



Universiteit  
Leiden  
The Netherlands

## Magnetic field effects on photosynthetic reactions

Liu, Y.

### Citation

Liu, Y. (2008, October 21). *Magnetic field effects on photosynthetic reactions*. Retrieved from <https://hdl.handle.net/1887/13153>

Version: Corrected Publisher's Version

License: [Licence agreement concerning inclusion of doctoral thesis in the Institutional Repository of the University of Leiden](#)

Downloaded from: <https://hdl.handle.net/1887/13153>

**Note:** To cite this publication please use the final published version (if applicable).

# **Magnetic Field Effects on Photosynthetic Reactions**

Yan Liu



# Magnetic Field Effects on Photosynthetic Reactions

proefschrift

ter verkrijging van  
de graad van Doctor aan de Universiteit Leiden,  
op gezag van de Rector Magnificus prof. mr. P. F. van der Heijden,  
volgens besluit van het College voor Promoties  
te verdedigen op dinsdag 21 oktober 2008  
klokke 15:00 uur

door

Yan Liu

geboren te Jiangyan, Jiangsu, China in 1978

## **Promotiecommissie**

Promotor: Prof. T. J. Aartsma  
Copromotor: Dr. P. Gast  
Referent: Prof. P. J. Hore (University of Oxford)  
Overige leden: Prof. J. Lugtenburg  
Dr. H. J. van Gorkom  
Dr. Alia  
Prof. J. M. van Ruitenbeek

This work was supported by the “Nederlandse organisatie voor Wetenschappelijk Onderzoek (NWO)” through “Chemische Wetenschappen (CW)” project 70098030.

### **Magnetic Field Effects on Photosynthetic Reactions.**

Thesis Universiteit Leiden.

ISBN/EAN: 978-90-9023566-0

Printed by PrintPartners Ipskamp B.V., the Netherlands

*To my parents  
and Hui*



# Abbreviations

ADMR	adsorption detected magnetic resonance
ADP	adenosine diphosphate
ATP	adenosine triphosphate
BChl	bacteriochlorophyll
BPheo	bacteriopheophytin
Chl	chlorophyll
cyt	cytochrome
DCMU	3-(3,4-dichlorophenyl)-1,1-dimethylurea
dQ	quinone-depleted
EDTA	ethylenediaminetetraacetic acid
EPR	electron paramagnetic resonance
Fd	ferredoxin
FM-ADMR	frequency modulated absorption detected magnetic resonance
HEPES	4-(2-hydroxyethyl)-1-piperazineethanesulfonic acid
hfi	hyperfine interaction
IC	interconversion
Im	imidazole
IR	infrared
ISC	intersystem crossing
LDAO	lauryldimethylamine oxide
LFE	low field effect
MES	2-(N-morpholino) ethanesulfonic acid
MFE	magnetic field effect
NADPH	nicotinamide-adenine dinucleotide phosphate



$^1\text{O}_2$	singlet oxygen
OD	optical density
OEC	oxygen-evolving system
$\text{P}_{680}$	primary electron donor in PS II
$\text{P}_{860}$	primary electron donor in purple bacteria
Pheo	pheophytin
PS I	photosystem I
PS II	photosystem II
$\text{Q}_A$	primary quinone acceptor
$\text{Q}_B$	secondary quinone acceptor
RB	Rose Bengal
Rb.	Rhodobacter
RC	reaction center
RNO	N,N-dimethyl-4- nitrosoaniline
RPM	radical pair mechanism
S-T mixing	singlet-triplet mixing
T-S spectrum	triplet-minus-singlet spectrum
TEMP	2,2,6,6-tetramethyl-piperidine
TEMPL	2,2,6,6-tetramethylpiperidinol
TMPD	2,2,6,6-tetramethyl-4-piperidone
wt	wild type

# CONTENTS

1. Introduction	1
2. Magnetic Field Effect on Singlet Oxygen Yield in Reaction Centers of <i>Rhodobacter sphaeroides</i>	
2.1 Luminescence detected singlet oxygen	24
2.2 Absorbance detected singlet oxygen	43
<i>A high magnetic field study</i>	
3. Frequency-Modulated Absorbance Detected Magnetic Resonance study on light-treated <i>Rhodobacter sphaeroides</i> R26 Reaction Centers	57
4. The influence of a Magnetic Field on Photoinhibition in <i>Synechocystis</i> sp. PCC 6803 cells	77
Thesis Summary	103
Samenvatting	107
Curriculum Vitae	111
Nawoord	113



**1**

# **Introduction**

## Magnetic Field Effects on Biological Systems

All living organisms on Earth are exposed to the geomagnetic field. In addition, exposure to man-made magnetic fields has increased significantly over the years, and for this reason the study of magnetic field effects (MFE) in biological systems, including humans, has gained interest, especially in the two recent decades. Public concern about possible hazardous effects of magnetic fields emitted from high power lines has led to several studies by means of behavioral experiments (Bernhardt, 1992; D'Andrea et al., 2003). A large number of clinical studies and much research have been conducted to explore the possible harmful effects on patients exposed to a strong, static magnetic field during magnetic resonance imaging (MRI) experiments (for a review, see Schenck, 2000). Moreover, adverse effects of exposure to magnetic fields have been indicated in a few epidemiological studies (Feychting & Ahlbom, 1993; Olsen et al., 1993; Ahlbom et al., 1993), and in cell cultures (Zhang et al., 2003). Although the hazardous effect of a magnetic field on living organisms, especially on humans, is still a matter of dispute, beneficial effects of magnetic fields have been identified: several species are well known to utilize the Earth magnetic field for orienting or guiding their migration (Schulten & Windemuth, 1986; Wiltschko & Wiltschko, 1995).

Yet it is still not fully understood which mechanism is causing the magneto-sensitivity. The majority of studies of magnetic field effects on living organisms discuss one of the following two theoretical magnetoreceptor mechanisms:

1. The magnetite mechanism
2. The radical pair mechanism

### *The magnetite mechanism*

Some types of bacteria and unicellular algae orient their movements along magnetic field lines (for a review, see Bazylinski & Frankel, 2004). The findings of crystals of magnetite ( $\text{Fe}_3\text{O}_4$ ) and greigite ( $\text{Fe}_3\text{S}_4$ ) in these organisms have stimulated the study of the possible sensory function of magnetite in animals. It has been suggested that the magnetite crystals can transfer the magnetic field information to the animal nerve system. One possibility is that magnetite adjacent to or inside the nerve

systems will exert a torque or pressure onto a secondary receptor when the magnetite aligns to the magnetic field. A second possibility is that the rotation of magnetite crystals opens an ion channel in the nerve system. In this way an animal could utilize the geomagnetic field to orient and to migrate. However, the role of magnetite crystals has been questioned because of the lack of convincing anatomic evidence for the presence of reasonably sized crystals. This has led to the suggestion that magnetic field sensitivity arises from very small crystals that typically exhibit superparamagnetism. These superparamagnetic crystals are thought to be much smaller than the magnetite crystals, i.e. much less than 50 nm. Unlike large magnetite crystals, a superparamagnetic crystal does not have a well-defined orientation of the magnetic moment in the absence of an external magnetic field. In the geomagnetic field, the superparamagnetic crystals can generate fields strong enough to attract or repel other nearby crystals. These magnetic field dependent inter-crystal interactions can potentially form a superparamagnetic cluster (Bacri et al., 1996; Shcherbakov & Winklhofer, 1999; Winklhofer et al., 2001). The superparamagnetic cluster is hypothesized to be located in the membrane of neurons. Depending on the orientation of the external field, the interacting clusters will compress or expand the membranes (Fleissner et al., 2003). The nerve system is sensitive to the membrane expansion or contraction. This potentially provides a possible means of detecting the orientation and/or the intensity of the external magnetic field. Furthermore, a model has been established to fully interpret the superparamagnetite mechanism in which the differences between magnetite crystal and superparamagnetic crystal concepts have been addressed (Davila et al., 2003). The superparamagnetic crystal model gained interest by the finding of very small superparamagnetic magnetite crystals in some fishes (Walker et al., 1997; 2000; Diebel et al., 2000); and birds, such as homing pigeons (Winklhofer et al., 2001).

However, the magnetite mechanism cannot explain the finding that in some species the magnetic field orientation is dependent on light intensity and its wavelength (Wiltschko et al., 1993; Muheim et al., 2002; Wiltschko & Wiltschko, 2002). Moreover, birds with their right eyes covered cannot perform magnetic field orientation in the lab (Wiltschko et al., 2002). Therefore light is considered to be a crucial factor for animal migration and/or orientation (Wiltschko & Wiltschko 1995; 1999; 2001; Wiltschko et al., 1993; 2000a; 2000b; 2001; 2002), pointing to the involvement of photoreceptors

rather than magnets in magnetoreception. Therefore, other (molecular) mechanisms, such as the Radical Pair Mechanism, may contribute to the magneto-sensitivity in these animals.

### ***The Radical Pair Mechanism***

It has been known for over three decades that magnetic fields can influence the rates and yields of certain classes of chemical reactions. Several mechanisms have been proposed (Leask, 1977; Lednev, 1991), but the only mechanism which gained widespread acceptance is the one involving pairs of radicals: the Radical Pair Mechanism (RPM) (Kaptein & Oosterhoff, 1969; Kaptein, 1971; Closs & Doubleday 1973; Brocklehurst & McLauchlan, 1996; Brocklehurst, 2002).

Despite very extensive research and concomitant basic understanding of magnetic field effects on chemical reactions via radical pair interactions, little evidence of radical pair involvement was obtained for biological systems, until the magnetic field-dependence of enzyme reactions was demonstrated and discussed by Harkins (Harkins & Grissom, 1994). In 1995, Grissom formulated several requirements for the observation of a magnetic field effect in enzyme reactions (for a review, see Grissom, 1995). Although in many enzymatic reactions radicals are involved, most of them do not generate radical pairs. In another word, most enzymes do not meet the criteria and it has been proved difficult to find magnetic-field sensitive enzymes. Though the model itself remains, Grissom's observations of magnetic field effects on horseradish peroxidase and ethanolamine ammonia lyase have recently been questioned by Jones (Jones et al., 2006; 2007).

The Radical Pair Mechanism was first invoked by Schulten (Schulten et al., 1978) to explain the ability of animals to sense the geomagnetic field and use it for their orientation or migration. Ritz et al. (2000) later on developed the hypothesis that magnetoreceptors located in a bird's retina generate a radical pair by photo-activation. The photo-generated radical pairs have specific magnetic properties, such that the anisotropy of the hyperfine interaction will cause the interconversion between the two spin states of the radical pairs, i.e. the singlet state and the triplet state, respectively. The magnetic field-dependence of this interconversion can affect the bird's vision in response to the magnetic field direction by two possible ways. The first possibility is

that the radical pair forming molecule, the magneto-photoreceptor, is involved in the photoreceptor, for example in the retina, i.e., in the visual pathway (Mouritsen & Ritz, 2005). The magnetic field modulates the light sensitivity of the magnetoreceptors differently in different parts of the retina because of the fixed orientation of the magnetoreceptors within the retinal cells and the hemispherical shape of the retina. The other suggestion is that a neurotransmitter is a product of a radical pair reaction. The magnetic field effects on the radical pair will influence the yield of this product, which results in the increase or decrease of the signal of the nerve cells which receive the neurotransmitters (Ritz et al., 2000; Timmel et al., 2001; Timmel & Henbest, 2004). The discovery of cryptochromes in the retina of two species of birds gave an experimental support to this hypothesis (Mouritsen et al., 2004; Möller et al., 2004; Ritz et al., 2004; for a review see Beason, 2005). The cryptochrome, a blue-green light photoreceptor, can form a radical pair on photoexcitation. This fact allows the suggestion that retinal cryptochromes can act as magneto-receptors in birds (Möller et al., 2004). However, it is still unclear how retinal cryptochromes would transfer the magnetic field information to the nerve system for further signal processing. Recently Maeda and his co-workers (Maeda et al., 2008) have shown that a triad molecule consisting of a carotenoid, porphyrin and fullerene can be used to detect magnetic field smaller than 50  $\mu$ T.

The work described in this thesis was undertaken to provide a 'proof of principle' demonstrating in vitro and in vivo that magnetic fields can significantly affect biological functionality. To this end magnetic field effects were investigated in a light-sensitive protein complex known to produce radical pairs: the photosynthetic reaction center.

## **Photosynthesis and Singlet oxygen**

In this thesis, light-induced Magnetic Field Effects are studied in different photosynthetic protein complexes as demonstrated in the following sections. The light-induced changes and the consequent products of the photosynthetic proteins are measured and detected using different spectroscopic techniques.



## ***The photosynthetic systems***

Photosynthesis is the process in which solar energy is converted to chemical energy, and takes place in higher plants, algae and some bacteria. It is directly or indirectly the sole energy resource for almost all living organisms. The oxygen produced by plants and cyanobacteria is essential for most life on earth. The primary act of photosynthesis is thought to be basically the same in the higher plants, algae and photosynthetic bacteria. It starts with the absorption of light by light-harvesting (or antenna) chromophores, followed by transfer of the excitation energy to the so-called reaction center, where the light energy is converted to chemical energy via charge separation. There are two types of photosynthetic reaction centers. They can be distinguished by their ability to reduce either sulfur clusters (FeS, Type I) or quinones (Type II) as terminal electron acceptors. Despite some differences between Type I and Type II reaction centers, the similarities of these two types is evident from the cofactor composition of the electron transfer system, the structure of the primary electron donor and the structural alignment of the electron transfer cofactors (Schubert et al., 1998). Type II reaction centers have been studied more extensively than Type I reaction centers. The studies on Type I reaction centers are not as extensive as on Type II reaction centers. The reason for this is that Type I reaction centers are integrated with a large number of light harvesting antenna pigments in a single pigment-protein complex, which complicates the measurements (for a review, see Heathcote et al., 2003). Type II reaction centers, on the other hand, were isolated from purple non-sulfur bacteria three decades ago (Reed & Clayton, 1968) and were in fact the first membrane protein whose structure was resolved by X-ray crystallography (Deisenhofer et al., 1984). Also in this thesis Type II reaction centers were used.

## ***The Reaction center of the purple bacterium Rhodobacter sphaeroides***

Purple bacteria are capable of photosynthetic energy conversion. In general, purple bacteria can be divided into two groups: purple sulfur and purple non-sulfur bacteria. These unicellular organisms contain only one type of reaction center for light induced charge separation. They cannot oxidize water but utilize sulfur compounds (for a review, see Dismukes et al., 2001) or organic compounds as electron donors to reduce

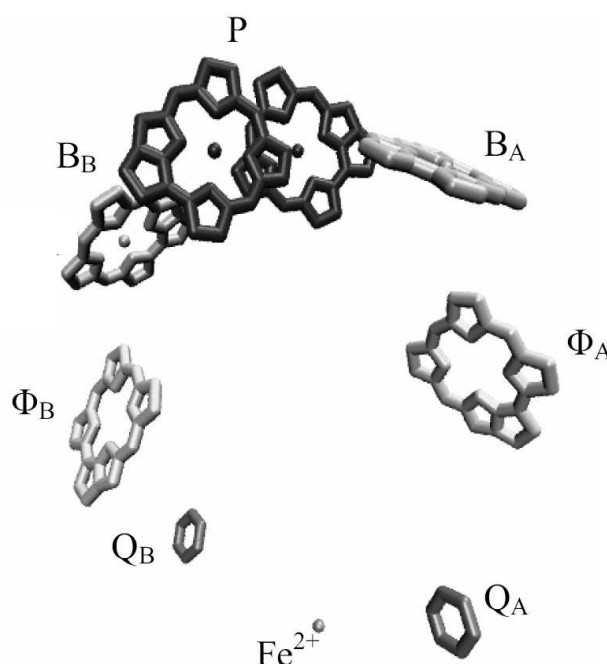


**Figure 1.**

The arrangement of the cofactors of the photosynthetic reaction center of *Rb. sphaeroides* R26. When a photon is absorbed by the primary donor, P860 (P in the figure) the primary donor loses an electron by transfer to the adjacent primary electron acceptor, BChl<sub>A</sub> (B<sub>A</sub> in the figure) in the time frame of picoseconds. The electron is subsequently transported to the nearby quinone Q<sub>A</sub>, via the Pheo<sub>A</sub> (Φ<sub>A</sub> in the figure) in about 200 ps. The final transfer step from Q<sub>A</sub> to Q<sub>B</sub> takes about 200 μs.

carbon dioxide to carbohydrates. *Rhodobacter sphaeroides* is a purple non-sulfur bacterium.

The reaction center (RC) of the non-sulfur purple bacterium *Rhodobacter (Rb.) sphaeroides* has been isolated and the structure of its carotenoidless mutant *Rb. sphaeroides* R26 has been elucidated using X-ray crystallography (Allen et al., 1987; Chang et al., 1991). The cofactors in the RC of the *Rb. sphaeroides* R26 are arranged with a near C<sub>2</sub> symmetry axis as depicted in Figure 1. The primary electron donor, a bacteriochlorophyll (BChl) dimer, P, is located near the periplasmic surface. Nearest to P are two mono-bacteriochlorophyll (BChl) molecules located on each side of the C<sub>2</sub> axis. Two quinones are located on the cytoplasmic side, with a non-heme iron located

in between on the C<sub>2</sub> axis. In Figure 1 the two symmetric branches are labeled A and B. The electron transport proceeds only along the A branch of the cofactors (Feher et al., 1989).

In addition to the above-mentioned chromophores, the wild type reaction center of *Rb. sphaeroides* contains also a carotenoid molecule, which is located close to the BChl of the B branch.

## ***Cyanobacteria***

Cyanobacteria are a very large group of ecologically diverse photoautotrophic gram-negative bacteria. They contain a complex intracellular membrane system (the thylakoid membrane), specialized light-harvesting systems and two photosystems, Photosystem (PS) I and Photosystem (PS) II (for a review, see Blankenship, 2002). Cyanobacteria are capable of performing oxygenic photosynthesis in the same way as algae and higher plants, using water as the ultimate electron donor.

*Synechocystis sp.* strain PCC 6803 is a unicellular cyanobacterium and has proved to be one of the best model organisms for studying the mechanism and regulation of oxygenic photosynthesis (Williams, 1988). The primary steps of photosynthesis in *Synechocystis sp.* PCC 6803 are illustrated in Figure 2. Two types of reaction centers, PS I and PS II, are linked to each other electronically. The primary photo-oxidant of PS II has a very high oxidation potential (> 1.2 V, van Gorkom & Schelvis, 1993) sufficient to split water into molecular oxygen and 4 protons, while the primary photo-reductant PS I has an extremely low redox potential (< -1.3 V), which provides energy for the reduction of NADP<sup>+</sup> to NADPH (nicotinamide-adenine dinucleotide phosphate) and formation of ATP (adenosine triphosphate) from ADP. NADPH and ATP are used to reduce CO<sub>2</sub> to carbohydrates in the so-called dark reactions.

The efficiency of photosynthesis can be influenced by many environmental conditions, such as salt concentration (Sharma & Hall, 1991; Jeanjean et al., 1993; Allakhverdiev et al., 2000), temperature (Crafts-Brandner & Salvucci, 2000; Öquist & Huner, 2003; Allakhverdiev & Murata, 2004; Yang et al., 2005; Murata et al., 2007), and light conditions (Nishiyama et al., 2001; for a review, see Murata et al., 2007) etc.

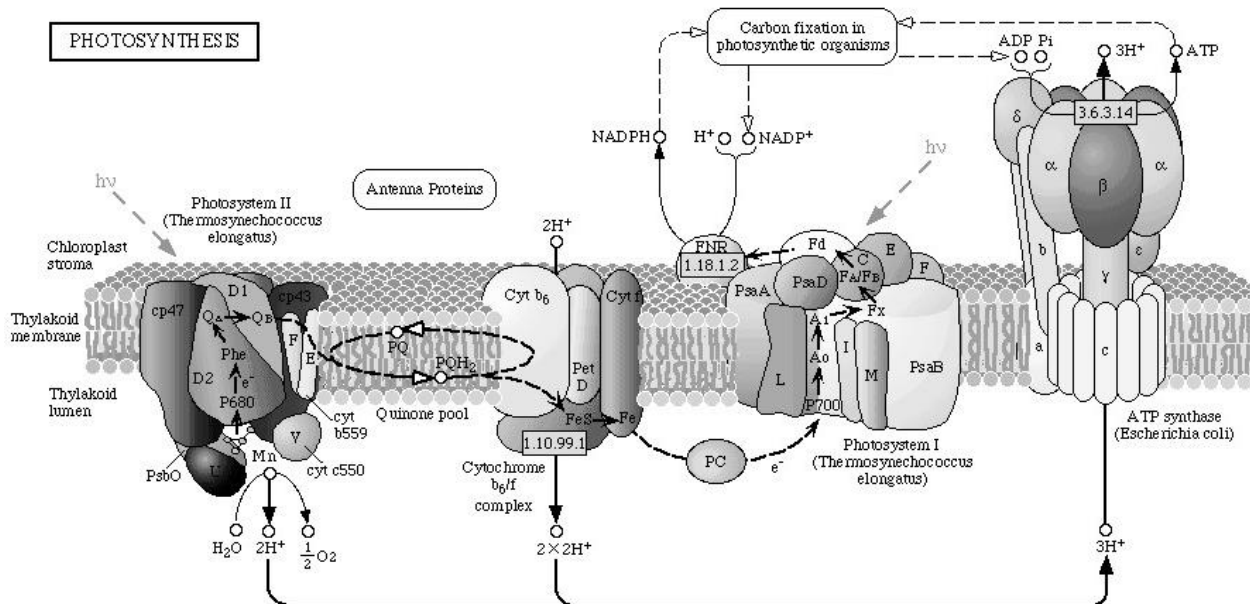


**Figure 2.**

*Schematic view of photosynthesis in *Synechocystis* sp. PCC 6803. One molecule  $O_2$  is released by oxidation of two water molecules in the oxygen evolving complex (OEC) after PS II has undergone 4 photon excitations ( $h\nu$ ) of the primary donor (P680) and 4 successive charge separations. The released electrons are transferred via a primary quinone  $Q_A$  to a secondary quinone acceptor  $Q_B$ , which is protonated upon two successive reductions, released from its pocket and replaced by oxidized quinone from the quinone pool.  $PQH_2$  transfers two electrons to cytochrome  $b_6/f$  (cyt  $b_6/f$ ). And then the electrons are transferred via plastocyanin (PC) to PS I. The reducing power of the PS I-acceptor ferredoxin (Fd) is used for the reduction of  $NADP^+$  to NADPH. The proton gradient generated by the light reactions is used by ATP synthase to generate the energy carrier ATP (adapted from <http://www.genome.jp/>).*

It has been noted that light can play two roles in photosynthesis efficiency. On the one hand, light may induce damage to photosystem II. On the other hand, it assists in the repair of photosystem II (Ohad et al., 1984). The molecular mechanisms for photo-induced damage and repair in PS II in *Synechocystis* sp. PCC 6803 (the subject of Chapter 4) are very similar to those in plants and it is therefore particularly useful

for studies of light-induced damage and repair.

## Singlet oxygen

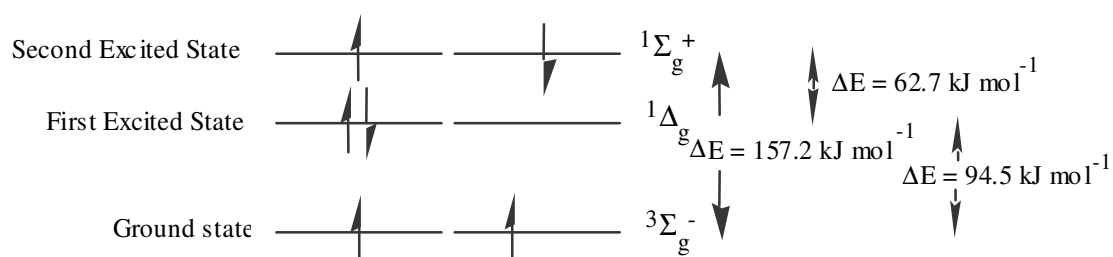
The oxidation of water by PS II results in the release of molecular oxygen, which has led to the evolution of multicellular organisms and the further development of life. Almost all living organisms on earth utilize oxygen for energy generation and respiration as well. However, there are hazards associated with living in an oxygen-rich environment, mainly due to the possible formation of oxygen free radicals and highly reactive singlet oxygen, a nonradical reactive oxygen species. The formation of such nonradical species is illustrated in the following sections.

### *Properties of singlet oxygen*

The ground state of spin state of oxygen is triplet unlike the singlet state of most natural compounds, whereas the lowest excited state of oxygen is singlet, as shown in Scheme 1 (Ameta et al., 1990).

The transition from the  $^1\Delta_g$  excited state to the  $^3\Sigma_g^-$  O<sub>2</sub> ground state is strictly forbidden because of spin selection rules. Since the lifetime of the second excited state ( $^1\Sigma_g^+$ ) is extremely short, which may be expected to undergo one-electron free radical reactions, the lowest excited state is the semi-stable state for singlet oxygen. This lowest excited state lies 94 kJ mol<sup>-1</sup> above the triplet ground state. Because of its singlet multiplicity no spin-restrictions exists for reactions of singlet oxygen, and due to its relatively high energy level, singlet oxygen is chemically extraordinary reactive.

Its lifetime in solution depends on the type of solvent (Table 1; Merkel & Kearns, 1972), due to vibrationally assisted relaxation. For example, the lifetime of singlet oxygen can be in the range of 4 μs in water, which has the highest frequency vibrations, and can be much longer than 1 ms as in CCl<sub>4</sub> for which vibrational frequencies are much lower.

**Scheme 1**

*Different energy states of oxygen molecule (Ameta et al., 1990).*

**Table 1.**

*Lifetime of singlet oxygen in various solvents, taken from Merkel & Kearns (1972)*

Solvent	Lifetime / $\mu\text{s}$
H <sub>2</sub> O	3.3
D <sub>2</sub> O	67
C <sub>6</sub> H <sub>5</sub> CH <sub>3</sub>	30
CH <sub>3</sub> OH	10.4
CH <sub>3</sub> OD	37
CD <sub>3</sub> OD	227
CH <sub>2</sub> Cl <sub>2</sub>	94
CHCl <sub>3</sub>	247
C <sub>6</sub> D <sub>6</sub>	700
CCl <sub>4</sub>	59,000

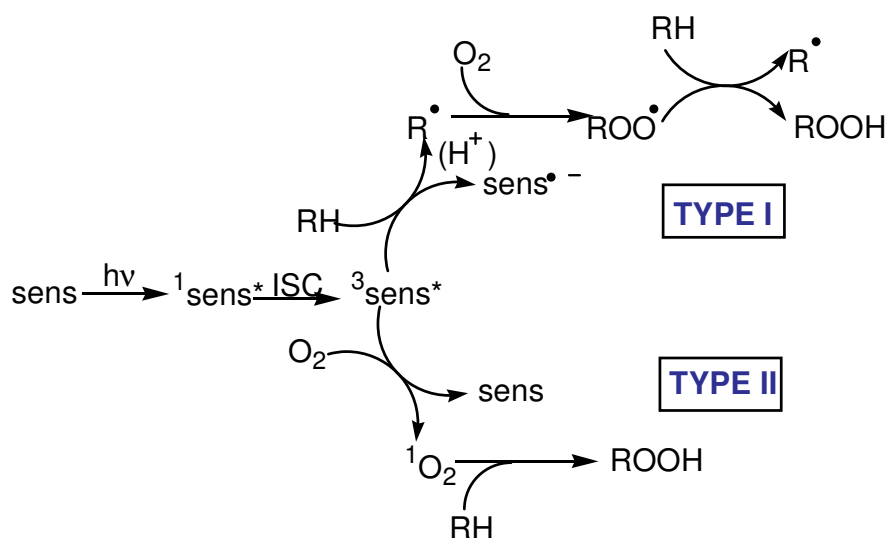


**Figure 3.**

Two types of photosensitization reactions. Type I generates radicals and Type II generates singlet oxygen (Phillips, 1994).

## Generation of singlet oxygen

Singlet oxygen can be formed in both, physical and chemical ways. The most common method of singlet oxygen production is by photosensitization reactions. In such a reaction, a photosensitizer, an agent that absorbs light and subsequently initiates a photochemical or photophysical alteration in the system, is irradiated to its singlet excited state, followed by conversion (called intersystem crossing, ISC) to its triplet excited state. The triplet excited sensitizer may now undergo radical reactions (Type I processes, i.e., radical generating via electron transfer or H-atom transfer) or produce singlet oxygen (Type II process, generating singlet oxygen ( $^1\text{O}_2$ ), via energy transfer from the triplet sensitizer to oxygen), as shown in Figure 3 (Phillips, 1994). It has been demonstrated that  $^1\text{O}_2$  can oxidize many kinds of biological molecules such as DNA, proteins and lipids (Briviba et al., 1997). Since oxygen is ubiquitous and efficiently quenches electronically excited (triplet) states,  $^1\text{O}_2$  is likely to be formed following irradiation in countless situations and involved in various chemical and biological processes as well as in several disease-related processes (Krinsky, 1979).

The quantum yield of singlet oxygen ( $\Phi_\Delta$ ) is a key property of photosensitizers.

It is defined as the number of singlet oxygen molecules formed per absorbed photon. The quantum yield is the product of three factors: 1) formation of the triplet state of the photosensitizer, the quantum yield of this process is the ISC efficiency or triplet yield ( $\Phi_T$ ); 2) trapping of the triplet state by molecular oxygen within its lifetime, the fraction of triplet states quenched by molecular oxygen is designated by  $S_Q$ ; 3) energy transfer from the trapped triplet state to molecular oxygen, the probability of energy transfer is  $S_\Delta$ , i.e. the fraction of encounter complexes which yields  $^1O_2$ . For many molecules the experimental value of  $S_\Delta$  is usually unity in case of long triplet lifetime. In summary,  $\Phi_\Delta = \Phi_T S_Q S_\Delta$ . Measured quantum yields show considerable variation with solvent, reaction conditions and measuring technique, therefore, measurements are always relative to a reference substance.

## Detection Methods

### *Direct luminescence detection.*

In solution, upon deactivation back to the ground state, the singlet oxygen molecule emits radiation in the near IR region, particularly at 1270 nm (Krasnovsky, 1979). It is an accurate method to detect the lifetime, quantum yield of singlet oxygen as well as rates of reactions with substrates in solution. After a nanosecond laser pulse is applied to excite the sensitizer, the decay of the singlet oxygen can be directly observed over time. The time dependence of the decay typically follows a monoexponential function, by which the lifetime of singlet oxygen in solution can be determined. The time-resolved method also allows direct determination of the rate constant by which singlet oxygen is consumed. This rate constant is the sum of rate constants of quenching by the solvent ( $k_d$ ), of physical quenching ( $k_q$ ), and of reaction of a substrate ( $k_r$ ), given by

$$k_{\text{obs}} = k_d + [S] (k_q + k_r),$$

where  $[S]$  presents the concentration of substrate which quenches singlet oxygen via a physical process or a chemical reaction, and the emission rate  $k_e$  is ignored as  $k_d \gg k_e$  (Schmidt & Afshari, 1990). By applying different substrate concentrations, the rate of reaction with substrate can be obtained.

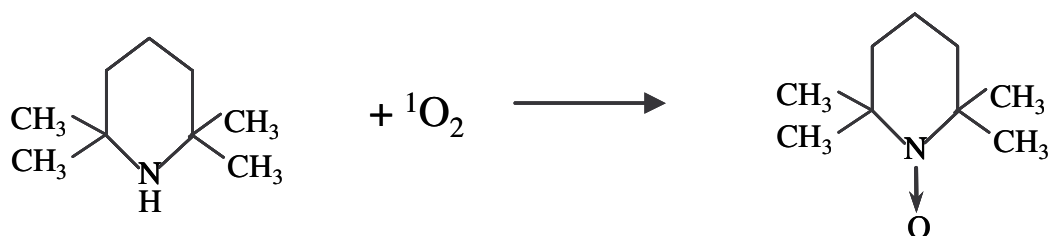


However, this technique is limited by the properties of the detecting apparatus. Photomultipliers have poor sensitivity in the near-IR region. Therefore photodiodes are the detectors of choice. We have utilized an InGaAs diode, due to its higher gain and faster response time compared with the traditional Ge photodiode. It is difficult to detect singlet oxygen when the lifetime is quite short and/or the intensity of emitted luminescence is low. Therefore, we have also used indirect detection methods in addition to direct luminescence detection.

### ***Indirect detection.***

#### *EPR Spin-trapping method*

Singlet oxygen is electron spin resonance (ESR, EPR) silent. However, long-lived nitroxide radicals can be generated by reaction with singlet oxygen and can be easily detected by EPR spectroscopy (Lion et al., 1976; Lion et al., 1980). Free radical production occurs, as shown below, when the chemical reaction is performed in the presence of the amine (in this scheme, the sterically hindered amine 2,2,6,6-tetramethylpiperidine (TEMP) is used as an example).

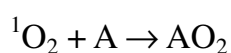


The EPR spectrum of the radical product consists of three lines and its intensity will be greatly increased with continuous illumination provided that neither additional intermediate quenchers are generated nor photobleaching of the dyes occurs during the illumination. Various amines are expected to generate EPR-sensitive radical products in the presence of singlet oxygen, such as TEMP, 2,2,6,6-tetramethyl-4-piperidone (TMPD), 2,2,6,6-tetramethylpiperidinol (TEMPL) etc. So far the most popular amine is TEMP, because of the extraordinarily long life time of the produced radicals produced.

#### *Optical Measurements*

The indirect optical detection method of singlet oxygen was introduced by

Kraljic and Mohsni (Kraljic & Mohsni, 1978) and is widely used in chemistry, material research, pharmacology and biology (Umemura et al., 1992; Ramu et al., 2001; Fiori et al., 2003). Here, generation of singlet oxygen by photosensitizer irradiation in the presence of dissolved oxygen is performed in a solution of N,N-dimethyl-4-nitrosoaniline (RNO). This results in the bleaching of RNO at 440 nm which is caused by an intermediate product of the reaction of singlet oxygen with an oxygen acceptor (A), usually imidazole. The imidazole reacts with singlet oxygen to form transannular peroxide which then oxidizes RNO, leading to a colorless oxidation product:



RNO has a yellow color, whereas the RNO-oxidation products are colorless. The reaction with singlet oxygen can thus be followed by spectrophotometry.

## Scope of this thesis

This thesis is aimed at the investigation of the Magnetic Field Effect (MFE), via the Radical Pair Mechanism (RPM), at the molecular and cellular level. Different photosynthetic protein complexes are used in this work. Magnetic field dependent light-induced changes and light-induced products from different photosynthetic protein complexes are illustrated.

The direct detection of a light generated product from photosynthetic reaction centers and the MFE on this product are studied in Chapter 2, where the first clear demonstration is given that a radical pair reaction in a protein can generate a toxic product in amounts that depend on the presence of an applied magnetic field.

The damage caused by light in photosynthetic proteins is further investigated in Chapter 3. It is concluded that a magnetic field partially protects from photo damage.

Finally, in Chapter 4, an *in vivo* study of the magnetic field effect on *Synechocystis sp.* PCC 6803 cells is demonstrated. The results suggest that a magnetic field of moderate strength can play a protective role against photoinhibition and that it could benefit plant growth.

## References

- Ahlbom A., Feychting M., Koskenvuo M., Olsen J.H., Pukkala E., Schulgen G., Verkasalo P. 1993, Electromagnetic-fields and childhood cancer, *Lancet*, 342: 1295–1296.
- Allakhverdiev S.I., Murata N. 2004, Environmental stress inhibits the synthesis de novo of proteins involved in the photodamage-repair cycle of photosystem II in *Synechocystis* sp. PCC 6803, *Biochim. Biophys. Acta*, 1657: 23–32.
- Allakhverdiev S.I., Sakamoto A., Nishiyama Y., Inaba M., Murata N. 2000, Ionic and osmotic effects of NaCl-induced inactivation of photosystems I and II in *Synechococcus* sp. *Plant Physiol.* 123: 1047–1056.
- Allen J.P., Feher G., Yeates T.O., Komiyama H., Rees D.C. 1987, Structure of the reaction center from *Rhodobacter sphaeroides* R-26: the protein subunits, *Proc. Natl. Acad. Sci. USA* 84: 6162–6166.
- Ameta S.C., Punjabi P.B., Chobisa C.S., Mangal N., Bhardwaj R. 1990, Singlet Molecular Oxygen, *Asian J. Chem. Rev.* 1: 106–124.
- Bacri J.C., Cabuil V., Cebers A., Menager C., Perzynski R. 1996, Flattening of ferro-vesicle undulations under a magnetic field, *Europhys. Lett.* 33: 235–240.
- Bazylnski D.A., Frankel R.B. 2004, Magnetosome formation in prokaryotes, *Nature Rev.* 2: 217–230.
- Beason R.C. 2005, Mechanisms of magnetic orientation in birds, *Integr. Comp. Biol.*, 45: 565–573.
- Bernhardt J.H. 1992, Non-ionizing radiation safety: radiofrequency radiation, electric and magnetic fields, *Phys. Med. Biol.* 37: 807–844.
- Blankenship R.E. 2002, *Molecular mechanisms of photosynthesis*, Blackwell Science, Oxford.
- Briviba K., Klotz L.O., Sies H. 1997, Toxic and signaling effects of photochemically or chemically generated singlet oxygen in biological systems, *Biol. Chem.*, 378: 1259–1265.
- Brocklehurst B. 2002, Magnetic fields and radical reactions: recent developments and their role in nature, *Chem. Soc. Rev.*, 31: 301–311.
- Brocklehurst B., McLauchlan K.A. 1996, Free radical mechanism for the effects of environmental electromagnetic fields on biological systems, *Int. J. Radiat. Biol.*, 69: 3–24.
- Chang C.H., El-Kabbani O., Tiede D., Norris J., Schiffer M. 1991, Structure of the membrane-bound protein photosynthetic reaction center from *Rhodobacter sphaeroides*, *Biochemistry*, 30: 5352–5360.
- Closs G.L., Doubleday C.E., 1973, Determination of the average singlet-triplet splitting in biradicals by measurement of the magnetic field dependence of CIDNP, *J. Am. Chem. Soc.* 95: 2735

–2736.

- Crafts-Brandner S.J., Salvucci M.E. 2000, Rubisco activase constrains the photosynthetic potential of leaves at high temperature and CO<sub>2</sub>, Proc. Natl. Acad. Sci. USA 97: 13430–13435.
- D'Andrea J.A., Adair E.R., de Lorge J.O. 2003, Behavioral and cognitive effects of microwave exposure, Bioelectromagnetics, 24: S39–S62.
- Davila A.F., Fleissner G., Winklhofer M., Petersen N. 2003, A new model for a magnetoreceptor in homing pigeons based on interacting clusters of superparamagnetic magnetite, Phys. Chem. Earth, 28: 647–652.
- Deisenhofer J., Epp O., Miki K., Huber R., Michel H. 1984, X-ray structure analysis of a membrane protein complex electron-density map at 3 Å resolution and model of the chromophores of the photosynthetic reaction center from *Rhodospseudomonas viridis*. J. Mol. Biol. 180: 385–398.
- Diebel C.E., Proksch R., Green C.R., Neilson P. 2000, Walker M.M. Magnetite defines a vertebrate magnetoreceptor, Nature, 406: 299–302.
- Dismukes G.C., Klimov V.V., Baranov S.V., Kozlov Y. N., DasGupta J., Tyryshkin A. 2001, The origin of atmospheric oxygen on earth: the innovation of oxygenic photosynthesis, Proc. Natl. Acad. Sci. USA 98: 2170–2175.
- Feher G., Allen J.P., Okamura M.Y., Rees D.C. 1989, Primary processes in bacterial photosynthesis: structure and function of reaction centers, Nature, 339: 111–116.
- Feychting M., Ahlbom A. 1993, Magnetic-fields and cancer in children residing near Swedish high-voltage power-lines, Am. J. Epidemiol. 138: 467–481.
- Fiori J., Ballardini R., Hrelia P., Andrisano V., Tarozzi A., Cavrini V. 2003, Investigation of the photochemical properties and in vitro phototoxic potential of bumetanide, Photochem. Photobiol. Sci. 2: 1011–1017.
- Fleissner G., Holtkamp-Rotzler E., Hanzlik M., Winklhofer M., Fleissner G., Petersen N., Wiltschko W. 2003, Ultrastructural analysis of a putative magnetoreceptor in the beak of homing pigeons, J. Comp. Neurol. 458: 350–360.
- Grissom C.B. 1995, Magnetic field effects in biology: a survey of possible mechanisms with emphasis on radical pair recombination, Chem. Rev. 95: 3–24.
- Harkins T.T., Grissom C.B. 1994, Magnetic field effects on B<sub>12</sub> Ethanolamine Ammonia Lyase: Evidence for a Radical Mechanism, Science, 263: 958 – 960.
- Heathcote P., Jones M.R., Fyfe P.K. 2003, Type I photosynthetic reaction centers: structure and function, Phil. Trans. R. Soc. Lond. B, 358: 231–243.
- Jeanjean R., Matthijs H.C.P., O Nana B., Havaux M., Joset F. 1993, Exposure of the cyanobacterium *Synechocystis* PCC6803 to salt stress induces concerted changes in respiration and

- photosynthesis, *Plant Cell Physiol.* 34: 1073–1079.
- Jones A.R., Hay S., Woodward J.R., Scrutton N.S. 2007, Magnetic field effect studies indicate reduced geminate recombination of the radical pair in substrate-bound adenosylcobalamin-dependent ethanolamine ammonia lyase. *J. Am. Chem. Soc.* 129: 15718–15727.
- Jones A.R., Scrutton N.S., Woodward J.R. 2006, Magnetic field effects and radical pair mechanisms in enzymes: A reappraisal of the horseradish peroxidase system. *J. Am. Chem. Soc.* 128: 8408–8409.
- Kaptein R., Oosterhoff L.J. 1969, Chemically induced dynamic nuclear polarization, *Chem. Phys. Lett.* 4: 195–197.
- Kaptein R. 1971, Simple rules for chemically induced dynamic nuclear polarization, *J Chem. Soc. Chem. Commun.* 14: 732–733.
- Kraljic I., Mohsni S.E. 1978, New method for the detection of singlet oxygen in aqueous solutions. *Photochem. Photobiol.* 28: 577–581.
- Krasnovsky A.A. 1979, Photo-luminescence of singlet oxygen in pigment solutions, *Photochem. Photobiol.* 29: 29–36.
- Krinsky N.I. 1979, Biological roles of singlet oxygen, *Singlet Oxygen*, Wasserman J.J. and Murray R.W. (eds), New York, Vol. 40, Academic Press, pp 579–641.
- Leask M.J.M. 1977, A physicochemical mechanism for magnetic field detection by migratory birds and homing pigeons, *Nature*, 267: 144–145.
- Lednev V.V. 1991, Possible mechanism for the influence of weak magnetic fields on biological systems, *Bioelectromagnetics*, 12: 71–75.
- Lion Y., Delmelle M., van der Vorst A. 1976, New method of detecting singlet oxygen production, *Nature*, 263: 442–443.
- Lion Y., Gandin E., van der Vorst A. 1980, On the production of nitroxide radicals by singlet oxygen reaction – an EPR study. *Photochem. Photobiol.* 31: 305–309.
- Maeda K., Henbest K.B., Cintolesi F., Kuprov I., Rodgers C.T., Liddell P.A., Gust D., Timmel C.R., Hore P.J. 2008, Chemical compass model of avian magnetoreception, *Nature*, 453: 387–390.
- Merkel P.J.B., Kearns D.R. 1972, Radiationless decay of singlet molecular oxygen in solution. An experimental and theoretical study of electronic-to-vibrational energy transfer, *J. Am. Chem. Soc.* 94: 7244–7253.
- Möller A. Sagasser S, Wiltschko W, Schierwater B. 2004, Retinal cryptochrome in a migratory passerine bird: a possible transducer for the avian magnetic compass, *Naturwissenschaften*, 91: 585–588.

- Möller A., Gesson M., Noll C., Phillips J.B., Wiltschko R., Wiltschko W. 2001, Light-dependent magnetoreception in migratory birds: previous exposure to red light alters the response to red light. In Orientation and Navigation – Birds, Humans and Other Animals, Proc. of the RIN 01 Conference, pp. 6-1–6-6. Oxford: Royal Institute of Navigation.
- Mouritsen H., Janssen-Bienhold U., Liedvogel M., Feenders G., Stalleicken J., Dirks P., Weiler R. 2004, Cryptochromes and neuronal-activity markers colocalize in the retina of migratory birds during magnetic orientation, Proc. Natl. Acad. Sci. USA, 101: 14294–14299.
- Mouritsen H., Ritz T. 2005, Magnetoreception and its use in bird navigation, Curr. Opin. Neurobiol. 15: 406–414.
- Muheim R., Bäckman J., Åkesson S. 2002, Magnetic compass orientation in European robins is dependent on both wavelength and intensity of light, J. Exp. Biol. 205: 3845–3856.
- Murata N., Takahashi S., Nishiyama Y., Allakhverdiev S.I. 2007, Photoinhibition of photosystem II under environmental stress, Biochim. Biophys. Acta, 1767: 414–421.
- Nishiyama Y., Yamamoto H., Allakhverdiev S.I., Inanba M., Yokota A., Murata N. 2001, Oxidative stress inhibits the repair of photodamage to the photosynthetic machinery. EMBO J. 20: 5587–5594.
- Ohad I., Kyle D.J., Arntzen C.J. 1984, Membrane-protein damage and repair – removal and replacement of inactivated 32-kilodalton polypeptides in chloroplast membranes, J. Cell Biol. 99: 481–485.
- Okamura M.Y., Isaacson R.A., Feher G. 1975, Primary acceptor in bacterial photosynthesis: obligatory role of ubiquinone in photoactive reaction centers of *Rhodospseudomonas sphaeroides*, Proc. Natl. Acad. Sci. USA, 72: 3491–3495.
- Olsen J.H., Nielsen A., Schulgen G. 1993, Residence near high-voltage facilities and risk of cancer in children, Br. Med. J. 307: 891–895.
- Öquist G., Huner N.P.A. 2003, Photosynthesis of over-wintering evergreen plants, Annu. Rev. Plant Biol. 54: 329–355.
- Phillips D. 1994, Photodynamic therapy, Sci. Progress. 77: 295–316.
- Ramu A., Mehta M.M., Leaseburg T., Aleksic A. 2001, The enhancement of riboflavin-mediated photo-oxidation of doxorubicin by histidine and urocanic acid, Cancer Chemother. Pharmacol. 47: 338–346.
- Reed D.W., Clayton, R.K. 1968, Isolation and composition of a photosynthetic reaction center complex from *Rhodospseudomonas sphaeroides*, Biochem. Biophys. Res. Comm. 30: 471–475.
- Ritz T., Adem S., Schulten K. 2000, A model for photoreceptor-based magnetoreception in birds, Biophys. J. 78: 707–718.

- Ritz T., Thalau P., Phillips J.B., Wiltschko R., Wiltschko W. 2004, Resonance effects indicate a radical-pair mechanism for avian magnetic compass, *Nature*, 429: 177–180.
- Schenck J.F. 2000, Safety of strong, static magnetic fields. *J. Magn. Reson. Imaging*, 12: 2–19.
- Schmidt R., Afshari E. 1990, Effect of solvent on phosphorescence rate constants of singlet molecular oxygen, *J. Phys. Chem.* 94: 4377–4378.
- Schubert W.D., Klukas O., Saenger W., Witt H.T., Fromme P., Krauss N. 1998, A common ancestor for oxygenic and anoxygenic photosynthetic systems: a comparison based on the structural model of photosystem I, *J. Mol. Biol.* 280: 297–314.
- Schulten K., Swenberg C., Weller A. 1978, A biomagnetic sensory mechanism based on magnetic field modulated coherent electron spin motion, *Z. Phys. Chem. NF*, 111: 1–5.
- Schulten K., Windemuth A. 1986, Model for a physiological magnetic compass. In: *Effects of steady magnetic fields*. Maret G., Kiepenheuer J., Feychtig M. (eds.), Berlin, Springer-Verlag, pp: 99–106.
- Schulten K. 1982. Magnetic field effects in chemistry and biology, *Adv. Solid State Phys.* 22: 61–83.
- Sharma P.K., Hall D.O. 1991, Interaction of salt stress and photoinhibition on photosynthesis in barley and sorghum, *J. Plant Physiol.* 138: 614–619.
- Shcherbakov V., Winklhofer M. 1999, The osmotic magnetometer: a new model for magnetite-based magnetoreceptors in animals, *Eur. Biophys. J.* 28: 380–392.
- Timmel C.R., Henbest K.B. 2004, A study of spin chemistry in weak magnetic fields, *Phil. Trans. R. Soc. Lond. A*, 362: 2573–2589.
- Timmel C.R., Cintolesi F., Brocklehurst B., Hore P.J. 2001, Model calculations of magnetic field effects on the recombination reactions of radicals with anisotropic hyperfine interactions, *Chem. Phys. Lett.* 334: 387–395.
- Umemura S., Kawabata K., Yumita N., Nishigaki R., Umemura K. 1992, Sonodynamic approach to tumor treatment, *Ultrasonics Symp. Proc.* 2: 1231–1240.
- van Gorkom H.J., Schelvis J.P.M. 1993, Kok's oxygen clock: what makes it tick? The structure of P680 and consequences of its oxidizing power, *Photosynth. Res.* 38: 297–301.
- Walker M.M., Diebel C.E., Green C.R. 2000, Structure, function, and use of the magnetic sense in animals (invited). *J. Appl. Phys.* 89: 4653–4658.
- Walker M.M., Diebel C.E., Haugh C.V., Pankhurst P.M., Montgomery J.C., Green C.R. 1997, Structure and function of the vertebrate magnetic sense, *Nature*, 390: 371–376.
- Williams J.G.K. 1988. Construction of specific mutations in photosystem II photosynthetic reaction center by genetic engineering methods in *Synechocystis* 6803, *Methods Enzymol.* 167:766–778.

- Wiltschko W., Gesson M., Wiltschko R. 2001, Magnetic compass orientation of European robins under 565 nm green light, *Naturwissenschaften*, 88: 387–390.
- Wiltschko W., Munro U., Ford H., Wiltschko R. 1993, Red light disrupts magnetic orientation of migratory birds, *Nature*, 364: 525–527.
- Wiltschko W., Traudt J., Güntürkün O., Prior H., Wiltschko R. 2002, Lateralization of magnetic compass orientation in a migratory bird, *Nature*, 419: 467–470.
- Wiltschko W., Wiltschko R. 1995, Migratory orientation of European robins is affected by the wavelength of light as well as by magnetic pulse, *J. Comp. Physiol. A*, 177: 363–369.
- Wiltschko W., Wiltschko R. 1999, The effect of yellow and blue light on magnetic compass orientation in European robins. *Erithacus rubecula*, *J. Comp. Physiol. A*, 184: 295–299.
- Wiltschko W., Wiltschko R. 2001, Light-dependent magnetoreception in birds: the behaviour of European robins, *Erithacus rubecula*, under monochromatic light of various wavelengths and intensities, *J. Exp. Biol.* 204: 3295–3302.
- Wiltschko W., Wiltschko R. 2002, Magnetic compass orientation in birds and its physiological basis, *Naturwissenschaften*, 89: 445–452.
- Wiltschko W., Wiltschko R., Munro U. 2000a, Light-dependent magnetoreception in birds: does directional information change with light intensity? *Naturwissenschaften*, 87: 36–40.
- Wiltschko W., Wiltschko R., Munro U. 2000b, Light-dependent magnetoreception in birds: the effect of intensity of 565-nm green light, *Naturwissenschaften*, 87: 366–369.
- Winklhofer M., Holtkamp-Rötzler E., Hanzlik M., Fleissner G., Petersen N. 2001, Clusters of superparamagnetic magnetite particles in the upper-beak tissue of homing pigeons: evidence of a magnetoreceptor, *Eur. J. Mineral.* 13: 659–669.
- Yang X., Liang Z., Lu C. 2005, Genetic engineering of the biosynthesis of glycinebetaine enhances photosynthesis against high temperature stress in transgenic tobacco plants, *Plant Physiol.* 138: 2299–2309.
- Zhang Q.M., Tokiwa M., Doi T., Nakahara T., Chang P.W., Nakamura N., Hori M., Miyakoshi J., Yonei S. 2003, Strong static magnetic field and the induction of mutations through elevated production of reactive oxygen species in *Escherichia coli soxR*, *Int. J. Radiat. Biol.*, 79: 281–286.





# 2

## **Magnetic Field Effect on Singlet Oxygen Yield in Reaction Centers of *Rhodobacter sphaeroides***

## 2.1 Luminescence detected singlet oxygen

### Summary

The yield of singlet oxygen ( $^1\Delta_g$ ,  $^1O_2$ ) photosensitized by quinone-depleted bacterial photosynthetic reaction centers, and the ensuing oxidative damage to the protein complex and its associated cofactors, are shown to be magnetic field-dependent.  $^1O_2$  formed by flash illumination of the carotenoidless mutant of *Rhodobacter sphaeroides* R26 is detected via its luminescence at 1270 nm. In a magnetic field of 1 mT, the  $^1O_2$  yield drops by 10% and by 50% for a field of 20 mT. The photobleaching of the 800 nm absorption band of the accessory bacteriochlorophylls, caused by the  $^1O_2$  attack on the reaction center, is about 45% less in a magnetic field of 15 mT than it is in the absence of an applied field. The origin of the magnetic field effect—the Radical Pair Mechanism—and the conditions under which the  $^1O_2$  yield might be increased by an applied magnetic field are discussed. We believe this to be the first clear demonstration that a radical pair reaction involving a protein can generate toxic products in amounts that depend on the presence of a weak applied magnetic field.

### Introduction

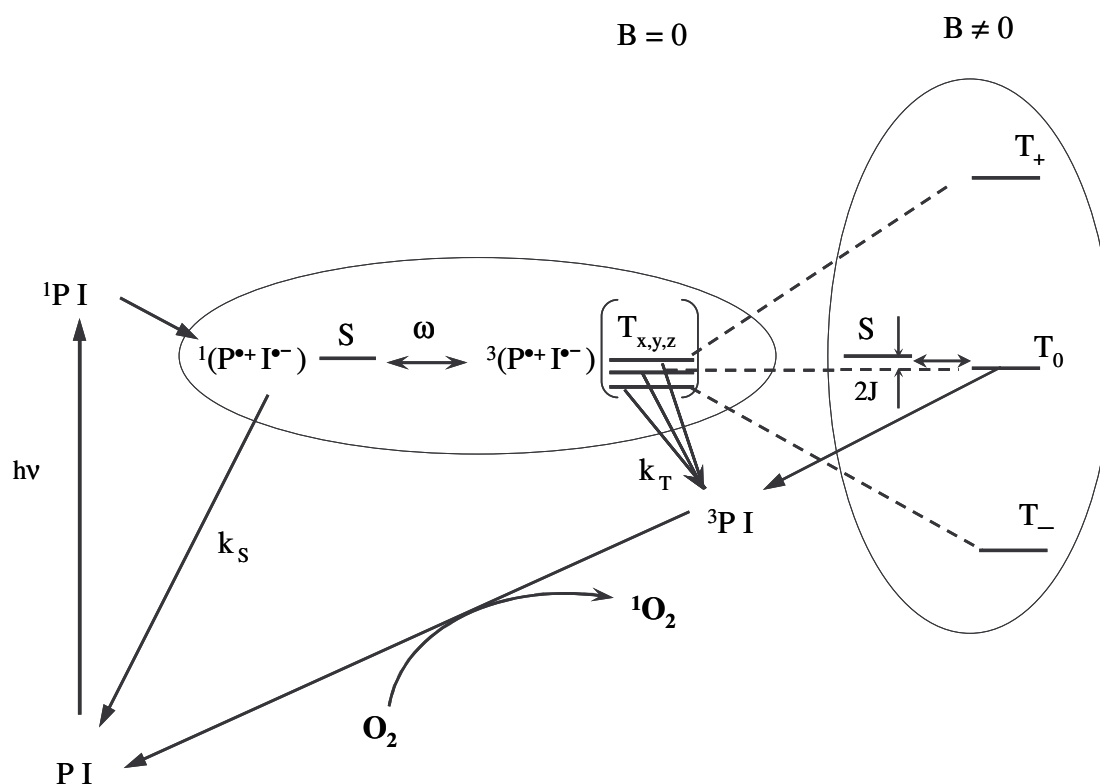
It has been well established that external magnetic fields can influence certain biological processes and can affect living organisms. Several enzymatic reactions are known to be field dependent (Harkins & Grissom, 1994; Grissom, 1995). Beneficial effects in living organisms are the proposed role of navigating in the earth magnetic field by several migratory species, and it has been shown that this field-sensitivity is often light-driven (Phillips & Borland, 1992; Wiltchko et al., 1993). Indications of adverse effects of exposure to magnetic fields on humans have been found in a few epidemiological studies (Feychting & Ahlbom, 1993; Olsen et al., 1993; Ahlbom et al., 1993), and in cell cultures (Zhang et al., 2003). The magnetic field strengths, for which these effects have been observed, range from sub-microTesla ( $\mu$ T) to several Tesla (T).

Although the influence of magnetic fields on the rates and product yields of a host of chemical reactions are well documented and can be understood in the

framework of the Radical Pair Mechanism (RPM) (Grissom, 1995; Brocklehurst, 2002; Brocklehurst & McLauchlan, 1996), it has so far proved impossible to demonstrate convincingly a biological RPM effect. Here we present proof that a biological system, for which it is known that the RPM is operative, can generate toxic products in amounts that depend on the presence of a relatively weak applied magnetic field. We show, to our knowledge, the first observation of magnetic field dependent singlet oxygen production in a biological system. These measurements could in principle explain beneficial and adverse effects for low and high magnetic fields, respectively.

### ***Radical Pair Mechanism***

A radical pair that is initially generated in the singlet state can be transformed to a triplet radical pair state via singlet-triplet conversion. It is driven by electron-nuclear hyperfine interactions and modified by the electron Zeeman interactions, which makes it sensitive to a magnetic field. In zero magnetic field, the four radical-pair spin states (the singlet and the three triplet states:  $T_x$ ,  $T_y$ ,  $T_z$ ) are coupled by the hyperfine interaction and are nearly degenerate. Therefore, S-T mixing can occur between the singlet and any of the three sublevel triplet states and thus the three sublevel triplet states are populated with approximately equal probability. When a magnetic field is applied with a strength that is equal to or weaker than the hyperfine interactions, an enhancement in the inter-conversion of singlet and triplet radical pairs is produced. Its origin lies in a change in the selection rules for singlet-triplet mixing under the influence of the hyperfine couplings (Brocklehurst & McLauchlan, 1996; Timmel et al., 1998). This effect is referred to as the low field effect (LFE). When the value of the external magnetic field equals the zero magnetic field energy difference between the singlet and triplet state ( $2J$ ), the initially populated singlet energy level will mix with one of triplet states, which depends on the direction of the external magnetic field. The population probability of the triplet state will therefore increase, which leads to an increase of the total triplet yield. This effect is known as  $2J$ -resonance (Werner et al., 1978; Lersch & Michel-Beyerle, 1983). When a magnetic field much larger than the hyperfine interactions is applied, two of the three triplet states ( $T_+$ ,  $T_-$ ) are separated from the singlet state energy level due to Zeeman interaction and not populated, since the energy differences between S and  $T_+$  or between S and  $T_-$  prevent mixing of these states. Only the  $T_0$  and S levels are then

**Scheme 1.**

Schematic view of electron transfer with and without a magnetic field in blocked RCs, where  $\omega$  indicates the frequency of interconversion of  $^1(P^+\Gamma)$  and  $^3(P^+\Gamma)$ ;  $k_S$  and  $k_T$  represent the rates of the two electron transfer processes.

energetically close which means that the singlet state can only mix with  $T_0$ . It results in a decrease of the quantum yield of triplet states in a magnetic field compared to the yield at zero-field when the triplet state is created from the radical pair triplet.

When a Radical Pair ( $P^+$  and  $\Gamma^-$  in this work) is created in the singlet radical pair state  $^1(P^+\Gamma)$  it can dephase with a dephasing rate  $\omega$  to the triplet radical pair state  $^3(P^+\Gamma)$  from which the molecular triplet state  $^3P$  can be populated. The dephasing rate,  $\omega$ , between singlet and triplet radical pair states is governed by differences in hyperfine interactions and  $g$ -value differences between  $P^+$  and  $\Gamma^-$  (Hoff et al., 1993), as shown in equation 1.

$$\omega(B) = \left[ \sum_j a_{P_j} m_{P_j} - \sum_k a_{I_k} m_{I_k} \right] + \Delta g \mu_B B \quad (1)$$

in which  $a_{P_j}$  and  $m_{P_j}$  are the hyperfine coupling constant and nuclear magnetic quantum number for nucleus  $j$  of radical  $P^+$ , with similar notation for radical  $I^-$ ;  $B$  is the magnetic field strength,  $\mu_B$  the Bohr magneton and  $\Delta g$  is the g-value difference between  $P^+$  and  $I^-$ .

At very high magnetic field, the term with  $\Delta g$  becomes the dominant factor (eq. 1) and the dephasing rate will increase linearly. The dephasing rate  $\omega$  competes with the recombination rate of  $^1(P^+I^-)$ ,  $k_S$ , and more triplet radical pairs will be generated in case of  $\omega \gg k_S$ . This results in an increase of the quantum yield of molecular triplets compared to a moderate magnetic field and at very high magnetic field the yield can even exceed the yield at zero-field (Goldstein et al., 1988).

### ***Magnetic Field Effect in purple bacteria***

In this work, the magnetic field effect is studied in photosynthetic reaction center of *Rhodobacter (Rb.) sphaeroides* wt and of its carotenoidless mutant R26. The cofactors of the reaction center of *Rb. sphaeroides* consist of a primary donor (P), which is a bacteriochlorophyll dimer, two accessory bacteriochlorophylls (B), two bacteriopheophytins (I), two quinones ( $Q_A$  and  $Q_B$ ) and one carotenoid (see Fig. 1 in Chapter 1). When a quantum of light is absorbed, the primary donor is excited into the first excited singlet state  $P^*$ . Then rapid charge separation occurs and an electron from  $P^*$  is transferred to I, thus forming the radical pair  $P^+I^-$ . Further charge stabilization leads to the formation of  $P^+Q_A^-$  in 200 ps followed by  $P^+Q_B^-$  in 100  $\mu$ s. In isolated reaction centers these two charged pairs recombine to the ground state in 0.1 and 1 second, respectively. When the quinones are removed or chemically reduced, the electron transfer to  $Q_A$  is blocked. In the blocked system,  $P^+I^-$  can then recombine to the ground state in several nanoseconds or to the triplet of P,  $^3P$ . This triplet has a yield of 15% (Parson et al., 1975) at room temperature in the absence of a magnetic field. The relative yield of singlet and triplet recombination can be influenced by an external magnetic field. In purple bacteria, both the zero-field splitting of the radical pair triplet

state and the energy difference of  $2J$  between  $^1(\text{P}^+\Gamma^-)$  and  $^3(\text{P}^+\Gamma^-)$  are small, leading to an equal population on the three triplet states in zero field. When a moderate magnetic field is applied ( $< 1\text{T}$ ) (Hoff et al., 1993), the S-T dephasing rate,  $\omega$ , can be considered constant because the hyperfine coupling term in equation 1 is dominant. Due to the Zeeman splitting, which leads to only S- $\text{T}_0$  mixing, the molecular triplet yield is about three times lower in a high magnetic field than in a zero magnetic field. When a very high magnetic field is applied ( $>1\text{T}$ ) (Chidsey et al., 1985; Hoff et al., 1993), the  $g$ -value difference between P and I ( $\sim 0.001$ ) results in an increased dephasing rate since the  $g$ -value difference becomes the dominant factor in equation 1 (Chidsey et al., 1985; Goldstein et al., 1988). The electron transfer kinetic scheme for reaction centers with removed quinones (blocked RCs) is shown in Scheme 1 in which the four energy levels of the radical pair with and without magnetic field are depicted.

The triplet state is potentially harmful to the reaction center, since it can be quenched by molecular oxygen by the following reaction, resulting in the formation of highly reactive singlet oxygen,  $^1\text{O}_2$



Singlet oxygen has been implicated in a variety of biological processes, including lipid peroxidation (Halliwell & Gutteridge, 1999). In wild-type reaction centers from the photosynthetic bacterium *Rb. sphaeroides*,  $^1\text{O}_2$  is not normally formed because  $^3\text{P}$  is rapidly quenched by a nearby carotenoid molecule: at room temperature the  $^3\text{P}$  lifetime is then a few hundred nanoseconds (Cogdell & Frank, 1987). In the carotenoidless mutant R26, however,  $^3\text{P}$  recombines to the ground state in about  $50 \mu\text{s}$  (Chidsey et al., 1985) in Q double-reduced and quinone-depleted RCs at room temperature under anaerobic conditions, allowing ample time for the formation of  $^1\text{O}_2$ , which is known to attack the reaction center (Tandori et al., 2001). Since the yield of  $^3\text{P}$  depends on the strength of the applied magnetic field, the amount of  $^1\text{O}_2$  is predicted to be also field-sensitive. This is of considerable interest because of the possible biological consequences of exposure to magnetic field.

## Materials and Methods

### *Sample Preparation*

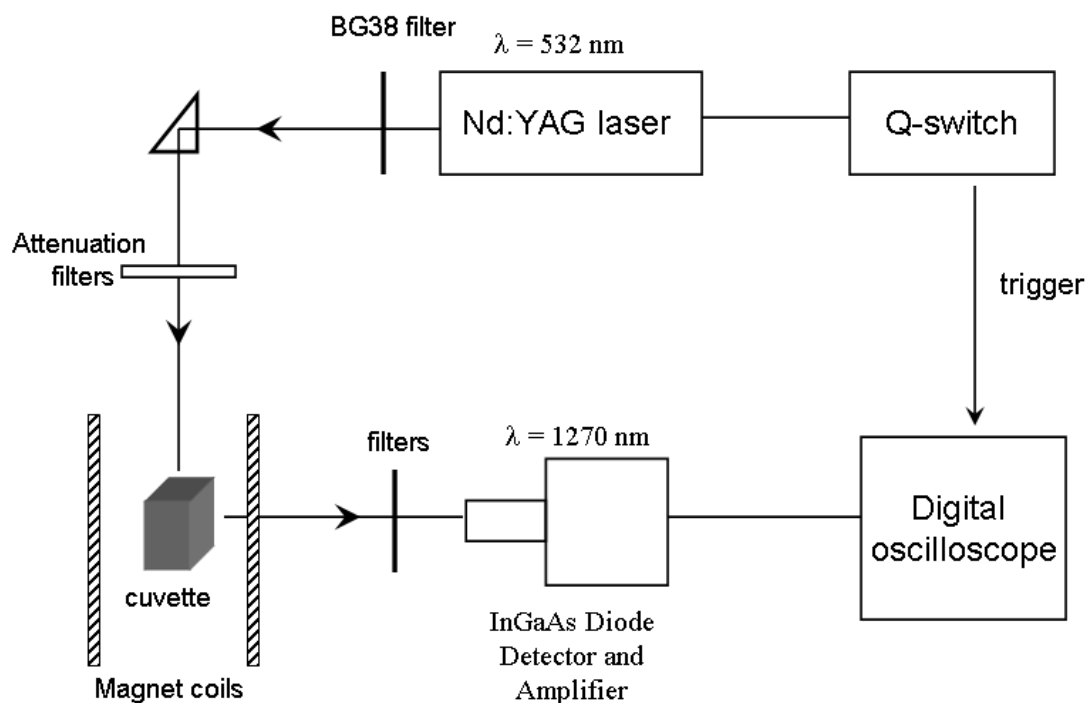
Reaction centers were isolated from *Rb. sphaeroides* wt and its carotenoidless mutant R26 with the use of lauryldimethylamine oxide (LDAO), as described by Clayton and Wang (Clayton & Wang, 1971). Quinones were removed with 10 mM o-phenanthroline and 4% LDAO as described (Feher & Okamura, 1978). After concentrating the solubilized RCs to about 100  $\mu$ M in TL buffer (10 mM Tris/HCl buffer, 1 mM EDTA, 0.1% LDAO, pH 8.0), using a 100 kD Amicon filter, the Q-depleted *Rb. sphaeroides* wt and R26 RCs were stored at  $-18$  °C. Before measurement, the RCs were thawed and suspended in perdeuterated buffer, resulting in final concentration of approximately 99.5%, in order to increase the singlet oxygen lifetime from 3  $\mu$ s ( $H_2O$ ) to about 67  $\mu$ s ( $D_2O$ ), containing 10 mM phosphate buffer, 1mM EDTA, 0.1% LDAO, pH = 8.0. Anaerobic conditions were achieved by bubbling with argon for 90 minutes. The oxygen saturation conditions were achieved by bubbling with oxygen for 60 minutes.

### *Singlet Oxygen Detection and Magnetic Field Effect*

Singlet oxygen was measured using time-resolved near-infrared luminescence at 1270 nm as described by Keene et al. (1986), shown in Scheme 2. The RCs were excited at 532 nm ( $A_{532} = 0.15$   $cm^{-1}$ ) from a Q-switched frequency-doubled Nd:YAG laser (Spectron Lasers SL 402, 16 ns pulse, energy per flash  $\leq 30$  mJ per pulse), operating at 1 Hz. The emission from the sample, contained in a 10 mm quartz cuvette, was filtered by a 1260 nm transmitting interference filter (bandwidth = 75 nm) in front of the detector, blocking excitation light. Emission was detected at  $90^\circ$  with respect to the laser beam by an InGaAs photodiode, amplified and then signals averaged (typically 1024 shots) on a digital oscilloscope (HP Infinium). The response time of the detection system was about 3  $\mu$ s. To minimize the effect of photodegradation, the sample (Q-depleted *Rb. sphaeroides* R26 RCs in  $O_2$  saturated  $D_2O$  buffer) was refreshed after one thousand flashes.

For the magnetic field effect measurements, the set-up is schematically shown





### ***Scheme 2.***

*Experimental set-up of singlet oxygen detection. For details, see the text.*

in Scheme 2. A magnetic field up to 100 mT was supplied by home-built solenoid magnet. The strength of the magnetic field was measured by a Gaussmeter Probe (Applied Magnetics Laboratory) with resolution of 0.1 mT.

Steady-state absorption measurements were carried out on a Shimadzu UV-visible spectrophotometer (Shimadzu UV-160A). All measurements were carried out at room temperature.

## **Results**

### ***Detection of singlet oxygen luminescence***

We studied the light-induced formation of  $^1\text{O}_2$  in Q-depleted reaction centers from wild-type *Rb. sphaeroides* and its carotenoidless mutant R26 suspended in a

perdeuterated buffer, saturated with oxygen. Singlet oxygen was monitored via its time-resolved near-infrared luminescence at 1270 nm following flash excitation of P at 532 nm (Krasnovsky, 1979; Khan & Kasha, 1979). A typical time-profile of the luminescence emission of singlet oxygen in D<sub>2</sub>O at 1270 nm is shown in Figure 1, using light excitation of the standard photosensitizer Rose Bengal (RB). Fluorescence and excitation light are responsible for an initial spike in the  $\mu$ s range. The 1270 nm emission from singlet oxygen is observed as a transient with a lifetime of about 60  $\mu$ s.

The lifetime of singlet oxygen in D<sub>2</sub>O ( $\tau_{\Delta} \approx 67 \mu$ s, Schmidt, 1989) is ~20 times longer than in H<sub>2</sub>O ( $\tau_{\Delta} \approx 3 \mu$ s) and hence D<sub>2</sub>O is commonly used as a means of detecting the formation of singlet oxygen. For this reason, the Q-depleted *Rb. sphaeroides* R26 RCs were suspended in ‘perdeuterated buffer’ after concentration. The H<sub>2</sub>O content of the buffer was then less than 0.5%. The lifetime of singlet oxygen in D<sub>2</sub>O will vary with the H<sub>2</sub>O content as H<sub>2</sub>O is a high effective singlet oxygen quencher. The decay rates of singlet oxygen generated from RB by light illumination were measured for different contents of H<sub>2</sub>O in D<sub>2</sub>O, as shown in Figure 2. The decay rate at low H<sub>2</sub>O content is linear with quencher concentration (Fig. 2 inset), in accordance with the Stern-Volmer equation (Krasnovsky, 1979). A lifetime of singlet oxygen of 60  $\mu$ s in 0% H<sub>2</sub>O is observed. At higher H<sub>2</sub>O concentrations, the curve starts to deviate from linearity, due to the instrumental time constant of ~3  $\mu$ s.

The singlet oxygen luminescence emission, generated from *Rb. sphaeroides* R26 RCs has a similar time profile as RB, but is much weaker. It was therefore needed to subtract from the luminescence signal from *Rb. sphaeroides* R26 RCs, the signal either from an anaerobic sample or from a sample containing the fast singlet oxygen quencher, sodium azide. Both methods are compared in Figure 3. The difference between the two methods is probably due to incomplete anaerobic condition. Therefore, the azide method is used in this work and kinetic traces were averaged over 1024 shots to achieve a good signal to noise ratio.

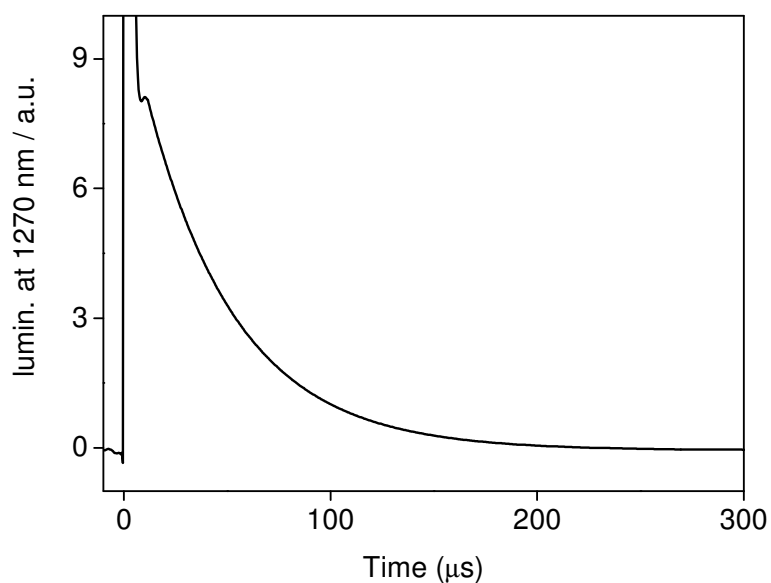


**Figure 1.**

*Luminescence emission from Rose Bengal (RB) in D<sub>2</sub>O after laser flash excitation.*

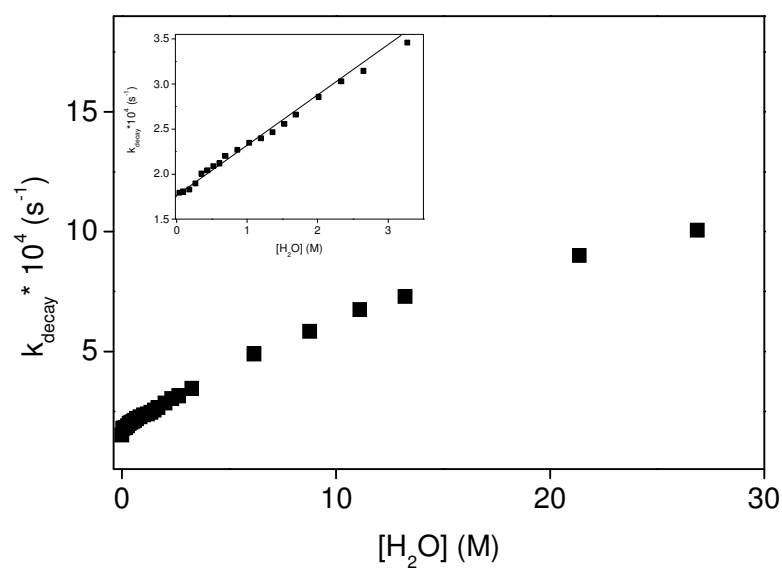


**Figure 2.**

*Decay rates of singlet oxygen (■) against H<sub>2</sub>O contents in D<sub>2</sub>O. Inset figure shows the decay rates of H<sub>2</sub>O in D<sub>2</sub>O at low concentrations.*

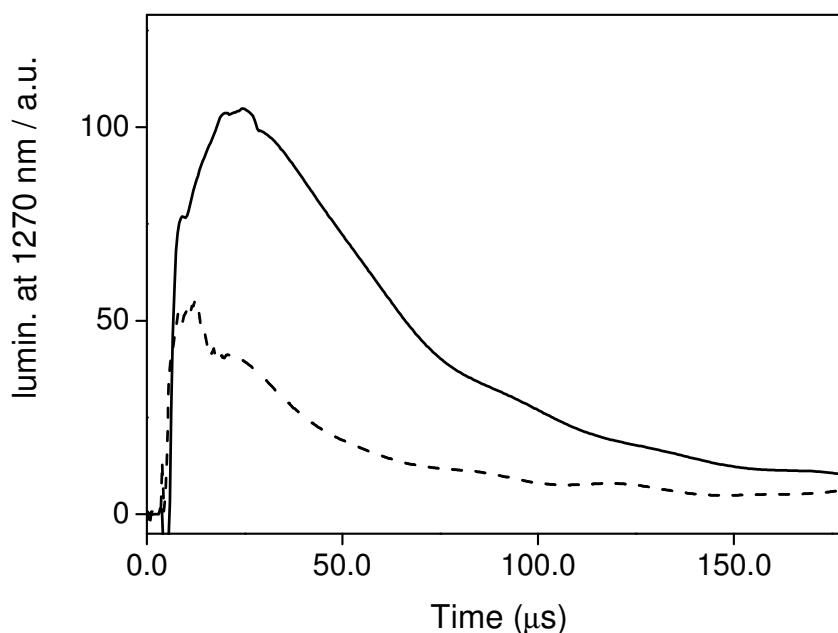


**Figure 3.**

*Corrected Near-IR emission signal of singlet oxygen, generated from oxygen saturated *Rb. sphaeroides* Q-depleted R26 RCs in  $\text{D}_2\text{O}$  by subtracting either the signal in the presence of sodium azide (solid line, 1 mM) or the signal under anaerobic conditions (dashed line).*

### ***Quantum Yield of Singlet Oxygen in *Rb. sphaeroides* R26 RCs***

Singlet oxygen was monitored via its time-resolved near-infrared luminescence at 1270 nm following flash excitation of P at 532 nm. The near-infrared emission signals were fitted to a monoexponential decay with amplitude  $S(0)$  at zero time. A signal decaying with a time constant of 43  $\mu\text{s}$  was observed for Q-depleted *Rb. sphaeroides* R26 RCs, whereas no long-lived ( $> 15 \mu\text{s}$ ) emission was found for wild-type reaction centers (Fig. 4), consistent with the very rapid triplet transfer to the carotenoid (Cogdell & Frank, 1987). The observed lifetime is somewhat shorter than that reported for  $^1\text{O}_2$  in  $\text{D}_2\text{O}$  (67  $\mu\text{s}$ ; Schmidt 1989), due to the presence of the protein complex, the solvent and residual  $\text{H}_2\text{O}$  in solution.

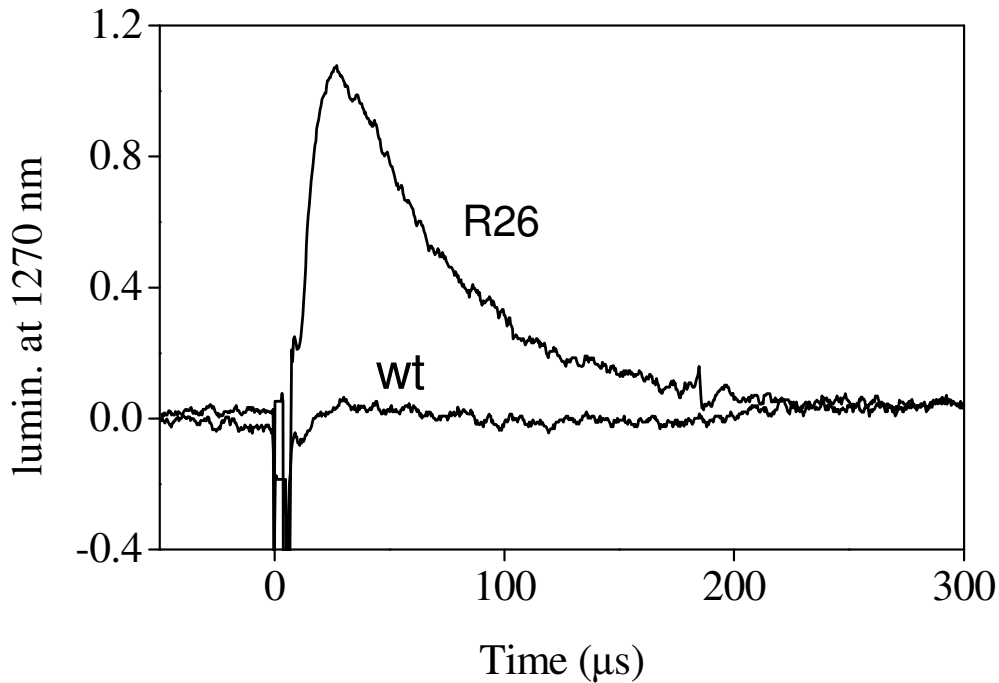


**Figure 4.**

Time-resolved  $^1O_2$  luminescence at 1270 nm from Q-depleted reaction centers of *Rb. sphaeroides* in oxygen-saturated perdeuterated buffer. R26: RCs from the carotenoidless R26 mutant; wt: carotenoid-containing wild-type RCs. Both kinetic traces were corrected for a laser-induced artifact by subtracting the signal in the presence of the  $^1O_2$  scavenger  $NaN_3$  (1mM).

$S(0)$ , the zero-time luminescence intensity is proportional to the quantum yield of singlet oxygen,  $\Phi_{\Delta}$ .  $S(0)$  values of a reference sensitizer for different laser energies, in this work RB, can be compared with those of RCs under the same experimental conditions, as shown in Figure 5.

Thus, the value of  $\Phi_{\Delta}$  for Q-depleted RCs of *Rb. sphaeroides* R26 can be determined from the following equation:

$$\Phi_{\Delta}^{sample} = \Phi_{\Delta}^{ref} \frac{\beta}{\alpha} \quad (3)$$

where  $\alpha$  and  $\beta$  correspond to the slopes of the lines in Figure 5 for RB and RCs, respectively.

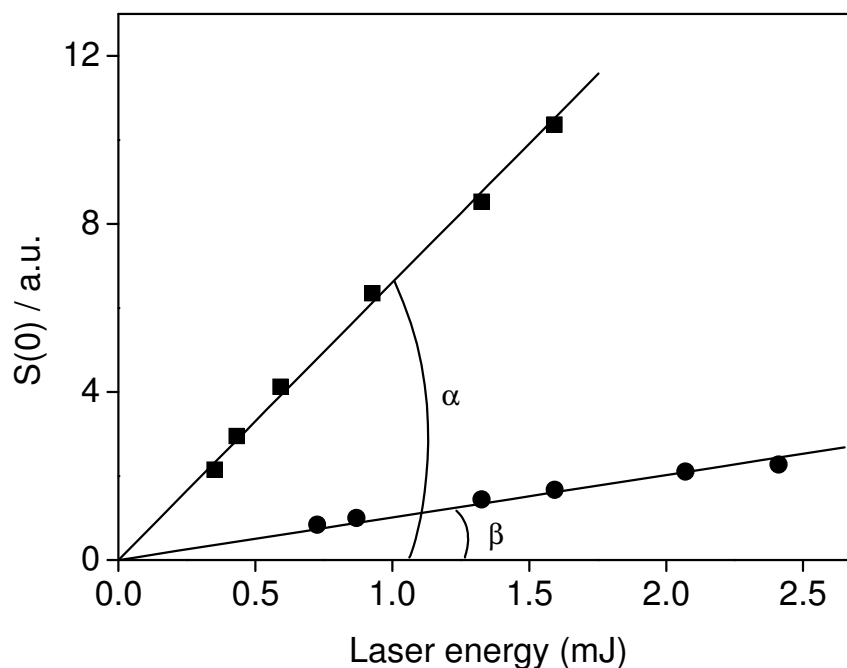


**Figure 5.**

Laser energy dependent  $^1O_2$  luminescence extrapolated from fitting the data for RB (squares) and Q-depleted (dQ) RCs from *Rb. sphaeroides* R26 (circles), with identical absorption at 532 nm ( $A_{532}$ ).

A quantum yield of singlet oxygen in Q-depleted RCs from *Rb. sphaeroides* R26 of  $9 \pm 4\%$  was obtained using RB as a standard reference with a yield of 75% in  $D_2O$  (Bilski et al., 1991).

### ***Magnetic field effect on singlet oxygen production***

When a magnetic field  $B$  is applied, the concentration of triplet will be changed by the RPM (Scheme 1), which will result in a change in the concentration of singlet oxygen. The lifetime of singlet oxygen generated in *Rb. sphaeroides* Q-depleted R26 RCs is not influenced by an external magnetic field (data not shown) but its luminescence intensity is dependent on the magnetic field strength. Singlet oxygen yields were obtained from the amplitude of a mono-exponential fit of the luminescence traces. A clear magnetic field effect on *Rb. sphaeroides* Q-depleted R26 RCs was

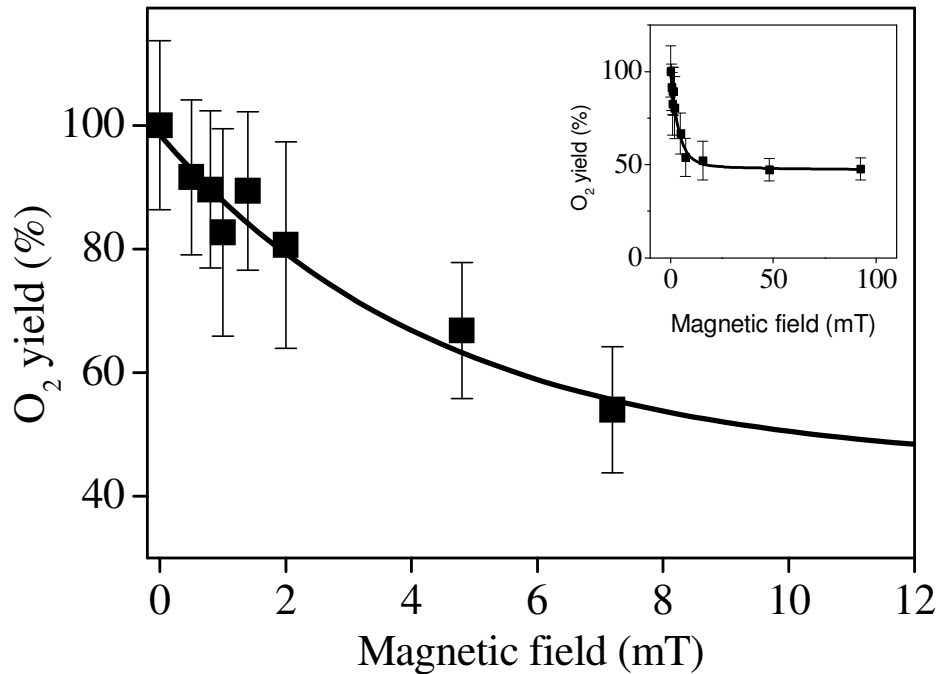


**Figure 6.**

Relative  $^1\text{O}_2$  yield in  $Q$ -depleted reaction centers from *Rb. sphaeroides* R26 RCs as a function of the applied magnetic field. The inset shows the same measurements made over a wider range of magnetic fields. Other conditions as in Fig 5.

obtained, shown in Figure 6. It appears that a magnetic field of a few mT has a profound effect on the  $^1\text{O}_2$  yield in R26 RCs: a 50 % reduction was observed for fields of 20-100 mT and even a 10 % reduction was observed for 1 mT. The total effect of 50% corresponds closely to the reduction in  $^3\text{P}$  yield observed at similar magnetic field strengths (Chidsey et al., 1985), and can thus be ascribed to the hyperfine mechanism outlined in the introduction.

The field strength needed to change the yield by one half of the final change,  $B_{1/2}$ , is  $3.9 \pm 0.5$  mT, which is slightly less than the  $B_{1/2}$ -values found for the yield of  $^3\text{P}$  (4.2 mT and 5.7 mT) (Chidsey et al., 1985; Vidal et al., 1986).

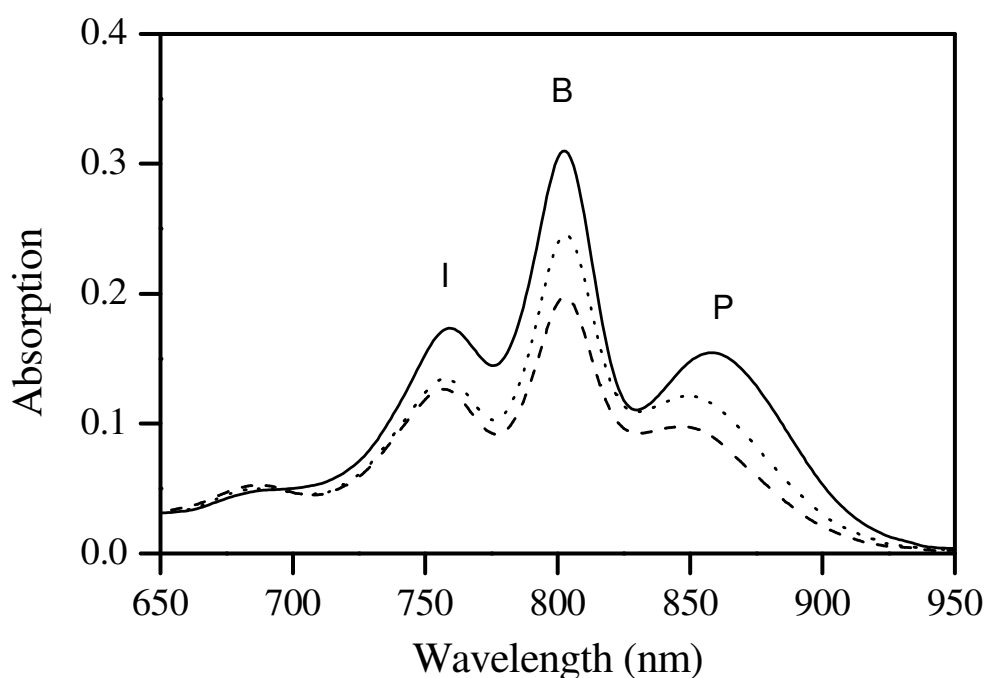


**Figure 7.**

*Absorption spectrum of Q-depleted reaction centers from Rb. sphaeroides R26 before (solid) and after (dashed) illumination at zero field. Dotted line: after illumination in a magnetic field of 15 mT.*

### ***Photodegradation of Q-depleted Rb. sphaeroides R26 RCs with and without magnetic field***

Figure 7 shows the absorption spectra of RCs in oxygen-saturated buffer before and after excitation with 12,000 laser flashes ( $\lambda_{exc} = 532$  nm) with and without magnetic field. The illumination has irreversibly attenuated the absorption bands at 760, 800 and 860 nm belonging to I, the accessory bacteriochlorophyll B, and P respectively, and a slight absorption increase around 680 nm has occurred. These changes are indicative of photobleaching, accompanied by disruption of the interactions between the chromophores and possibly by changes in the RC structure. They provide a measure of the extent of the photodegradation caused by  $^1O_2$  (Tandori et al., 2001). The bleaching of the 800 nm band is about 45% smaller in a field of 15 mT than it is in zero-field.



This finding corroborates the measurements shown in Fig. 6 and demonstrates directly that a relatively modest magnetic field affords substantial protection for the RC against  $^1\text{O}_2$ -induced damage. Wild-type reaction centers were much more stable under these light conditions and the total photobleaching was only 15 % and no magnetic field dependence was found (data not shown).

## Discussion

We have demonstrated that in Q-depleted RCs from *Rb. sphaeroides* R26 the singlet oxygen yield after laser excitation is dependent on the applied magnetic field. In time-resolved measurements a 50 % decrease of singlet oxygen yield was measured and consequently a reduced photodegradation was observed in steady-state experiments. Thus the magnetic field protects this protein from photodegradation. Just a few milli-Tesla has a profound effect on the singlet oxygen yield while lifetimes remain constant, in the range of 40-46  $\mu\text{s}$ .

For an applied magnetic field to have a damaging effect in this context, it would need to *promote* the formation of  $^1\text{O}_2$ . There are two ways in which a weak magnetic field ( $< 1$  mT) could cause such an increase. First, there is the “Low Field Effect” which has an opposite phase to the effects reported here and occurs for fields smaller than the average hyperfine interactions in the radical pair (Brocklehurst & MacLauchlan, 1996; Timmel et al., 1998). Second, and similar in appearance to the LFE, is the “ $2J$  resonance” that arises from energy-level crossings at field strengths that match the radical pair’s exchange interaction (Lersch & Michel-Beyerle, 1983). That neither of these mechanisms operates efficiently here is due to the short lifetime of the radical pair and, in the case of the LFE, to the presence of the exchange and dipolar interactions between the two electron spins. A  $2J$  resonance in the yield of  $^3\text{P}$  has been found for *Rb. sphaeroides* (Norris et al., 1987) but only at temperatures below 0 °C. In very strong magnetic fields ( $>5$  T), the triplet yield becomes larger than in the absence of an applied field as a result of the difference in Zeeman interactions of the two radicals (Brocklehurst & MacLauchlan, 1996; Goldstein et al., 1988). The size of this effect and the field at which it occurs are determined by the difference in the two  $g$ -values, which is quite small for  $\text{P}^+$  and  $\Gamma$  but can be much higher for other radical pairs, such that relatively modest fields could cause the photosensitised  $^1\text{O}_2$  yield to

rise above that in zero field.

These effects are not necessarily restricted to reaction centers or indeed to  $^1O_2$  produced by photosensitisation. For example,  $^1O_2$  is formed during lipid peroxidation by the self reaction of peroxy radicals (the Russell mechanism): a process which could conceivably show RPM effects (Miyamoto et al., 2003).

## **Conclusions**

This work demonstrated the magnetic field effect on a biological system in which the Radical Pair Mechanism is involved. A decreased  $^1O_2$  yield by an applied magnetic field is observed, and a possible increased yield is discussed. We believe this to be the first clear demonstration that a radical pair reaction involving a protein can generate toxic products in amounts that depend on the presence of a weak applied magnetic field.

## References

- Ahlbom A., Feychting M., Koskenvuo M., Olsen J.H., Pukkala E., Schulgen G., Verkasalo P. 1993, Electromagnetic-fields and childhood cancer, *Lancet*, 342: 1295–1296.
- Bilski P., Dabestani R., Chignell C. F. J. 1991, Influence of cationic surface on the photoprocess of eosin and Rose-Bengal in aqueous-solution, *Phys. Chem.* 95: 5784–5791.
- Brocklehurst B. 2002, Magnetic fields and radical reactions: recent developments and their role in nature, *Chem. Soc. Rev.* 31: 301–311.
- Brocklehurst B., McLauchlan K.A. 1996, Free radical mechanism for the effects of environmental electromagnetic fields on biological systems, *Int. J. Radiat. Biol.*, 69: 3–24.
- Clayton R.K., Wang R.T. 1971, Absolute yield of bacteriochlorophyll fluorescence in vivo, *Methods Enzymol.* 23: 696–704.
- Chidsey C.E.D., Takiff L., Goldstein R.A., Boxer S.G. 1985, Effect of magnetic-fields on the triplet-state lifetime in photosynthetic reaction centers – evidence for thermal repopulation of the initial radical pair, *Proc. Natl. Acad. Soc. USA* 82: 6850–6854.
- Cogdell R.J., Frank H.A. 1987, How carotenoids function in photosynthetic bacteria, *Biochim. Biophys. Acta* 895: 63–79.
- Feher G., Okamura M. Y. 1978, *The Photosynthetic Bacteria*, Clayton R. K. and Sistron W.R. (Eds.) pp: 349.
- Feychting M., Ahlbom A. 1993, Magnetic-fields and cancer in children residing near Swedish high-voltage power-lines, *Am. J. Epidemiol.* 138: 467–481.
- Goldstein R.A., Takiff L., Boxer S.G. 1988, Energetics of initial charge separation in bacterial photosynthesis – the triplet decay rate in very high magnetic-fields, *Biochim. Biophys. Acta* 934: 253–263.
- Grissom C. B., 1995, Magnetic-field effects in biology – a survey of possible mechanisms with emphasis on radical-pair recombination, *Chem. Rev.* 95: 3–24.
- Halliwell B., Gutteridge J.M.C. 1999, *Free Radicals In Biology And Medicine*, Third Edition, Oxford: Clarendon Press, 1999. pp. 617–783.
- Harkins T.T., Grissom C.B., 1994, Magnetic-field effects on B<sub>12</sub> ethanolamine ammonialyase – evidence for a radical mechanism, *Science*, 263: 958–960.
- Hoff A.J., Gast P., van der Vos R., Vrieze J., Franken E.M., Lous E.J. 1993, Magnetic-field effects – MARY, MIMS and MODS, *Z. Physik. Chem.*, 180: 175–192.
- Keene J.P., Kessel D., Land E.J., Redmond R.W., Truscott T.G. 1986, Direct detection of singlet oxygen sensitized by hematoporphyrin and related-compounds, *Photochem. Photobiol.* 43: 117–120.
- Khan A.U., Kasha M. 1979, Direct spectroscopic observation of singlet oxygen emission at 1268 nm

- excited by sensitizing dyes of biological interest in liquid solution, Proc. Natl. Acad. Soc. USA76: 6047–6049.
- Krasnovsky A.A. 1979, Photo-luminescence of singlet oxygen in pigment solutions, Photochem. PhotoBiol. 29: 29–36.
- Lersch W., Michel-Beyerle M.E. 1983, Magnetic-field effects on the recombination of radical ions in reaction centers of photosynthetic bacteria, Chem. Phys., 78: 115–126.
- Miyamoto S., Martinez G.R., Medeiros M.H.G., Di Mascio P. 2003, Singlet molecular oxygen generated from lipid hydroperoxides by the Russell mechanism: Studies using O-18-labeled linoleic acid hydroperoxide and monomol light emission measurements, J. Amer. Chem. Soc. 125: 6172–6179.
- Norris J.R., Lin C.P., Budil D.E.J. 1987, Magnetic resonance of ultrafast chemical reactions, J. Chem. Soc., Faraday Trans. 83: 13–27.
- Olsen J.H., Nielsen A., Schulgen G. 1993, Residence near high-voltage facilities and risk of cancer in children, G. Br. Med. J. 307: 891–895.
- Parson W.W., Roderick K.C., Cogdell R.J. 1975, Excited states of photosynthetic reaction centers at low redox potentials, Biochim. Biophys. Acta, 387: 265–278.
- Phillips J.B., Borland S.C. 1992, Behavioral evidence for use of a light-dependent magnetoreception mechanism by a vertebrate, Nature, 359: 142–144.
- Schmidt R. 1989, Influence of heavy-atoms on the deactivation of singlet oxygen ( $^1\Delta_g$ ) in solution, J. Amer. Chem. Soc. 111: 6983–6987.
- Tandori J., Hideg E., Nagy L., Maroti P., Vass I. 2001, Photoinhibition of carotenoidless reaction centers from Rhodobacter sphaeroides by visible light. Effects on protein structure and electron transport, Photosynth. Res. 70: 175–184.
- Timmel C.R., Till U., Brocklehurst B., McLauchlan K.A., Hore P.J. 1998, Effects of weak magnetic fields on free radical recombination reactions, Mol. Phys. 95: 71–89.
- Vidal M.H., Setif P., Mathis P. 1986, Influence of magnetic-fields of the P<sub>870</sub> triplet-state in *Rps. Sphaeroides* reaction centers, Photosynth. Res. 10: 347–354.
- Werner H.J., Schulten K., Weller A. 1978, Electron-reansfer and spin exchange contributing to magnetic-field dependence of primary photo-chemical reaction of bacterial photosynthesis, Biochim. Biophys. Acta 502: 255–268.
- Wiltshko W., Munro U., Ford H., Wiltshko R. 1993, Red-light disrupts magnetic orientation of migratory birds, Nature, 364: 525–527.
- Zhang Q.M., Tokiwa M., Doi T., Nakahara T., Chang P.W., Nakamura N., Hori M., Miyakoshi J., Yonei S. 2003, Strong static magnetic field and the induction of mutations through elevated production of reactive oxygen species in Escherichia coli soxR, Int. J. Radiat. Biol. 79: 281–286.



## 2.2 Absorbance-detected singlet oxygen

### A high magnetic field study

#### Summary

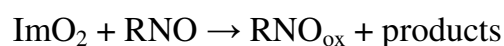
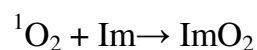
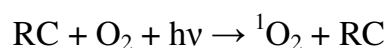
As in Chapter 2.1, the magnetic field dependence of singlet oxygen formation by quinone-depleted reaction centers isolated from carotenoidless mutant of *Rhodobacter sphaeroides* R26 was investigated. Here, singlet oxygen was detected via the irreversible bleaching of N,N-dimethyl-4-nitrosoaniline (RNO) by the reaction product of singlet oxygen with imidazole.. This can be measured after illumination in a magnetic field, which allowed the use of much higher field strengths than in Chapter 2.1. The results confirm the decrease of the singlet oxygen yield at low field strengths and show in addition that the singlet oxygen yield rises at magnetic fields above 1 T, as predicted by the involvement of the radical pair mechanism in its production.

#### Introduction

In the previous section, we investigated the dependence on low magnetic fields of singlet oxygen production in quinone-depleted reaction centers (RCs) from *Rhodobacter (Rb.) sphaeroides* by means of time-resolved near-infrared luminescence detection at 1270 nm. This magnetic field dependence of singlet oxygen yield was explained by its formation via recombination of the  $P^+I^-$  radical pair to the bacteriochlorophyll triplet state, and the radical pair mechanism (RPM) gave a straightforward explanation for the decreased singlet oxygen yield at low magnetic fields. According to the RPM, the mixing frequency,  $\omega$ , between singlet  $^1[P^+I^-]$  and triplet  $^3[P^+I^-]$  radical pair states is governed by differences in hyperfine interactions and g-tensor differences between  $P^+$  and  $I^-$ . In a low magnetic field, the hyperfine term dominates, whereas the term containing the g-tensor difference will become important at high magnetic fields (for details, see Chapter 2.1). Therefore, the mixing frequency

of singlet and triplet states is increased at higher magnetic field and may lead to an increased triplet yield. Thus, an increased yield of  $^1\text{O}_2$  from and increased light-induced damage to the RCs is expected at high magnetic fields. To verify this prediction we have studied singlet oxygen production by *Rb. sphaeroides* R26 RCs by a different method that allowed the use of higher magnetic fields.

The method is based upon the optical bleaching of N,N-dimethyl-4-nitrosoaniline (RNO) at 440 nm caused by a product of the reaction of  $\text{O}_2$  with imidazole (Im),  $\text{ImO}_2$ , as shown in the following reactions.



This method was introduced by Kraljic and Mohsni (1978), and is widely used in chemistry, material research, pharmacology and biology (Umemura et al., 1992; Gomes et al., 2001; Ramu et al., 2001; Inbaraj et al., 2002; Fiori et al., 2003). Because of its high sensitivity, this detection method has been used before to detect singlet oxygen generation in thylakoids (Xu et al., 2000) and other photosynthetic complexes (Telfer et al., 1994; Chakraborty & Tripathy, 1992).

## Materials and Methods

### *Samples preparation*

Reaction centers of *Rb. sphaeroides* R26 were isolated and quinone-depleted as in the previous section. Rose Bengal (RB), N,N-dimethyl-4-nitrosoaniline (RNO), and imidazole, were purchased from Aldrich.

### *Optical Detection*

The sample was placed in a quartz cuvette and was illuminated by continuous white light from a tungsten lamp. A 10 cm water filter combined with a heat filter was used to prevent sample heating. The reaction mixture (1.6 ml) contained 60  $\mu\text{M}$  RNO, 800  $\mu\text{M}$  imidazole and 1  $\mu\text{M}$  photosensitizer (RB and/or RCs). All agents were

dissolved in 50 mM TL buffer (50 mM Tris, 0.1% LDAO, 1mM EDTA, with pH 8.0). The irradiation was generally carried out in an open cuvette in equilibrium with the air.

A magnetic field up to 1.3 T was provided by a Varian E-9 X-band EPR magnet. The strength of the magnetic field was measured by a Gaussmeter Probe (Applied Magnetics Laboratory) with a resolution of 0.1 mT. At 1.3 T, the temperature increase of the sample was less than 1 °C and was ignored.

Absorption spectra before and after illumination were recorded on a Shimadzu UV-Vis spectrometer. All measurements were performed at room temperature.

## Results

In these measurements, imidazole was used as a singlet oxygen trap. No damage was observed when 800  $\mu$ M imidazole was added to *Rb. sphaeroides* R26 RCs and was kept in the dark for 1.5 hours (data not shown). The absorption spectrum of RCs containing 800  $\mu$ M imidazole and 60  $\mu$ M RNO is shown in Figure 1A. Photosensitized bleaching of RNO by RCs in the presence of imidazole is shown in Figure 1B.

The bleaching of the RNO absorbance measured at 440 nm in the Q-depleted RCs as a function of irradiation time is shown in Figure 2. The RNO bleaching photosensitized by Rose Bengal (RB) is for comparison.

The rate of bleaching of the RNO absorbance at 440 nm for various photosensitizers can be compared by correcting for the molar absorption and incident light-intensity. The rate of bleaching of RNO obeys the following equation as  $ImO_2$  is a reaction intermediate:

$$-\frac{d[RNO]}{dt} = -\frac{d[Im]}{dt} = (I_{ab}\phi_{\Delta}) * \frac{k_r [Im]}{k_d} \quad (1)$$

where  $k_r$  is the rate constant for quenching of singlet oxygen by Im,  $k_d$  the overall rate constant for deactivation of singlet oxygen by Im as well as solvent and other quenchers, and  $I_{ab}$  is the excitation rate of the photosensitizer and  $\phi_{\Delta}$  its quantum yield of singlet oxygen production. Therefore, under identical measuring condition and when the changes of Im are small compared to the initial concentration of Im, the singlet oxygen yield of photosensitizer can be determined from the ratio of the slopes with



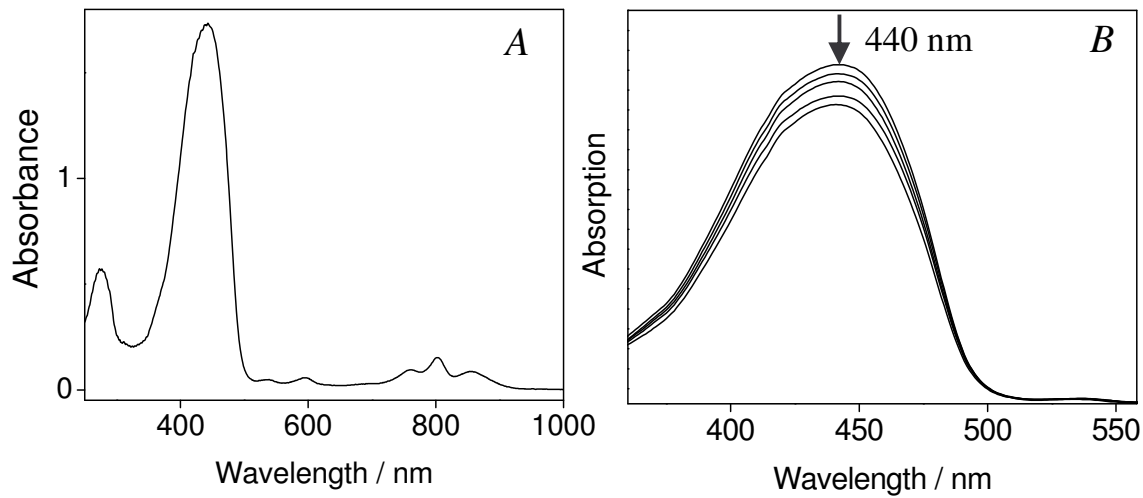


**Figure 1.**

A. Absorption spectrum of *Q*-depleted *Rb. sphaeroides* R26 RCs (1  $\mu\text{M}$ ) in the presence of RNO (60  $\mu\text{M}$ ) and 800  $\mu\text{M}$  imidazole. B. Absorption spectra of RNO (60  $\mu\text{M}$ ) in the presence of imidazole (800  $\mu\text{M}$ ) in 50 mM TL buffer measured during the photosensitizing reaction with *Q*-depleted *Rb. sphaeroides* R26 RCs (1  $\mu\text{M}$ ) at 3-min intervals.

respect to a reference photosensitizer with known singlet oxygen yield such as RB. Assuming the quenching constant of singlet oxygen by Im is equal when different photosensitizers are used (details will be discussed later on), the quantum yield of singlet oxygen from *Q*-depleted *Rb. sphaeroides* R26 RCs was calculated as follows:

$$\Phi_{\Delta}^{\text{RCs}} = \Phi_{\Delta}^{\text{RB}} \times \frac{I_{ab}^{\text{RB}}}{I_{ab}^{\text{RCs}}} \times r \quad (2)$$

where  $\Phi_{\Delta}^{\text{RB}}$  is the singlet oxygen quantum yield of the standard, Rose Bengal (0.76) in this work.  $I_{ab}$  is the absorbed quanta by the RCs and the standard, respectively, which were used at the same concentration.  $r$  is the ratio of the slopes of RNO bleaching for RCs and for RB, respectively. Taking into account the emission spectrum of the lamp and the absorption characteristics of RB and RCs, an upper limit of 1% is calculated for quantum yield of singlet-oxygen in RCs. This value is much lower than what was

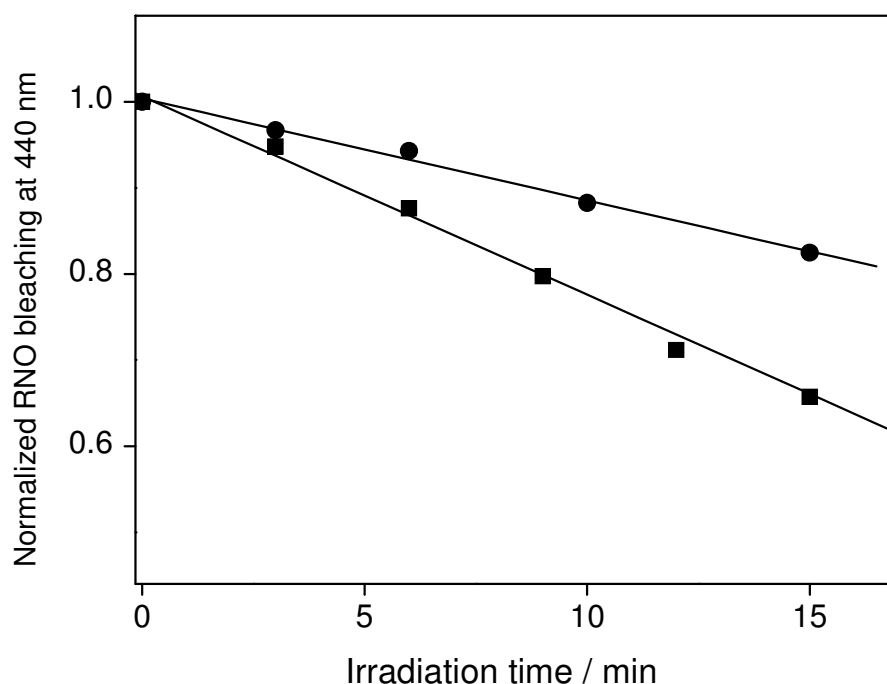


**Figure 2.**

Photosensitized RNO (60  $\mu\text{M}$ ) bleaching measured at 440 nm in the presence of imidazole (800  $\mu\text{M}$ ) in 50 mM TL buffer with 1  $\mu\text{M}$  RB (■) and 1  $\mu\text{M}$  Q-depleted Rb. *sphaeroides* R26 RCs (●).

obtained in direct luminescence detection (9%, Chapter 2.1) and indicates that singlet oxygen quenching by RC components was an order of magnitude faster than that by Im, which is not surprising since the  $^1O_2$  is produced inside the RC.

The bleaching of RNO is presumably caused by the reaction with the transannular peroxide intermediate that is formed as a result of a reaction between singlet oxygen and imidazole. To confirm the involvement of singlet oxygen, RNO bleaching assays were performed in the presence of the specific singlet oxygen quencher sodium azide, which reacts with singlet oxygen about 100 times faster than imidazole (Wilkinson & Brummer, 1981). When 8  $\mu\text{M}$  sodium azide was added, in the presence of 800  $\mu\text{M}$  imidazole, the rate of RNO bleaching by Q-depleted RCs was decreased by 60%, Fig. 3).

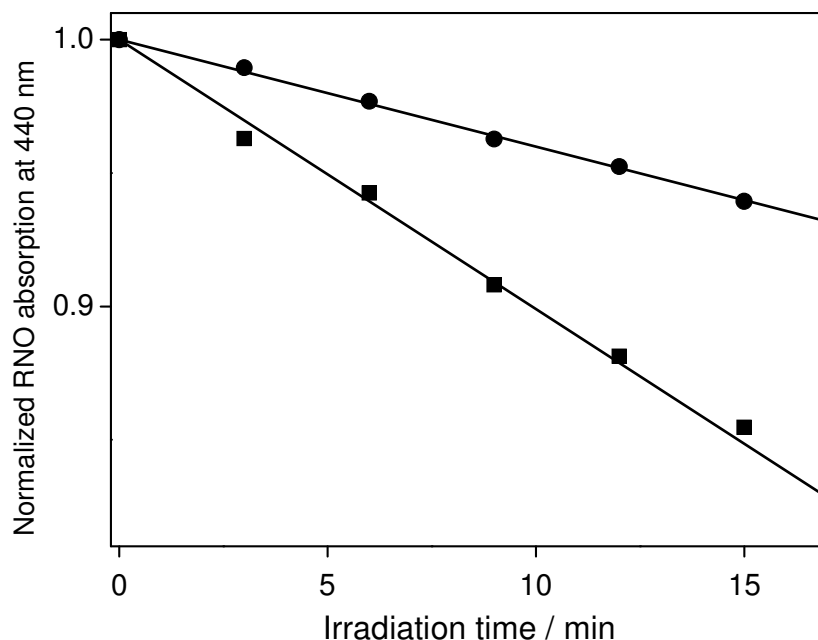


**Figure 3.**

*RNO (60  $\mu\text{M}$ ) bleaching measured at 440 nm by Q-depleted *Rb. sphaeroides* R26 RCs (1  $\mu\text{M}$ ) in the absence (■) and presence (●) of sodium azide (8  $\mu\text{M}$ ) as a function of irradiation time.*

It has been reported that RNO cannot only bleach in the presence of singlet oxygen but also in the presence of  $\cdot\text{OH}$  (Min, 2002; Min & Boff, 2002). The contribution of OH radicals in the RNO bleaching could be minimized by using metal chelates such as EDTA and specific hydroxyl radical scavenger such as ethanol (Peiser et al., 1982). The TL buffer contains EDTA and hence the effect of 5% ethanol on RNO bleaching at 440 nm was conducted and the results are shown in Figure 4. Addition of ethanol had only a minor effect on the slope of the RNO bleaching.

Figure 5 shows RNO photo-bleaching by Q-depleted *Rb. sphaeroides* R26 RCs in the presence of imidazole, in magnetic fields, with strengths ranging from 0 to 1.3 T, as a function of irradiation time. As described above, the slopes of RNO photo-bleaching are proportional to the singlet oxygen yields under these conditions.

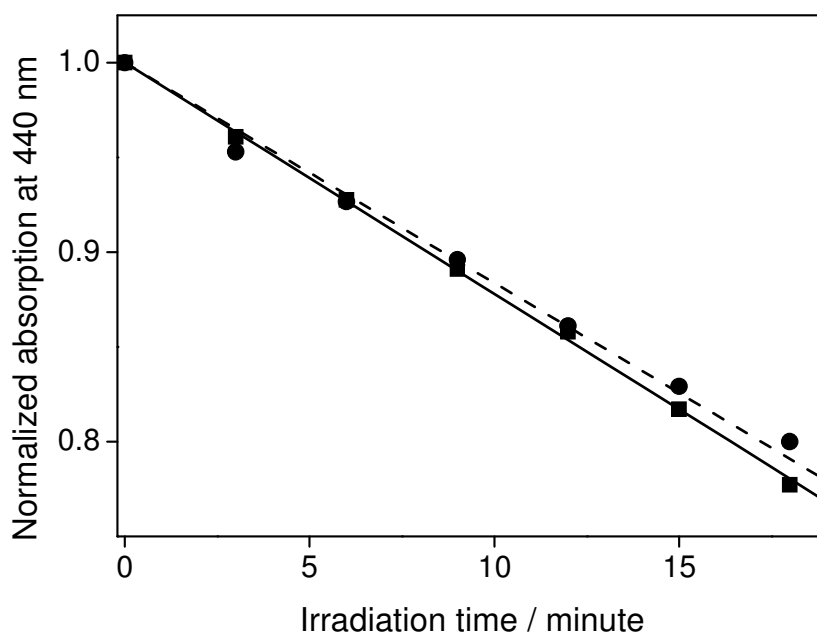


**Figure 4.**

Photosensitized RNO ( $60 \mu\text{M}$ ) bleaching measured at 440 nm by Q-depleted *Rb. sphaeroides* R26 RCs ( $1 \mu\text{M}$ ) in the absence (—) and presence (---) of 5% ethanol as a function of irradiation time.

The singlet oxygen yields were calculated by using the RB standard and plotted as function of magnetic field strengths in Fig. 6. For comparison, the magnetic field effect on the triplet yield in Q-depleted *Rb. sphaeroides* R26 RCs reported by Chidsey et al. (1985) is also shown (open circles). A clear magnetic field effect on the singlet oxygen yield by photoexcitation of Q-depleted *Rb. sphaeroides* R26 RCs is observed, which amounts to about half inhibition in the range of 20 to 900 mT, similar to the results found in Chapter 2.1. The field strength needed to change the yield by one half of the maximum change,  $B_{1/2}$ , is  $5.2 \pm 0.5$  mT, is slightly different from the  $B_{1/2}$ -values found in Chapter 2.1 (3.9 mT) and from the yield of  $^3\text{P}$  (4.2 mT and 5.7 mT) (Chidsey et al., 1985; Vidal et al., 1986). However, the magnetic effect on the RNO bleaching is clearly decreased at a field strength above 1T in agreement with the triplet yield measurements of Chidsey et al.(1985). Together with the results described in Chapter 2.1, these measurements convincingly demonstrate the involvement of the RPM in the magnetic field effect on singlet oxygen production.

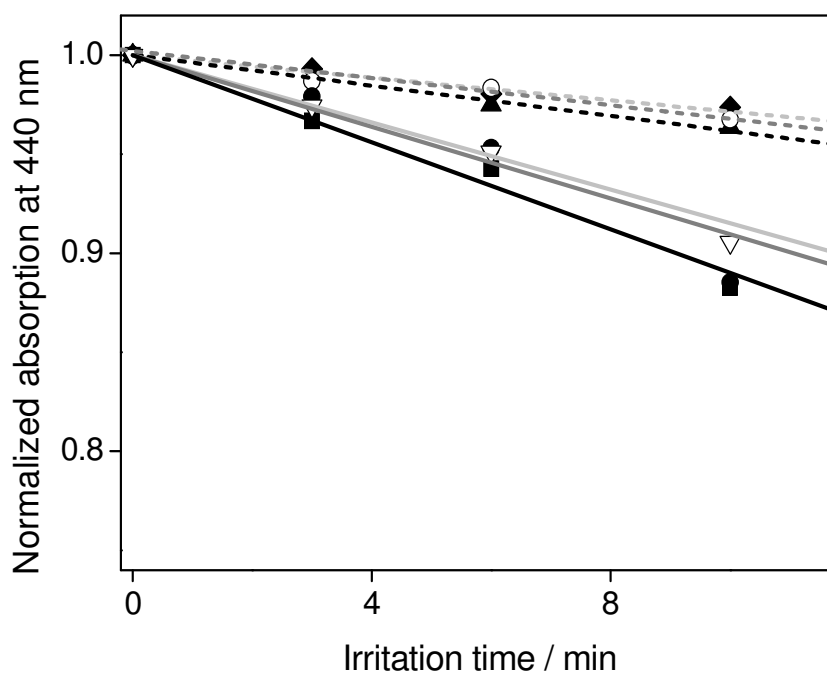


**Figure 5.**

*Photosensitized RNO (60  $\mu\text{M}$ ) bleach by Q-depleted Rb. sphaeroides R26 RCs (1  $\mu\text{M}$ ) at different magnetic fields: zero-field (■, black solid line), 2.5 mT (●, grey solid line), 20 mT (▲, black dashed line), 120 mT (◆, grey dashed line), 932 mT (○, light-grey dashed line), 1.3 T (▽, light-grey solid line).*

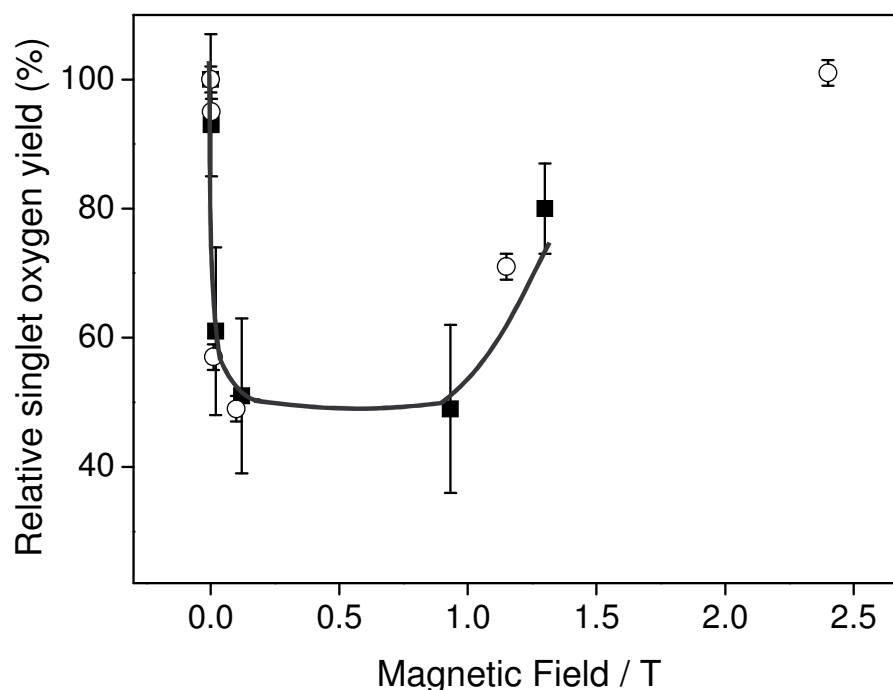


**Figure 6.**

Singlet oxygen yields from *Q*-depleted *Rb. sphaeroides* R26 RCs, normalized at zero magnetic field, as a function of magnetic field strengths (■); triplet yield (○) from *Q*-depleted *Rb. sphaeroides* R26 RCs versus magnetic field was taken from Chidsey *et al.* (1985). The values and error bars for RNO-bleaching were obtained from four independent measurements. The solid line is a guide to the eye. The drawn line needs to be redone, especially at low fields.

## Discussion

### *Singlet oxygen yield*

As shown in Chapter 2.1, a 9% quantum yield of singlet oxygen was found using the time-resolved luminescence measurement. Here a much lower singlet oxygen quantum yield of 1% was obtained by optical RNO-bleaching measurement, using the photosensitizer RB as a standard. This difference can be explained by the different detection methods. With the time-resolved luminescence method, the specific luminescence emitted by singlet oxygen is detected, regardless of its location. By the

chemical trapping method used here, however, the singlet oxygen produced in the hydrophobic core of the RC is likely to react with RC components before it diffuses out of the RC and can react with imidazole.

### ***High magnetic field effect***

The effect of low magnetic fields effect on the singlet oxygen production has been discussed in Chapter 2.1. According to the RPM, the mixing-frequency,  $\omega$ , linearly increases at high magnetic fields because the  $\Delta g$  term dominates. It leads to an increased triplet yields when  $\omega$  is slower than the recombination rate  $k_T$  (for details, see Scheme 1 in Chapter 2.1). At very high magnetic fields, when  $\omega$  much exceeds  $k_T$ , the triplet yield will become magnetic field independent and approach a limit value of  $k_T/(k_S + k_T)$ , which may be even higher than the triplet yield at zero field (Boxer et al., 1982). In this work, a substantial decrease of the magnetic field effect on singlet oxygen production has been observed at magnetic fields above 1 T, as illustrated in Figure 6, which is characteristic for the RPM.

### ***EPR spin-trapping***

In addition to the RNO detection method, we have also explored the method of EPR spin trapping as a means for detection of singlet oxygen. This method has been frequently used in the past to detect singlet oxygen in photosynthetic materials (Hideg et al., 1994a; 1994b; Spetea et al., 1997; Krieger et al., 1998; Fufezan et al., 2002; Tandori et al., 2002) exposed to light.

Singlet oxygen, which is a strong electrophile, can oxidize sterically hindered amines, like 2,2,6,6-tetramethyl-piperidine (TEMP), to nitroxyl (N-oxyl) radicals, which are detectable by EPR (Lion et al., 1976; 1980). However, Moan & Wold (1979) have studied the radical formation by reaction with singlet oxygen for TEMP and several other sterically hindered amines for different pH values. TEMP was found to trap singlet oxygen only under extreme alkaline conditions, e.g.  $\text{pH} \geq 11$ . We have found that such extreme alkaline conditions cause severe damage to *Rb. sphaeroides* R26 RCs, as shown in Fig. 7.

Under high pH conditions ( $\text{pH} = 11$ ) and an incubation time of 2 hours, the absorption bands of the RCs at 860 and 800 nm, belonging to P and B, respectively, are

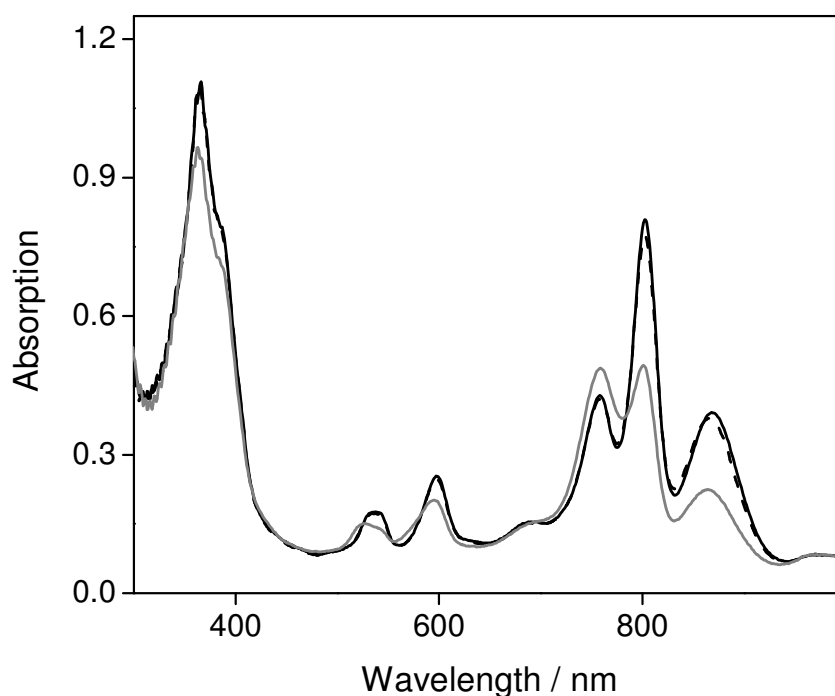


**Figure 7.**

*Absorption spectra of Q-depleted Rb. sphaeroides R26 RCs at different pH values: initial absorption spectrum (—, black) of Q-depleted Rb. sphaeroides R26 RCs; absorption spectrum (---) of Q-depleted Rb. sphaeroides R26 RCs incubated at pH 8.0 for 2 hours; absorption spectrum (—, grey) of Q-depleted Rb. sphaeroides R26 RCs incubated at pH 11.0 for 2 hours.*

reduced, and around 680 nm the absorption is increased. These changes in the absorption spectrum are indicative of disruption of the interactions between the chromophores and of changes in the reaction center structure. Based on our observations, TEMP is not a suitable spin-trap to detect singlet oxygen in these biological systems.

Surprisingly TEMP is frequently used as a spin-trap in the study of photosynthetic materials. Hideg (Hideg et al., 1994a) have used TEMP (10mM) to study  $^1O_2$  formation during photoinhibition in thylakoid membranes from spinach at pH = 7.5 (HEPES 40 mM) and concluded that  $^1O_2$  was generated from the donor triplet state and that D1 damage and the generation of  $^1O_2$  are related. In related work Hideg et al (1994b) demonstrated with the use of TEMP that singlet oxygen formation in



thylakoids membranes from spinach (in 40 mM HEPES, pH 7.5) during photoinhibition is related to acceptor-side damage. Spetea et al. (1997) concluded from spin trapping experiments with TEMP (10 mM) that singlet oxygen formation in the same thylakoids was dependent on pH (7.0 - 4.0) and was less at low pH. Krieger et al. (1998) applied TEMP (10 mM) to measure singlet oxygen production in PS II-enriched membrane fragments from spinach under photoinhibition (80 mM MES pH = 6.5) and found that the  $^1\text{O}_2$  formation was unexpectedly low in  $\text{Cl}^-$ -depleted PS II. Fufezan et al. (2002) applied TEMP (10 mM) to investigate singlet oxygen production in herbicide-treated PS II enriched membrane fragments (50 mM MES pH = 6.5) and found that singlet oxygen production was less in DCMU than in Bromoxynil treated samples. Tandori et al. (2002) used TEMP (10 mM) to measure light-induced  $^1\text{O}_2$  production in RCs from *Rhodobacter sphaeroides* wt and the carotenoidless mutant R26 (10 mM Tris pH = 8). They found that the R26 mutant was less stable under strong illumination than the wt RCs and that it was related to singlet oxygen formation. Our results and the work of Moan & Wold (Moan & Wold, 1979) would discredit the validity of these investigations: either they have been conducted at very high pH, where the photosystems are not stable, or at pH values where TEMP is a very inefficient singlet oxygen trap.

## Conclusions

These results both in low magnetic fields and high magnetic fields clearly demonstrate the involvement of the RPM in singlet oxygen production in R26 RCs. In addition, our failed experiments with the spin-trap TEMP question previously obtained results with TEMP.

## References

- Arnoux B., Gaucher J.F., Ducruix A., Reiss-Husson F. 1995, Structure of the photochemical reaction center of a spheroidene-containing purple-bacterium, *Rhodobacter sphaeroides* Y, at 3 Å resolution, *Acta. Cryst. D* 51: 368–379.
- Boxer S.G., Chidsey C.E.D., Roelofs M.G., 1982, Use of Large Magnetic Fields To Probe Photoinduced Electron-Transfer Reactions: An Example from Photosynthetic Reaction Centers, *J. Am. Chem. Soc.* 104: 1452–1454.
- Chakraborty N., Tripathy B.C. 1992, Involvement of singlet oxygen in 5-aminolevulinic acid-induced photodynamic damage of cucumber (*cucumis sativus* L) chloroplasts, *Plant Physiol.* 98: 7–11.
- Chidsey C.E.D., Takiff L., Goldstein R.A., Boxer S.G. 1985, Effect of magnetic-fields on the triplet-state lifetime in photosynthetic reaction centers – evidence for thermal repopulation of the initial radical pair, *Proc. Natl. Acad. Sci. USA* 82: 6850–6854.
- Gomes A.J., Lunardi C.N., Gonzalez S., Tedesco A.C. 2001, The antioxidant action of *Polypodium leucotomos* extract and kojic acid: reactions with reactive oxygen species. *Braz. J. Med. Biol. Res.* 34: 1487–1494.
- Fiori J., Ballardini R., Hrelia P., Andrisano V., Tarozzi A., Cavrini V. 2003, Investigation of the photochemical properties and in vitro phototoxic potential of bumetanide, *Photochem. Photobiol. Sci.* 2: 1011–1017.
- Fufezan C., Rutherford A.W., Krieger-Liszkay A. 2002, Singlet oxygen production in herbicide-treated photosystem II. *FEBS Lett.* 532: 407–410.
- Hideg E., Spetea C., Vass I. 1994a, Singlet oxygen production in thylakoid membranes during photoinhibition as detected by EPR spectroscopy, *Photosynth. Res.* 39: 191–199.
- Hideg E., Spetea C., Vass I. 1994b, Singlet oxygen and free-radical production during acceptor induced and donor-side induced photoinhibition – studies with spin-trapping EPR spectroscopy, *Biochim. Biophys. Acta* 1186: 143–152.
- Inbaraj J.J., Bilski P., Chignell C.F. 2002, Photophysical and photochemical studies of 2-phenylbenzimidazole and UVB sunscreen 2-phenylbenzimidazole-5-sulfonic acid. *Photochem. Photobiol.* 75: 107–116.
- Kraljic I. Mohsni S.E. 1978, A new method for the detection of singlet oxygen in aqueous solutions, *Photochem. Photobiol.* 28: 577–581.
- Krieger A., Rutherford A.W., Vass I., Hideg E. 1998, Relationship between activity, D1 loss, and Mn binding in photoinhibition of photosystem II. *Biochemistry* 37: 16262–16269.

- Lion Y., Delmelle M., van der Vorst A., 1976, New method of detecting singlet oxygen production, *Nature*, 263: 442–443.
- Lion Y., Gandin E., van der Vorst A., 1980, On the production of nitroxide radicals by singlet oxygen reaction – an EPR study, *Photochem. Photobiol.* 31: 305–309.
- Min D. B. Boff J., 2002, Singlet Oxygen Oxidation of Foods, *Comprehensive Reviews on Food Science and Safety*. 58–72.
- Min D.B. 2002, Chemistry of Singlet and Triplet Oxygen Oxidation in Foods, *Food Science and Industry*, 35: 57–63.
- Moan J., Wold E. 1979, Detection of singlet oxygen production by ESR, *Nature*, 279: 450-451.
- Peiser G.D., Lizada M.C.C., Yang S.F. 1982, Sulfite-induced lipid peroxidation in chloroplasts determined by ethane production, *Plant Physiol.* 70: 994–998.
- Ramu A., Mehta M.M., Leaseburg T., Aleksic A. 2001, The enhancement of riboflavin-mediated photo-oxidation of doxorubicin by histidine and urocanic acid, *Cancer Chemother. Pharmacol.* 47: 338–346.
- Spetea C., Hideg E., Vass I. 1997, Low pH accelerates light-induced damage of photosystem II by enhancing the probability of the donor-side mechanism of photoinhibition. *Biochim. Biophys. Acta* 1318: 275–283.
- Tandori J., Hideg E., Nagy L., Maroti P., Vass I. 2001, Photoinhibition of carotenoidless reaction centers from *Rhodobacter sphaeroides* by visible light. Effects on protein structure and electron transport, *Photosynth. Res.* 70: 175–184.
- Telfer A., Bishop S.M., Phillips D., Barber J. 1994, Isolated photosynthetic reaction center of photosystem II as a sensitizer for the formation of singlet oxygen, *J. Biol. Chem.* 269: 13244–13253.
- Umemura S., Kawabata K., Yumita N., Nishigaki R., Umemura K. 1992, Sonodynamic approach to tumor treatment, *Ultrasonics Symp. Proc.* 2: 1231–1240.
- Vidal M.H., Setif P., Mathis P. 1986, Influence of magnetic-fields of the P870 triplet-state in *Rps. sphaeroides* reaction centers, *Photosynth. Res.* 10: 347–354.
- Wilkinson F., Brummer J.G. 1981. Rate constants for the decay and reactions of the lowest electronically excited singlet state of molecular oxygen in solution, *J. Phys. Chem. Ref. Data.* 10: 809–1000.
- Xu Z.F., Luo G.H., Wang A.G., Chen Y.Z. 2000, Detection of singlet oxygen by the bleaching of RNO in thylakoids, *Prog. Biochem. Biophys.* 27: 78–81.

# 3

**Frequency-Modulated  
Absorbance Detected  
Magnetic Resonance  
study on light-treated  
*Rhodobacter  
sphaeroides* R26  
Reaction Centers**

## Summary

An absorption band at 860 nm belonging to the bacteriochlorophyll dimer in *Rhodobacter sphaeroides* R26 reaction centers (RCs) exhibits a blue shift towards 850 nm upon short-term light treatment. The light-minus-dark differential spectra of the short-term light treated R26 RCs, which were performed at room temperature and liquid helium temperature, respectively, showed similar features as of untreated samples. Frequency-Modulated Absorption Detected Magnetic Resonance (FM-ADMR) of light treated R26 RCs was performed at 2 K, in which the same zero-field splitting parameters were obtained as for the untreated samples. The FM-ADMR detected Triplet-minus-Singlet spectra of light-treated R26 RCs showed similar features as control samples and no contribution from the 850 nm band was found when monitored at the  $|D| \pm |E|$  frequency of untreated R26 RCs, which indicated that the 850 nm band did not produce the same triplet as the untreated sample. Moreover the FM-ADMR spectrum of light-treated RCs when monitoring at 850 nm did not reveal a different triplet. We conclude that the shifted 850 nm absorption band must be attributed to a modified form of the RC, which does not contribute to charge separation and does not produce a triplet under light.

## Introduction

### *Light effect on Rhodobacter sphaeroides R26 reaction centers*

The absorption spectrum of RCs from *Rhodobacter (Rb.) sphaeroides* R26 shows at room temperature a specific band at 860 nm, which is associated with the  $P \rightarrow P^*$  transition of the primary donor. When excess light is applied to quinone-depleted or chemically reduced R26 RCs this band bleaches. The photobleaching of this band was suggested to be the result of photodamage by singlet oxygen generated by the donor triplet state,  $^3P$ , as suggested by Tandori (Tandori et al., 2001). In the previous chapter (Ch. 2) we have demonstrated the involvement of singlet oxygen and observed the photodegradation after prolonged illumination (Liu et al., 2005). The photobleaching caused a reduction of the absorption peaks at 760, 800 and

860 nm. Surprisingly, the photobleaching at 860 nm was accompanied by a band shift to 850 nm. In the following section we have further investigated the characteristic of this band shift, and its influence on the functioning of the RC, using low-temperature absorption spectroscopy, absorption difference spectroscopy and frequency-modulated absorbance detected magnetic resonance (FM-ADMR).

## **Materials and Methods**

### ***Sample preparation***

Reaction centers were isolated from the carotenoidless mutant R26 of *Rb. sphaeroides* with the use of lauryldimethylamine oxide (LDAO). Quinones were removed with 10 mM o-phenanthroline and 4% LDAO as described in the literature (Feher & Okamura, 1978). After concentrating to about 100  $\mu$ M RCs in TL buffer (10 mM Tris/HCl buffer, 1 mM EDTA, 0.1% LDAO, pH 8.0), using a 100 kD Amicon filter, the Q-depleted *Rb. sphaeroides* R26 RCs were stored at  $-18^{\circ}\text{C}$  for further study. For low temperature measurements, the sample was diluted with 67% glycerol to ensure formation of a clear glass, and the optical density (OD) was adjusted to about 0.35/2 mm at 800 nm.

### ***Light-treated sample preparation***

To induce photobleaching, the RCs were diluted to about 4  $\mu$ M in TL buffer and exposed to light from a tungsten lamp, with an intensity of about 20 mW/cm<sup>2</sup> for 5 minutes, a 10 cm water column was used as a heat filter. This sample will be designated as light-treated RCs. After illumination, the RCs were concentrated to about 0.35/2 mm at 800nm. Untreated samples follow the same procedure with the omission of the light treatment.

Quinone reconstitution was done by incubating the RCs in a solution containing a 50-fold excess of ubiquinone-10 (Okamura et al., 1975).

### ***Light-minus-dark differential spectra measurement***

Absorption spectra were measured in a Shimadzu UV-visible photo spectrophotometer (Shimadzu UV-160A). For the light-minus-dark differential spectra

at room temperature, the quinone-reconstituted sample was excited inside the Shimadzu spectrometer by actinic light from a tungsten lamp filtered by a 5 cm water and a CS4-96 cut-off filter. The reference sample contained RCs of the same concentration and was shielded from the actinic light.

Low temperature absorption and absorption difference measurements were done by placing the sample into the liquid helium cryostat used for ADMR spectroscopy. The light-minus-dark absorption difference spectrum at 2 K was obtained by subtracting the dark spectrum from the light spectrum, which was obtained by illuminating the sample by actinic light filtered by CS4-96 cut-off filter and water filter.

### ***ADMR technique***

#### *Effect of microwave power on triplet population*

Even in the absence of a magnetic field, the three energy levels of a triplet state are not degenerate with their relative energies separated by the so-called zero-field splitting parameters D and E. Each of three triplet states has its own population rate,  $p_i$  and decay rate,  $k_i$ , which are determined by the structure of the molecule and the triplet population mechanism. Then, assuming that the ground-state population is much larger than the triplet state population, the steady-state concentration of a triplet sublevel  $i$ ,  $[T_i]$ , is proportional to the ratio of the sublevel population rate  $p_i$  and the sublevel decay rate  $k_i$ :

$$[T_i] \propto K \frac{p_i}{k_i} \quad (1)$$

where  $K$  is the overall triplet population rate.

When a strong microwave field is applied with a frequency such that the photon energy equals the energy difference between two triplet sublevels, the microwave field is said to be resonant and the triplet sublevels are coupled by the microwave field. Thus the two coupled triplet sublevels can be treated as if they were one level and this will give rise to changes of the population probabilities and decay rates of these sublevels, and therefore the total triplet population will change in an applied microwave field (Hoff, 1996). When the microwave is off, the total concentration of two triplet sublevels  $i$  and  $j$  is:

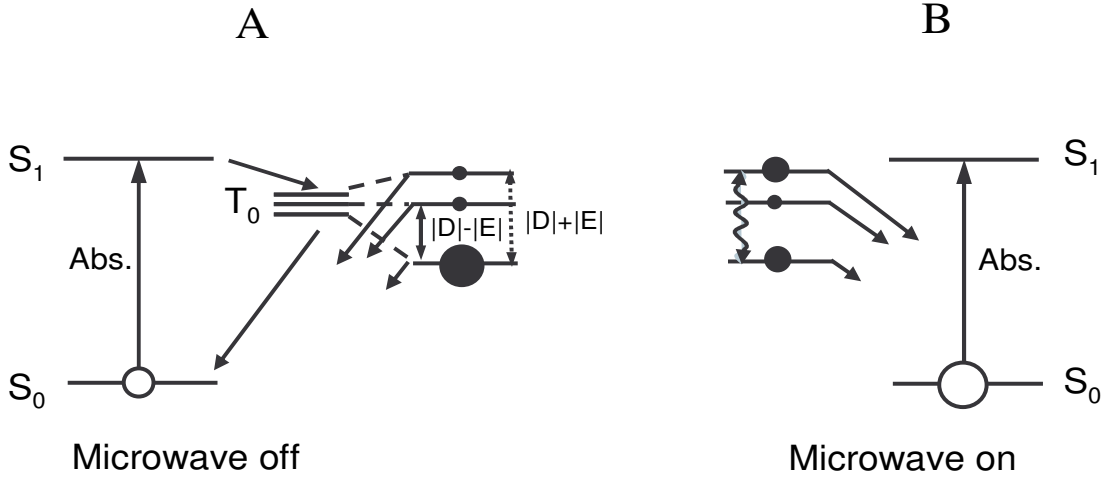


**Figure 1.**

*Principle of ADMR. Open circles denote relative equilibrium population of the singlet ground state, filled circles that of the triplet sublevels. When the microwave field is off (A), the lowest energy triplet sublevel will be predominantly populated. When a strong microwave field corresponding to the energy difference between two triplet sublevels is applied (B), it leads to a new equilibrium value of the singlet ground state population, hence to a change in the absorbance.*

$$[T_i] + [T_j] \propto K \left( \frac{p_i}{k_i} + \frac{p_j}{k_k} \right) \quad (2)$$

and when the resonant microwave field is on, the total concentration of these two sublevels is changed to be proportional to:

$$2K \left[ \frac{\frac{1}{2}(p_i + p_j)}{\frac{1}{2}(k_i + k_j)} \right] = 2K \frac{p_i + p_j}{k_i + k_j} \quad (3)$$

In general, the populating probabilities and decay rates of the three triplet sublevels are all different. Therefore, the total triplet population is changed when a microwave field is applied.

Such changes of triplet concentrations induced by microwaves can be detected



optically by a change in fluorescence, phosphorescence and/or absorption. In this work, the magnetic resonance is detected by absorbance, which has been labelled as Absorbance Detected Magnetic Resonance, ADMR (Figure 1).

### ***Normal ADMR T–S spectrum***

The most essential components of a conventional ADMR set-up are the light source, the microwave source, a cryostat and a light detector. The details of these components are described by Maki (1984) and Hoff (1989; 1990). During the measurement, the sample is continuously illuminated at super-fluid helium temperature to create steady-state conditions between the triplet excited states and the singlet ground state; the concentrations of other intermediate states can be neglected since the triplet state is the slowest decaying excited state. Therefore the total concentration of the ground state and the triplet state is constant and any changes in the triplet state population result in an equal but opposite change in that of the ground state:  $\Delta[S_0] = -\Delta[T]$ .

The absorption change induced by the microwaves in the ADMR experiment is proportional to the difference between the extinction coefficients of a molecule in the triplet and in the ground state at the detection wavelength, and to the change in population of the ground state (van der Vos, 1994):

$$\frac{\Delta I(\lambda)}{I(\lambda)} \propto (\epsilon_S(\lambda) - \epsilon_T(\lambda))\Delta[S_0] \quad (4)$$

Hence, if the optical absorption of the molecule in the triplet state is different from that in the singlet ground state, the change in triplet concentration can be detected by monitoring the change in transmittance induced by the microwave radiation. This leads to the high sensitivity of ADMR spectroscopy since the optical probing occurs with photons at much higher energy than the microwave quantum. When the optical wavelength is scanned and the microwave frequency is kept constant, the triplet-minus-singlet (T–S) spectrum can be obtained. T–S spectra of several reaction centers were studied by, e.g. den Blanken and Hoff (den Blanken & Hoff, 1982; den Blanken et al., 1984).

Two types of ADMR spectra can be obtained. In the first one, the spectrum is recorded by monitoring the absorbance at a wavelength where the singlet absorption differs from the triplet absorption, while sweeping the microwave frequency through the resonance bands of the triplet manifold. In the second type, the microwave frequency is fixed at one of the resonance bands of the triplet state, and the optical wavelength is scanned.

### ***Helix vs Loop-gap***

In the conventional ADMR technique, the sample is inserted into a helix connected to the microwave source. The advantage of a helix is that it is an almost non-resonant device and thus can be used over a large range of microwave frequencies. The disadvantage, however, is that most of the microwave energy is reflected by the helix, making microwave excitation of the sample inefficient. To overcome this problem we have used a resonant cavity, i.e. a loop-gap resonator, with the advantage of a much better coupling between the microwaves and the sample. The disadvantage of the loop gap is the in principle very limited bandwidth over which the microwave frequencies can be scanned. This problem has been circumvented in our work as follows.

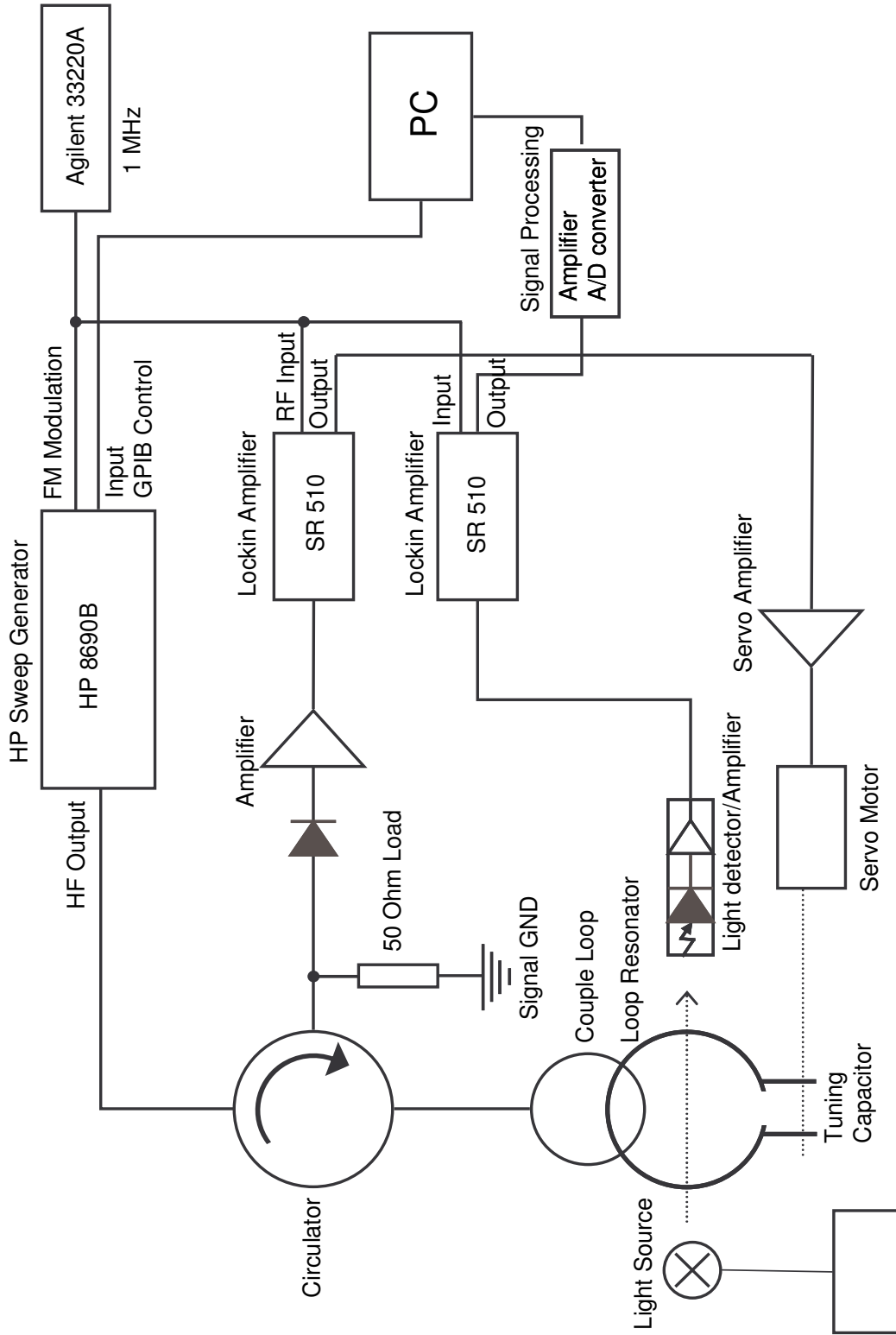
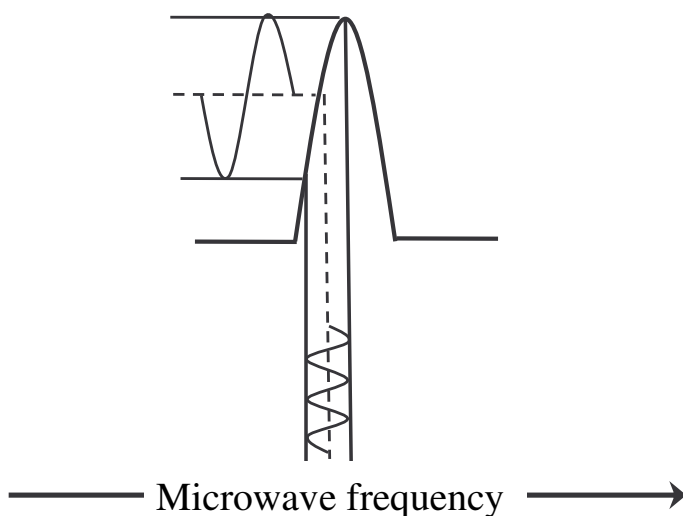


Figure 2. Schematic view of FM-ADMR set-up. For details, see the text.



**Figure 3.**

*Schematic view of the effect of frequency modulation of the microwave power on a zero field transition. The microwave frequency is modulated (vertical sine waves), which results into modulation of the detected signal (horizontal sine wave).*

The loop-gap resonator originally used by van der Vos et al.(1991) was first modified such that it could be mechanically tuned in the range of 400-900 MHz in super fluid helium at temperature of 2 K. To achieve locking of the loop-gap a servomotor was installed that controlled the distance between the two plates of the loop gap and thereby its resonant frequency. The applied microwave radiation was then frequency-modulated (FM), with a modulation depth much less than the half-width of the loop-gap resonance profile. The reflected signal from the loop-gap resonator was demodulated by a lock-in-amplifier. The output DC signal from the lock-in-amplifier was fed into an amplifier, which was connected to the servomotor. This feeds back mechanism ensured that the loop gap remained locked to the frequency (Fig. 2).

### ***FM-ADMR***

The FM-ADMR measurements were performed with a home-built set-up as shown in Figure 2. The sample was illuminated by a 250 W tungsten lamp. The light was IR-filtered by 8 cm of water-cell (8 cm path length). It was focused onto the sample by a condensor lens for continuous excitation, and also serves as the detection

beam. The transmitted light was detected at selected wavelengths via a monochromator with a photodetector placed at the exit slit.

The setup is essentially the same as described earlier (van der Vos, 1994; Meray, 2003), with the helix replaced by a loop-gap cavity. The loop-gap is locked to the microwave frequency with an accuracy of 0.2 MHz. The maximum scanning speed of the motor is 2 MHz/s. Three circulators (310-470 MHz; 400-700 MHz and 630-900 MHz) are employed in order to cover different frequency scan ranges. The microwave frequency is modulated with a minimum width of 1 MHz, via an Agilent/HP 33220A waveform generator. The microwaves are generated by a HP 8690B sweep oscillator. For demodulation two Stanford Research System SR510 lock-in amplifiers are used: one for demodulating the reflected microwaves from the loop gap and one for demodulating the signal from the photo detector. As a result of the frequency modulation of the microwave field, rather than the usual amplitude modulation, and subsequent lock-in detection, the ADMR spectra are obtained as the first derivative instead of the absorption bands (Figure 3). With this FM-ADMR technique a 2 times higher S/N was achieved. For T-S spectroscopy at a fixed microwave frequency the wavelength is scanned in steps of 1 nm. Sweeper, counter and lock-in amplifier were all interfaced by an IEEE bus and all data were acquired by computer.

## Results

The room-temperature absorption spectra of untreated and light-treated Q-depleted R26 RCs are shown in Figure 4. The most significant change in the absorption spectrum of the light-treated R26 RCs is the 10 nm shift to shorter wavelength of the 860 nm band of the primary donor P.

In these experiments, the electron acceptor  $Q_A$  was removed in order to block forward electron transport which leads to the formation of the long-lived radical pair  $P^+T^-$  and subsequent triplet formation (see details in Hoff et al., 1993). When these quinone-depleted RCs are reconstituted with ubiquinones (UQ), e.g. ubiquinone-10, as described by Okamura et al. (Okamura et al., 1975), the long-lived charge separated state  $P^+Q^-$  can be observed. The absorption changes due to  $P^+Q^-$  formation under illumination are shown in Figure 5. These light induced absorbance changes are

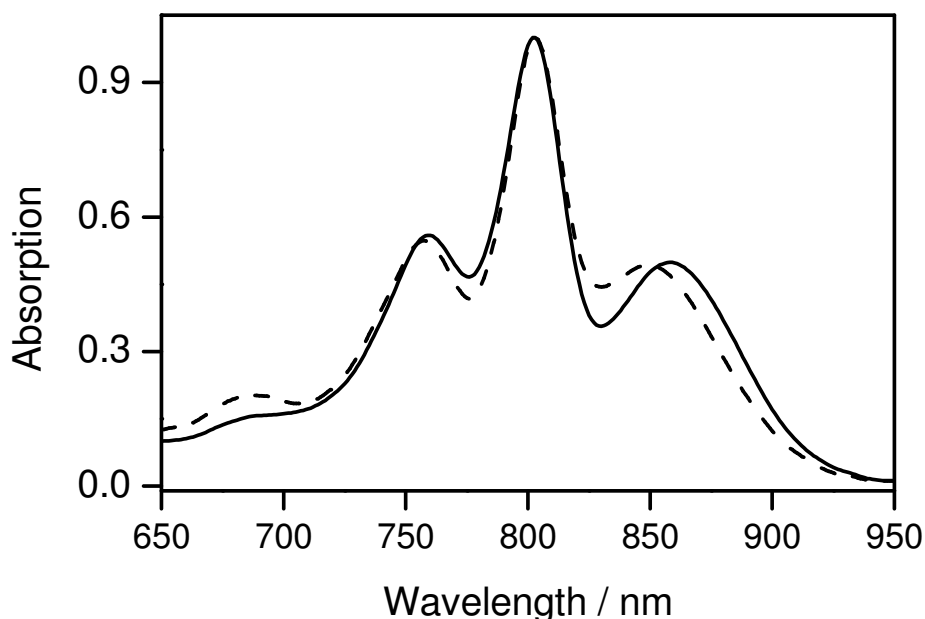


**Figure 4.**

Room-temperature absorption spectra of untreated (solid line) and light-treated R26 RCs (dashed line); spectra were normalized at 800 nm.

completely reversible within 2 min in the dark (data not shown). The bleached absorption band around 860 nm is due to the oxidation of P to P<sup>+</sup>, which is accompanied by the blue shift of the absorption band of the accessory BChls towards 796 nm. These two BChl molecules are located nearest to the dimer (Clayton, 1966). This blue shift results in a negative band centered around 800 nm and a positive band centered at 770 nm. The shift of the absorption band of Bpheo at 760 nm, which is partly obscured by the larger shift of the accessory BChls, is also linked to photo-oxidation of P. It leads to a positive band around 785 nm in the light-minus-dark differential spectrum, which is in agreement with the results described by Slooten (1972). At room temperature, the positive bands at 770 and 785 nm are not separated; see also Figure 7. Additional, but smaller changes are also present in the Soret band (data not shown).

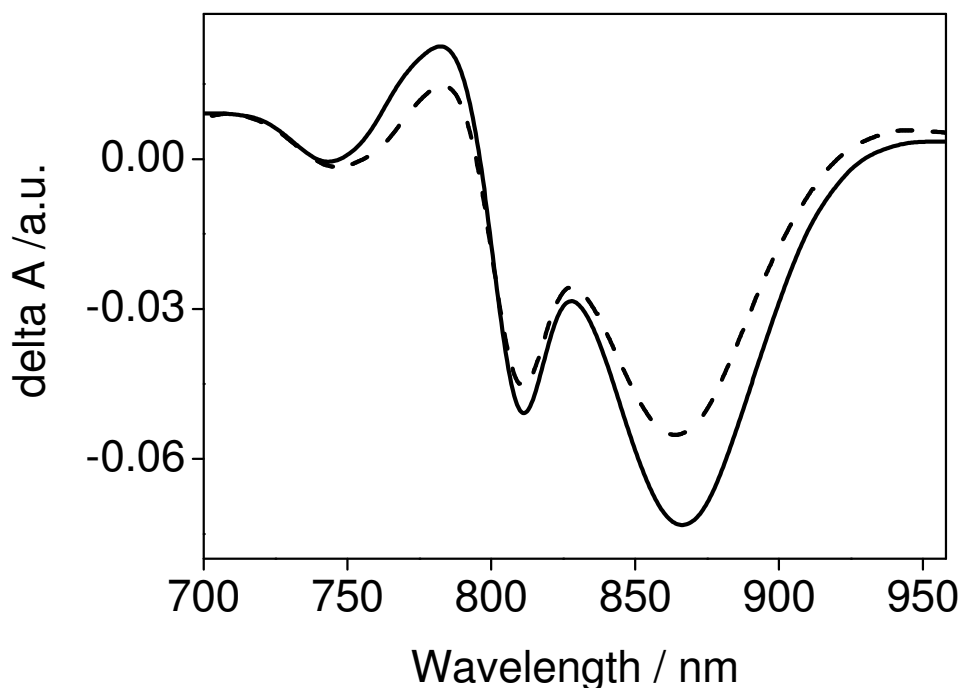


**Figure 5.**

*Room-temperature spectra of reversible light-induced absorption changes in untreated R26 RCs (solid line) and light-treated R26 RCs (dashed line). Initial concentration of samples are kept the same as described above (see “Materials and Methods”).*

The results show that the features of the light-minus-dark absorption difference spectra for the untreated and light-treated R26 RCs are almost identical. No additional signal belonging to the shifted absorption band at 850 nm was observed in the light-minus-dark absorption spectrum. However, the signal amplitude in the light-treated RCs is smaller than that in untreated RCs. This finding suggests that the absorption band shift of P (Fig. 4) might be caused by the fact that in a fraction of the RCs the absorption band at 860 nm has shifted and can be regarded as preliminary evidence that the functionality of RCs is slightly reduced due to the light treatment.

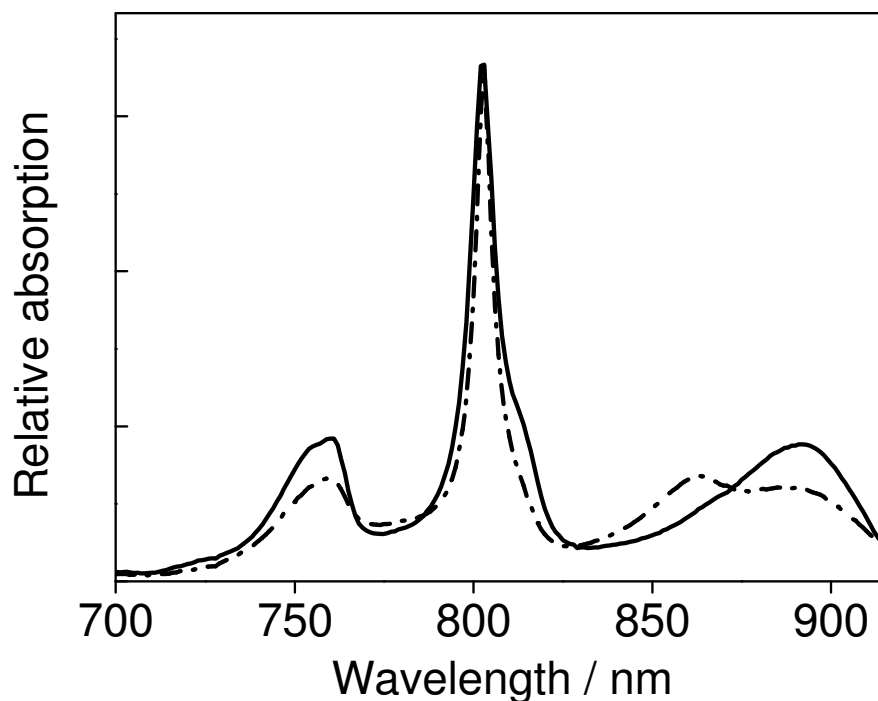


**Figure 6.**

*Absorption spectra of untreated (solid line) and light-treated R26 RCs (dash-dotted line) at 2 K. The initial concentration of both samples is identical as shown in the section of “Materials and Methods”.*

To clarify the characteristics of the light-treated R26 RCs, the absorption spectra as well as the light-minus-dark differential absorption spectra and FM-ADMR were measured at cryogenic temperature ( $\sim 2$  K), where the resolution is better because of line narrowing. Figure 6 shows the absorption spectra of untreated and light-treated R26 RCs at 2 K. The red-shifted band of the BChl dimer, P, was observed at 890 nm in both samples, which is consistent with the work published by McElroy et al. (1974). In addition, a band at 866 nm appeared in light-treated RCs accompanied with a narrower band around 802 nm. Thus it appears that the band at 850 nm seen at room temperature in light-treated RCs is split into two at low temperature, one at 866 nm and one at 890 nm.



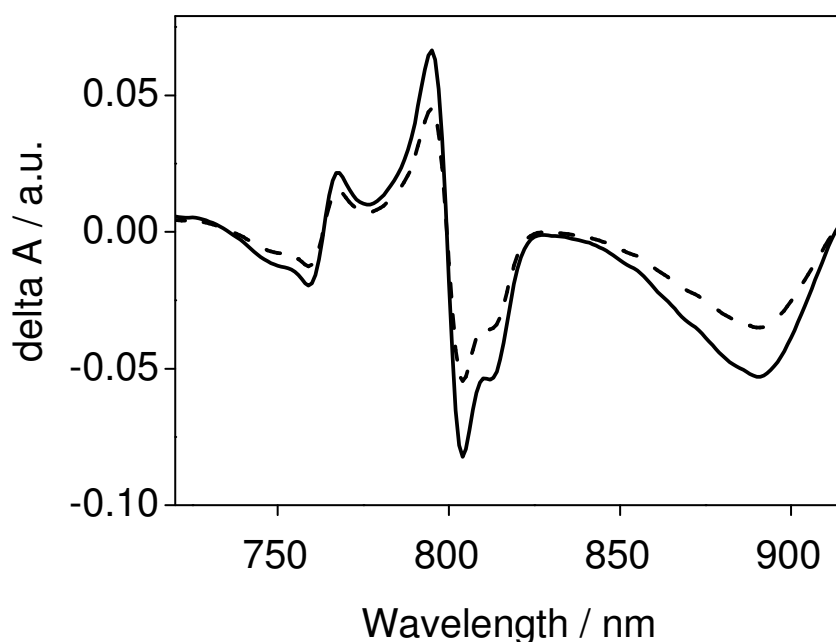


**Figure 7.**

*Spectra of reversible absorption changes induced by actinic light in the untreated Q-reconstituted R26 RCs (solid line) and the light-treated Q-reconstituted R26 RCs (dashed line) at 2 K. Initial sample concentrations were the same as described before.*

Figure 7 shows the differential spectra (light-minus-dark) of quinone reconstituted untreated and light-treated R26 RCs performed at 2K. Both exhibit the same features except that the magnitude of absorption changes is smaller in the light-treated RCs than in untreated RCs. It should be noted that no additional band at 866 nm was observed from the light-treated RCs. These findings are in agreement with the preliminary conclusion from the room temperature measurements that the 866 nm absorption band at helium temperature belongs to non-functional RCs.

The FM-ADMR spectra of untreated and light-treated RCs taken at 2 K are shown in Figure 8. Setting the detection wavelength at the peak of the primary donor absorption, 890 nm, two first-derivative signals, centered at 467 and 658 MHz are found in both light treated and untreated samples, corresponding to the  $|D|-|E|$  and

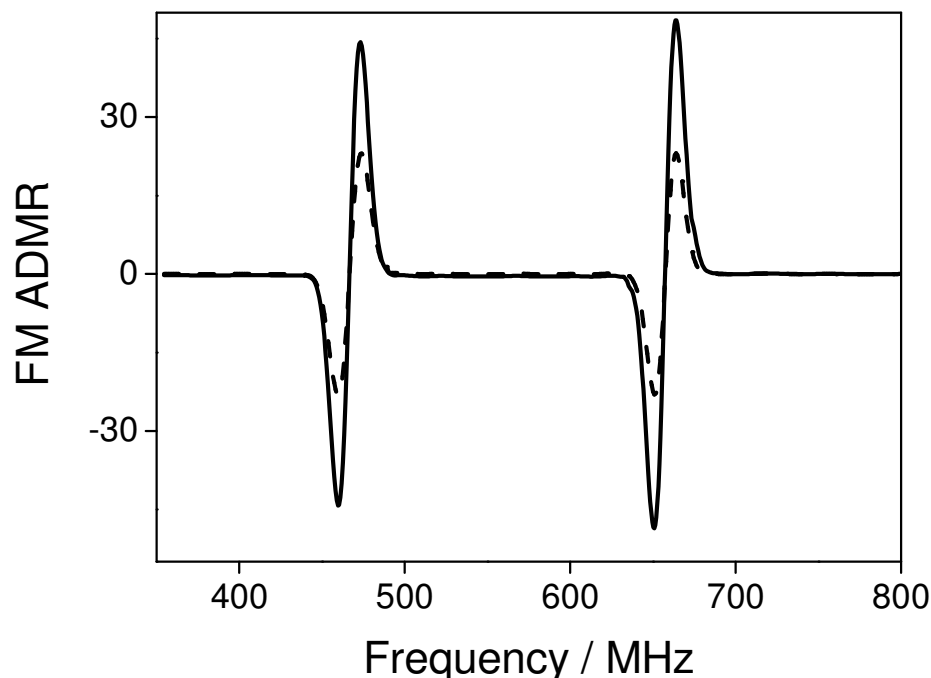


**Figure 8.**

*FM-ADMR spectra of untreated (solid line) and light-treated (dashed line) R26 RCs detected at 890 nm at 2 K with modulation amplitude of 1 MHz and scan speed of 0.61 MHz/s. Concentration of both samples were the same.*

$|D|+|E|$  transitions, respectively. No additional zero-splitting parameters are found from the light-treated sample when the microwave field was scanned from 350 to 800 MHz and monitoring at the absorption band at 890 nm.

Figure 9 shows the FM-ADMR-detected T–S spectra of both untreated and light-treated samples recorded at the same  $|D|-|E|$  frequency, 467 Hz. Both spectra show similar properties. Similar results were obtained when the T–S spectra were recorded at the  $|D|+|E|$  transition (658 nm, data not shown). Between 760 and 830 nm a number of sharp features are present. The 890 nm band shows a broad wing, representing the singlet absorption band of the primary donor, P, bleached by the formation of the triplet state,  $P^T$ . No contribution of the 866 nm band was observed in the T–S spectrum for the light-treated RCs. This fact indicates that the 866 nm band of

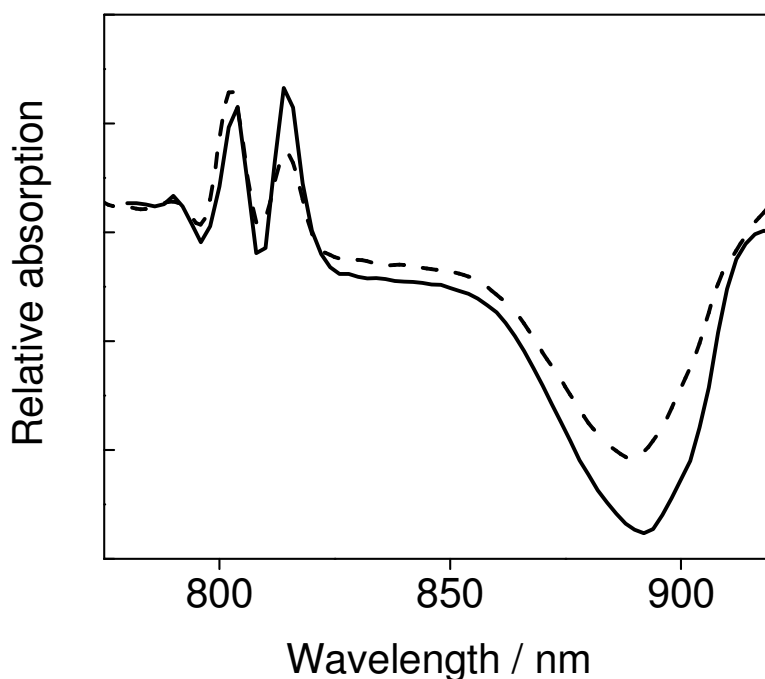


**Figure 9.**

*FM-ADMR T-S spectra of untreated R26 RCs (solid line) and light-treated R26 RCs (dashed line) are recorded at 2 K. Initial sample concentrations are the same as described above (see “Materials and Methods”).*

light-treated RCs does not produce a triplet with the same  $D$  and  $E$  values as the untreated RCs. The FM-ADMR spectrum of light treated RCs was therefore recorded with the detection wavelength set at 860 nm. The result is shown in Fig 10. Besides the previously found  $|D|-|E|$  and  $|D|+|E|$  transitions, no other triplet transition in the range of 350 to 800 MHz was detected.

## Conclusions

The low temperature absorption spectra demonstrate clearly that the RT band of the light-treated RCs at 850 nm is caused by a blue shift of the donor band in a fraction of the RCs. At 2 K this band now absorbs at 866 nm instead of 890 nm. However, the light-minus-dark differential spectra of untreated and light-treated samples show identical features both at room temperature and at 2 K. But the

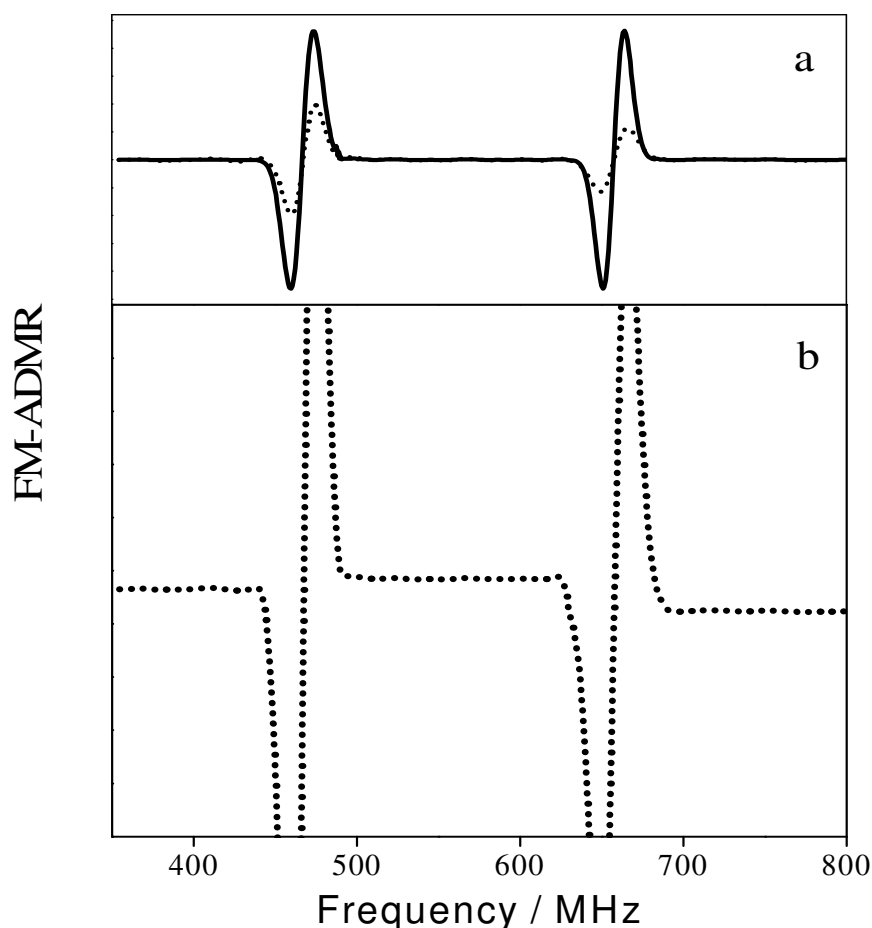


**Figure 10.**

*a) FM-ADMR spectra of light-treated R26 RCs detected at 890 nm (solid line) and 860 nm (dotted line), respectively; b) amplified FM-ADMR spectrum of light-treated R26 RCs detected at 860 nm. Experimental conditions are the same as in Figure 6.*

magnitude of the absorption changes in the light-treated sample was found smaller than in the untreated sample. This leads to the conclusion that the RCs absorbing at 866 nm do not generate any long-lived  $P^+$ .

In addition, the FM-ADMR spectra prove that the RCs absorbing at 866 nm do not produce any triplet. These findings suggest that the conformation of RC proteins is changed by light exposure. These damaged RCs are not photoactive and do not generate charge separation.

## References

- Clayton R.K. 1966, Spectroscopic analysis of bacteriochlorophylls *in vitro* and *in vivo*, *Photochem. Photobiol.* 5: 669–677.
- den Blanken H.J., Hoff A.J. 1982, High-resolution optical absorption-difference spectra of the triplet-state of the primary donor in isolated reaction centers of the photosynthetic bacteria *Rhodospseudomonas-viridis* measured with optically detected magnetic resonance at 1.2 K, *Biochim. Biophys. Acta* 681: 365–374.
- den Blanken H.J., Meiburg R.F., Hoff A.J. 1984, Polarized triplet-minus-singlet absorbance difference spectra measured by absorbance-detected magnetic resonance. An application to photosynthetic reaction centers, *Chem. Phys. Lett.* 105: 336–342.
- Feher, G., Okamura, M. Y. 1978, *The Photosynthetic Bacteria*, Clayton R. K. and Sistrun W.R. (Eds.) pp. 349.
- Hoff A.J. 1989, Optically-detected magnetic resonance of triplet states. In: *Advanced EPR. Application in biology and biochemistry*. Hoff A.J. (Ed.), Elsevier, Amsterdam, pp. 633–684.
- Hoff A.J. 1990, Triplet states in photosynthesis: linear dichronic difference spectra via magnetic resonance. In: *Physical methods in plant sciences Vol II, Modern methods in plant analysis*. Linkins H.F., Jackson J.F. (eds.). Springer-Verlag, Berlin, pp. 23–57.
- Hoff A.J. 1996, Optically Detected Magnetic Resonance (ODMR) of Triplet States in Photosynthesis. In: *Advances in Photosynthesis*. Amesz J. and Hoff A.J. (Eds.), *Biophysical Techniques in Photosynthesis, Vol 3*, Kluwer Academic Publishers, Dordrecht, pp. 277–298.
- Hoff A.J., Gast P., van der Vos R., Vrieze J., Franken E.M., Lous E.J. 1993, Magnetic-field effects – MARY, MIMS and MODS, *Z. Physik. Chem.*, 180: 175–192.
- Liu Y., Edge R., Henbest K., Timmel C.R., Hore P.J., Gast P. 2005, Magnetic field effect on singlet oxygen production in a biochemical system, *Chem. Commun.* 2: 174–176.
- Maki A.K. 1984, Techniques, theory and biological applications of optically-detected magnetic resonance (ODMR), In: *Biological magnetic resonance*. Berliner L.J. and Reuben J. (eds.), *Biological Magnetic Resonance Vol 6*, Plenum Press, New York. pp. 187–294.
- McElroy J.D., Mauzerall D.C., Feher G. 1974, Characterization of primary reactions in bacterial photosynthesis II: kinetic study of the light-induced signal ( $g=2.0026$ ) and the optical absorbance changes at cryogenic temperature. *Biochim. Biophys. Acta.* 333: 261–278.
- Meray N. 2003, Doctoral Thesis, Leiden University.
- Okamura M.Y., Isaacson R.A., Feher G. 1975, Primary acceptor in bacterial photosynthesis: obligatory role of ubiquinone in photoactive reaction centers of *Rhodospseudomonas spheroids*,

- Proc. Natl. Acad. Sci. USA. 72: 3491–3495.
- Slooten L. 1972, Electron acceptors in reaction center preparations from photosynthetic bacteria, *Biochim. Biophys. Acta* 275: 208–218.
- Tandori J., Hideg E., Nagy L., Maroti P., Vass I. 2001, Photoinhibition of carotenoidless reaction centers from *Rhodobacter sphaeroides* by visible light. Effects on protein structure and electron transport, *Photosynth. Res.* 70: 175–184.
- van der Vos R. 1994, Doctoral Thesis, Leiden University.
- van der Vos R., Carbonera D., Hoff A.J. 1991, Microwave and optical spectroscopy of carotenoid triplets in light-harvesting complex LHC II of spinach by absorbance-detected magnetic resonance, *Appl. Magn. Res.* 2: 179–202.



# 4

## **The influence of a Magnetic Field on Photoinhibition in *Synechocystis* sp. PCC 6803 cells**



## Summary

We have investigated the effects of an external magnetic field *in vivo* on the photodamage to photosystem II caused by photoinhibition in *Synechocystis* cells. Activities before and after photoinhibition were measured by detecting the oxygen production of photosystem II. The degree of photoinhibition decreased with increasing magnetic field (< 200 mT) and increased again when the magnetic field strength exceeded 200 mT. The photo-induced deactivation rate at 200 mT was found to be 30% less compared to zero magnetic field. These findings are explained within the framework of acceptor side photoinhibition with triplet state formation through recombination of the primary radical pair. The results show that a magnetic field of moderate strength can play a protective role against photodamage in these organisms and suggest that it could benefit plant growth.

## Introduction

In our previous work (Liu et al., 2005, and Chapter 2), we have shown that a magnetic field can partially protect the reaction center (RC) from purple bacteria against photodamage: about 40% less irreversible photobleaching was observed after illumination with intense light pulses in a magnetic field. The origin of this protection was the lower donor triplet state formation in a magnetic field resulting in less singlet oxygen formation and reduced photobleaching. This magnetic field effect in this type of RCs was only observed when the primary quinone acceptor  $Q_A$  was removed, and only for RCs that did not contain carotenoid. Similar effects may also occur in plant photosynthesis, either in photosystem I (PS I) and/or photosystem II (PS II). A prerequisite will be that under certain conditions singlet oxygen is produced and that this is (partly) generated through the RC donor triplet state that is formed *via* the radical pair mechanism.

As in purple bacteria, no reaction center triplet is formed during normal photosynthetic reactions in plant PS I and PS II. However, under reducing conditions, the typical AEEAAE (A = enhanced absorption, E = emission) electron spin polarized triplet spectrum has been observed by EPR in both plant PS I and II (Rutherford &

Mullet, 1981; Rutherford et al., 1981; van Mieghem et al., 1989; Vass et al., 1992a; Feikema et al., 2005). This spin polarization pattern of the triplet spectrum is characteristic for radical pair involvement in triplet state formation. Thus it may be possible that under such conditions, both in PS I and in PS II singlet oxygen is formed and that the amount is influenced by a magnetic field.

Besides strongly reducing conditions, another condition in which plants may produce singlet oxygen is during photoinhibition. Photoinhibition is the gradual loss of activity of the photosynthetic machinery when higher plants and algae are exposed to light intensities that are much higher than under normal growth condition. Such high light conditions will affect photosystem I activity by about 30% (Sonoike & Terashima, 1994), but the main factor in the light stress response in oxygenic photosynthetic organisms is PS II, the complex of proteins and pigments that oxidizes water and reduces plastoquinone during photosynthesis. The singlet oxygen that is generated in this process induces protein damage, especially by inactivation of the D1 protein. The damaged D1 protein, however, can be rapidly re-synthesized and reassembled into a new functional PS II; this is called D1 protein turnover (Ohad et al., 1984). This turnover keeps PS II active in spite of singlet oxygen damage, as long as the expression rate of the D1 protein compensates for its degradation rate. Under very high light intensities, the photodamage increases and the turnover rate of the D1 protein will not be sufficient to repair PS II. Consequently PS II is degraded and the photosynthetic process will cease. As soon as the light stress is lifted, D1 will be re-synthesized and normal photosynthesis will be restored.

Direct detection of singlet oxygen production during photoinhibition has been achieved by Macpherson et al. (1993) and Telfer et al. (1994) by monitoring its typical decay at 1270 nm. Hideg et al. (1994a; 1994b) have used EPR spin traps. Mishra et al. (1994) have studied the effects of singlet oxygen quenchers. These results give strong evidence for singlet oxygen formation under conditions of photoinhibition.

The mechanism of photoinhibition of PS II has been under debate for several decades (for reviews, see Prasil et al., 1992; Aro et al., 1993). To date two hypothetical photoinhibition mechanisms exist: the “donor side” and the “acceptor side” model (for a review, see Adir et al., 2003). Donor-side photoinhibition states that damage to PS II is caused when the high redox potential oxidant  $P_{680}^+$ , which is estimated to be 1.26 and

1.41 V (Rappaport et al., 2002), irreversibly oxidizes a pigment protein or a component of the protein backbone. This type of photodamage has a high yield when the oxygen-evolving complex is chemically destroyed (Callahan et al., 1986; Chen et al., 1992), but the oxygen-evolving complex may also fail to reduce  $P_{680}^+$  even under natural conditions. This random failure has been suggested to explain the photoinhibition *in vivo* (Anderson et al., 1998). Recently an alternative donor site mechanism was proposed (Hakala et al., 2005; Ohnishi et al., 2005). Hakala et al. (2005) demonstrated that the action spectrum of photoinhibition resembles the absorption spectrum of Mn IV of the oxygen-evolving complex, rather than that of chlorophyll. This would demonstrate that the oxygen-evolving complex is the first target in photoinhibition; after the release of a manganese ion from PS II, subsequent oxidative damage would then occur at the PS II reaction center because  $P_{680}^+$  would not be reduced. In the acceptor-side model the triplet of  $P_{680}$  is formed through recombination, when the PS II acceptor side is modified by strong illumination on intact systems (Setlik et al., 1990; Vass et al., 1992; Vass & Styring, 1992; van Mieghem et al., 1989); subsequent back reaction of the triplet state to the ground state in the presence of oxygen may then lead to singlet oxygen formation (Macpherson et al., 1993; Hideg et al., 1994a; 1994b; 1998; 2001; Telfer et al., 1994). Other external conditions that affect the D1 repair rate such as salt concentration, low temperature and  $H_2O_2$  (Allakhverdiev & Murata, 2004), as well as singlet oxygen (Nishiyama et al. 2004) can induce photoinhibition. In addition to these models there is evidence that triplet states from certain antenna complexes are involved in photoinhibition. It was found that the amount of photoinhibition did not depend on the antenna size (Sinclair et al., 1996), nor was it affected by added singlet state quenchers (Tyysjarvi et al., 1999; Santabarbara et al., 2001; Santabarbara & Jennings, 2005). Based on these findings it was suggested that a small population of uncoupled antenna Chlorophyll (Chl) molecules, 1-3 per RC (Santabarbara & Jennings, 2005), could give rise to the observed photoinhibition.

Carotenoids have been proposed to be protective against photoinactivation (Horton et al., 1996). The carotenoid in RCs of purple bacteria, which is located quite close to the bacteriochlorophyll (BChl) donor, is an efficient quencher of triplet BChl (Frank & Cogdell, 1993). This explains why so far the protective effect of a magnetic field in RCs from *Rb. sphaeroides* was only observed in the carotenoidless mutant R26.

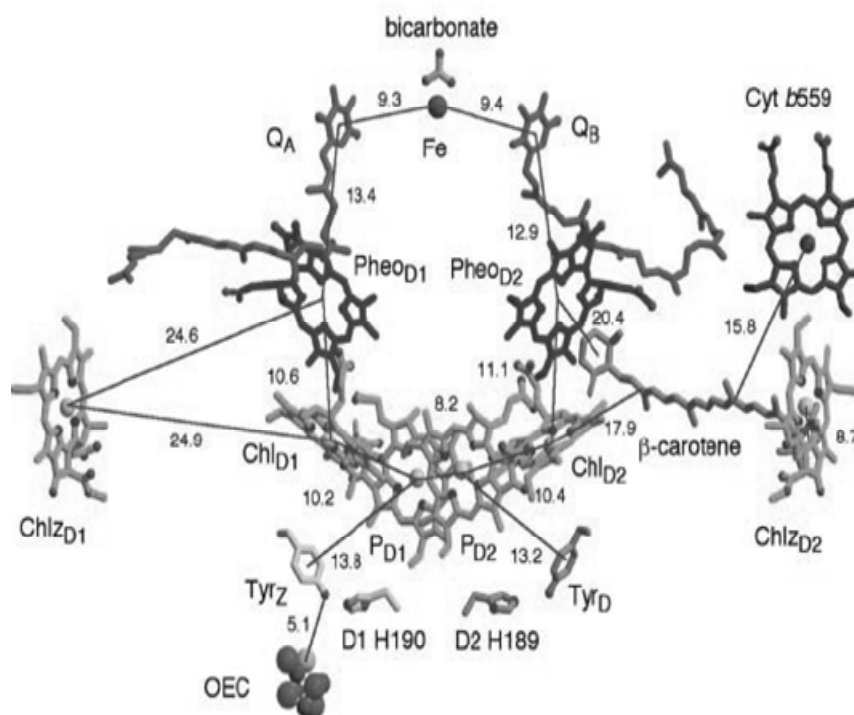


Figure 1. Cofactor arrangement in PSII. Distances are given in Å (Figure was taken from Kamiya and Shen (Kamiya and Shen 2003)).

In the PS II RC (Fig. 1), two  $\beta$ -carotene molecules are present (Kamiya & Shen, 2003; Ferreira et al., 2004). The distance between these carotenes and the triplet carrying Chl, however, is more than 17 Å, which is too long to allow direct quenching. In an isolated PS II reaction center, a 30 %  $P_{680}$  triplet yield and less than 3% Car triplet have been observed (Takahashi et al., 1987; Durrant et al., 1990). Thus the primary function of the carotenoid in the PS II reaction center is believed to quench singlet oxygen produced from triplet Chl rather than directly quenching triplet Chl (Telfer, 2002; van Gorkom & Schelvis, 1993). Singlet oxygen has a short half life time of 200 ns in cells (Gorman & Rodgers, 1992) and its diffusion distance has been calculated to be up to 10 nm in a physiologically relevant situation (Sies & Menck, 1992). This indicates that carotene can only partially quench formed singlet oxygen in the PS II reaction center. If singlet oxygen produced from triplet Chl is not quenched by carotenoids (Trebst et al., 2003), it could well react with the D1 protein as a target molecule.

Based on the above it is likely that singlet oxygen, generated from the reaction center donor triplet state is involved in photoinhibition. We have therefore investigated

whether magnetic fields may influence the extent of photoinhibition in the cyanobacteria *Synechocystis* sp.

## **Materials and Methods**

### ***Samples preparation***

*Synechocystis* sp. PCC 6803 cells were routinely grown in BG 11 medium at 28 °C, gently bubbled with sterile air containing 1% CO<sub>2</sub>. The cylindrical culture tube (4 cm internal diameter) was irradiated by 4 incandescent light bulbs to give 60 μE·s<sup>-1</sup>·m<sup>-2</sup>. After 4-6 days the cells were harvested by centrifugation for 20 minutes at 5000×g at 4 °C. The chlorophyll concentration of the cell cultures was determined by measuring the absorbance at 645 and 663 nm of a pigment extract using 80% acetone and 20% water (Arnon, 1949).

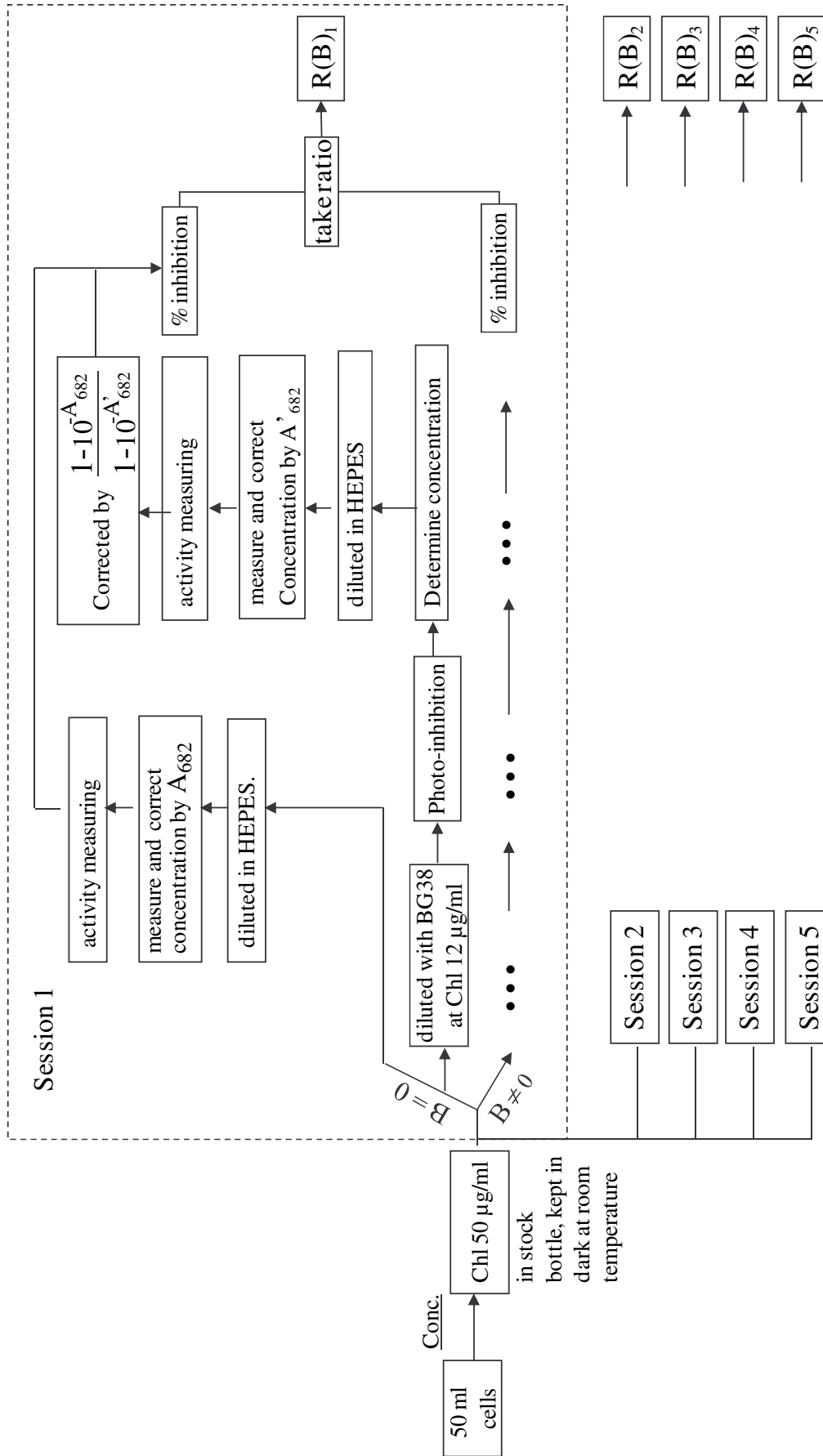
### ***Measurements of photosynthetic activity***

The activity of PS II in *Synechocystis* cells before and after photoinhibition was measured by a home built instrument that monitors the photosynthetic oxygen evolution using a Clark-type oxygen electrode (Bartos et al., 1975). The oxygen electrode was calibrated with air-saturated and nitrogen-saturated distilled water. The measurements were conducted at 28 °C in the presence of 1 mM 1,4-benzoquinone as the electron acceptor. Prior to the activity measurement, the cells were diluted and suspended in 10 mM HEPES-NaOH buffer at pH 7.0 in a 1.7 ml container with a concentration of 12 μgChl·ml<sup>-1</sup>. Actinic light was provided by an incandescent lamp in combination with a 5 cm water filter and a Calflex c filter at a saturating light intensity of 1.5 mE ·s<sup>-1</sup>·m<sup>-2</sup>.

During activity measurements, the stock solution of cells was kept in the dark at room temperature.

### ***Light intensity measurement***

Light intensities were measured with a YSI radiometer, model 65. For O<sub>2</sub> evolution measurements, incident light was measured at the outer chamber surface. The obtained values were only indicative of the relative photon flux density reaching the inner chamber.



Scheme 1. Schedule of experimental procedure

### ***Magnetic Field Effect on photoinhibition and recovery***

Cells taken from 4-6 days cultures were diluted to  $20 \mu\text{gChl}\cdot\text{ml}^{-1}$  in BG-11 medium and were placed in a 4-wall-clear 10 mm quartz cuvette, which was open to the air; the cuvette was in contact with water from a temperature bath operating at room temperature. The cuvette was placed between the two poles of a magnet. A Pt-100 resistor recorded the temperature; the temperature variation during a one-day measurement was less than  $2 \text{ }^\circ\text{C}$ . For illumination a 250 W halogen lamp was used. The light was filtered by 10-cm water and heat filters; maximum light intensity at the cuvette was controlled at  $3 \text{ mE}\cdot\text{s}^{-1}\cdot\text{m}^{-2}$ . The temperature increase during illumination at maximum light intensity for about 2 hours was less than  $1 \text{ }^\circ\text{C}$ .

A Varian E-9 magnet with its field direction perpendicular to the light pathway supplied the external magnetic field. Magnetic field intensities were measured using a RFL Gauss meter type 912. Zero magnetic field was established using Helmholtz coils mounted on the magnet poles to correct for the remnant field of the magnet (about 5 mT). After the photoinhibition treatment, the cells were taken out and concentrated for oxygen-evolving activity measurements. Each photoinhibition measurement in a magnetic field was always preceded by a photoinhibition measurement at zero magnetic field. The activity of the cells was always measured before and after illumination. For recovery after photoinhibition, the cells were taken out of the magnet and diluted to  $7 \pm 1 \mu\text{gChl}\cdot\text{ml}^{-1}$  in BG 11 medium and incubated at  $28 \text{ }^\circ\text{C}$  in light at  $50 \mu\text{E}\cdot\text{s}^{-1}\cdot\text{m}^{-2}$  and bubbled with sterile air containing 1%  $\text{CO}_2$ .

Experiments were performed as shown in scheme 1. Results presented in this chapter correspond to the average results of 3-5 independent experiments, and error bars represent standard deviation.

## **Results**

### ***Oxygen-evolution measurement***

The activity of PS II in *Synechocystis* cells was monitored by measuring the oxygen evolution under continuous illumination. An example is show in Figure 2. The initial oxygen evolution rates, expressed in  $\mu\text{mol}\cdot(\text{mgChl})^{-1}\cdot\text{h}^{-1}$  were obtained by a linear fit of the first 125 s after light was turned on. Reproducibility of the oxygen

evolution rate was better than 87%.

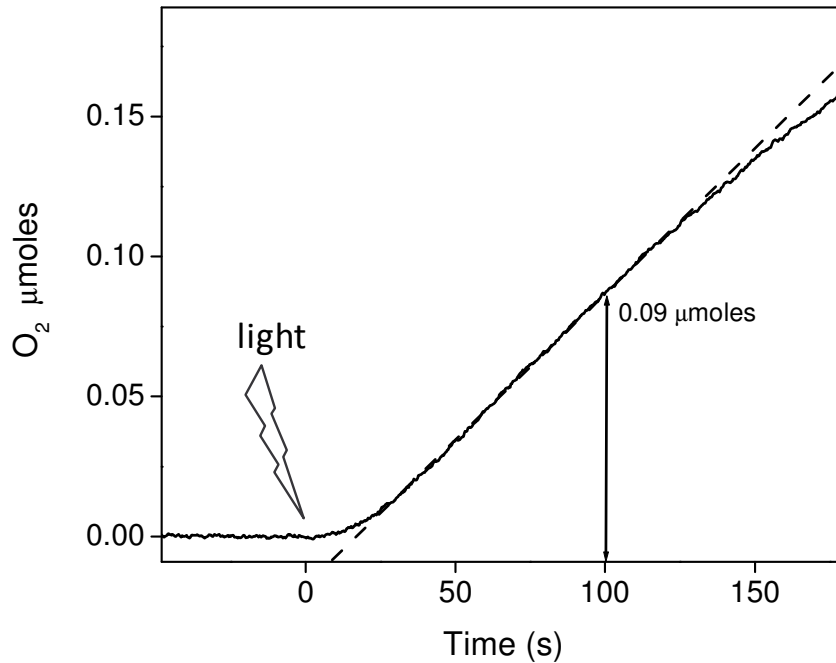


**Figure 2.**

*Typical oxygen evolution time trace from *Synechocystis* cells with a concentration of  $12 \mu\text{g Chl}\cdot\text{ml}^{-1}$ . Light was turned on at time  $t = 0$ . A linear fit (dashed line) was used to calculate the rate of oxygen evolution.*

In Figure 3 we show the O<sub>2</sub> evolution rates for different chlorophyll concentrations of the cell suspension. A clear linear relation was observed in the low concentration range. At values above  $25 \mu\text{g Chl}\cdot\text{ml}^{-1}$  the curve started to deviate from linearity. Therefore, in order to be able to correct for the slight variation of the Chl concentration of the samples during one session of measurements, we used a concentration of about  $12 \mu\text{gChl}\cdot\text{ml}^{-1}$  for the O<sub>2</sub> evolution measurements.



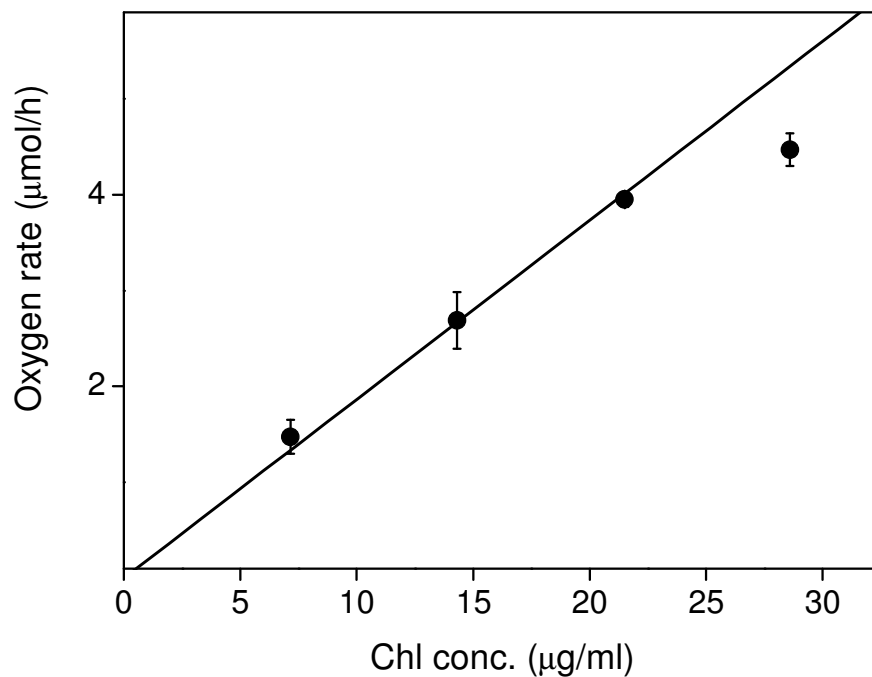


**Figure 3.**

*O<sub>2</sub> evolution rate as measured in Synechocystis cells for different chlorophyll concentrations.*

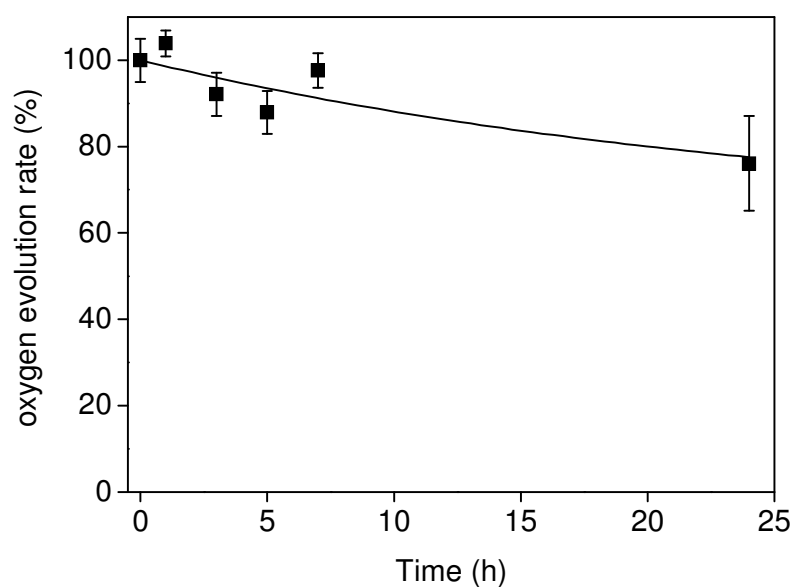


**Figure 4.**

*Changes of activity in Synechocystis cells as a function of dark period at room temperature.*

### ***Effect of dark period on cell activities***

During the photoinhibition experiments, the harvested cells were kept at room temperature in the dark. Since one complete set of experiments lasted up to 10 hours (10 samples were illuminated for 1 hour, 5 at zero field and the other 5 at a certain magnetic field), it was important to investigate the effect of this dark period on the activity of the cells. This is shown in Figure 4 where the oxygen evolution rate is plotted vs the length of the dark period. There was about a 25% decrease in activity after 25 hours dark incubation; after 10 hours of darkness, the activity had dropped about 10 %, which is close to the reproducibility of the oxygen evolution measurements. The conclusion is that these cells can safely be kept for at least 10 hours in the dark.

### **Photoinhibition experiments**

The effect of different light strengths on the oxygen evolution rate in *Synechocystis* sp. PCC 6803 is shown in Figure 5. The cells were illuminated with white light with intensities ranging from  $10 \mu\text{E} \cdot \text{s}^{-1} \cdot \text{m}^{-2}$  to  $3000 \mu\text{E} \cdot \text{s}^{-1} \cdot \text{m}^{-2}$  for a period of 120 minutes. It is seen that the activity gradually decreases with increasing illumination intensity and illumination time. After illumination with the maximum intensity, the activity has decreased five-fold after 120 minutes. Figure 5 shows how photodamage to *Synechocystis* cells varies with light intensity; drawn lines represent mono-exponential fits (see discussion).

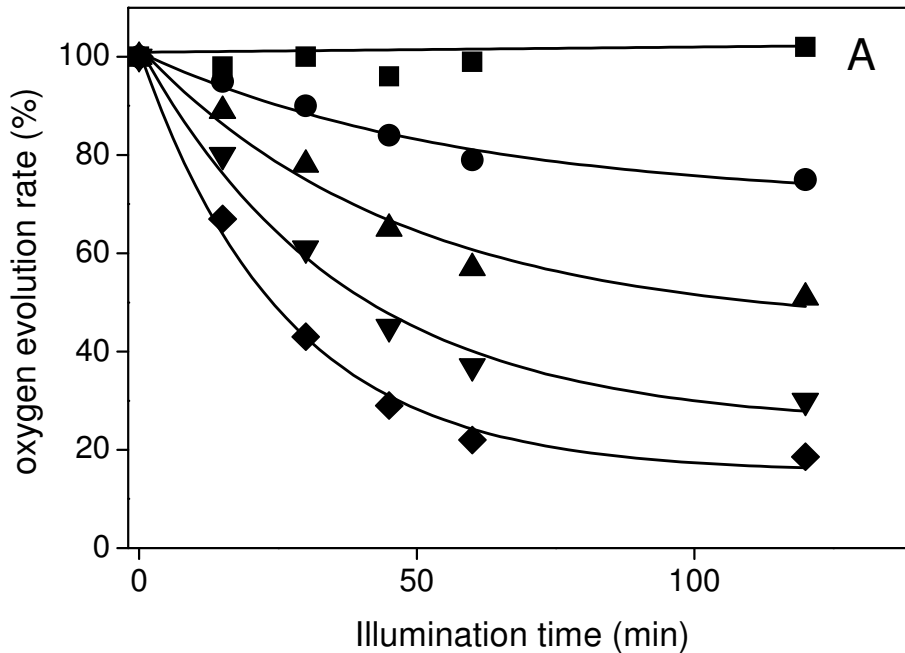


**Figure 5.**

Light induced inactivation of PS II in *Synechocystis* PC 6803 at 25 °C in growth BG-11 medium under normal aerobic conditions. Profile of photodamage to PS II by light at 10  $\mu\text{E}\cdot\text{s}^{-1}\cdot\text{m}^{-2}$  (■), 1.2  $\text{mE}\cdot\text{s}^{-1}\cdot\text{m}^{-2}$  (●), 1.5  $\text{mE}\cdot\text{s}^{-1}\cdot\text{m}^{-2}$  (▲), 2  $\text{mE}\cdot\text{s}^{-1}\cdot\text{m}^{-2}$  (▼) and 3  $\text{mE}\cdot\text{s}^{-1}\cdot\text{m}^{-2}$  (◆). Cell activity was evaluated in terms of oxygen evolution in the presence of 1mM 1,4-benzoquinone and 1mM  $\text{K}_3(\text{FeCN})_6$ . 100% activity was equal to  $188 \pm 21 \text{ O}_2 \mu\text{mol}\cdot(\text{mgChl})^{-1}\cdot\text{h}^{-1}$ . The error bars shown in the results were obtained from three independent measurements.

### ***Repair of Photodamaged cells***

We monitored the recovery of PS II activity after photoinhibition by means of oxygen evolution (Fig. 6). When the cells were exposed to white light with an intensity of 3  $\text{mE}\cdot\text{s}^{-1}\cdot\text{m}^{-2}$  for 60 minutes, the activity of PS II decreased to approximately 23%. After subsequent exposure of cells to weak light at 30  $\mu\text{E}\cdot\text{s}^{-1}\cdot\text{m}^{-2}$  for 4 hours, the activity of PS II returned to 80 % of the original value. When the cells were exposed to the same light intensity but twice as long, the cells activity decreased to 18%. However, during the subsequent weak light exposure at 28 °C, no recovery of activity was observed (Fig. 6). Thus long illumination leads to almost total loss of activity and

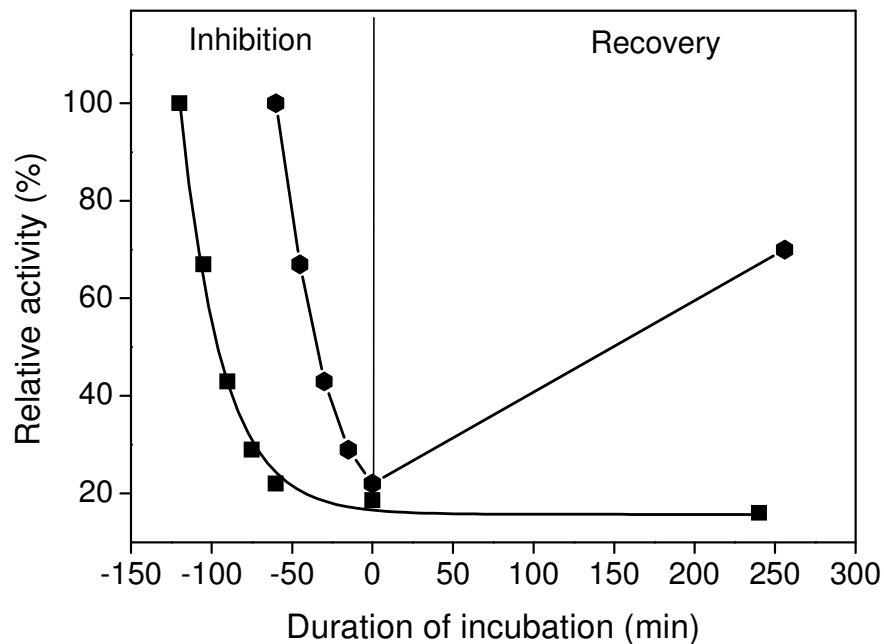


**Figure 6.**

*Recovery of activity under two light intensities. Cells were pretreated under photoinhibiting conditions ( $3 \text{ mE} \cdot \text{s}^{-1} \cdot \text{m}^{-2}$ ). After 1 hour illumination time (hexagon), the activity decreased to 23% of the original value. After 2 hours illumination, a loss of 82 % of its activity was observed (square). The cells were then subjected to standard growth condition under weak light at  $30 \mu\text{E m}^{-2} \text{ s}^{-1}$  in a water-bath at  $28^\circ\text{C}$ . Cells activities were measured after 4 hours recovery treatment.*

cannot be considered to be reversible photoinhibition; irreversible damage must have occurred. Therefore we limited the exposure time to high light conditions during the photoinhibition experiments to 60 minutes.

### ***Magnetic Field Effect on photoinhibition of cells***

We examined the effect of a magnetic field on the photoinhibition of PS II in *Synechocystis* cells. The cells were suspended in growth medium BG-11 and were treated under photoinhibiting conditions with and without an external magnetic field. In Figure 7 the remaining oxygen-evolving activity of the cells after exposure to light

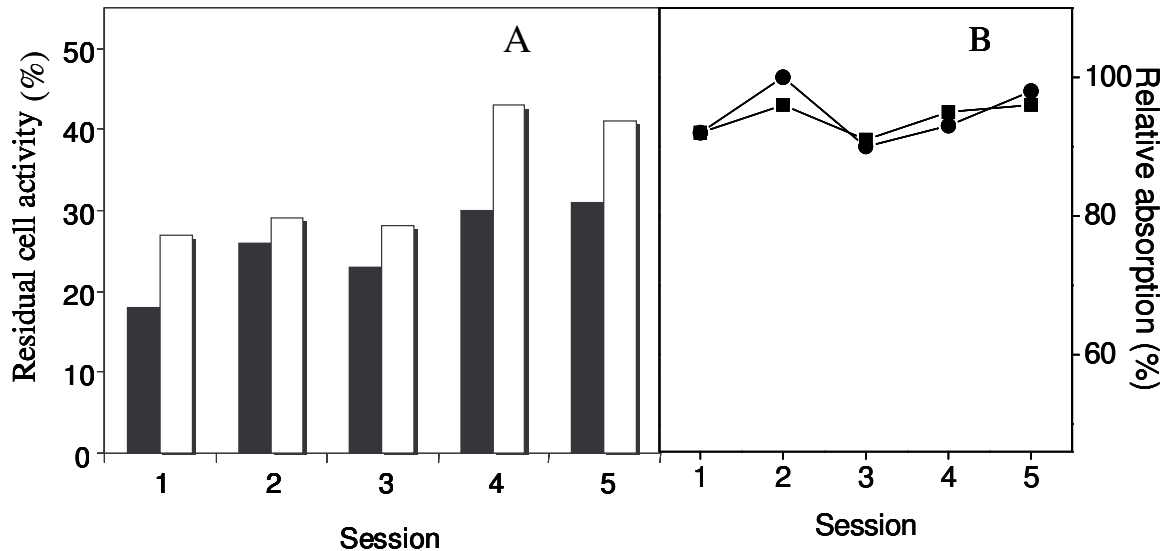


**Figure 7.**

A, Remaining oxygen-evolving activities of PS II of *Synechocystis* cells after photoinhibition at zero-field (black bars) at 200 mT magnetic field (white bars) were obtained in five independent measurements. B, Relative absorptions were measured before and after photoinhibition treatments in each measuring session. Absorption (squares) used for zero-field, circles for 200 mT magnetic field.

for 60 minutes with an intensity of  $3 \text{ mE} \cdot \text{s}^{-1} \cdot \text{m}^{-2}$  is shown, at zero magnetic field and at 200 mT. These experiments were repeated 5 times. Despite the fact that we corrected these values for slight changes in Chl concentration and variation in photo-activity just before photoinhibition, there still remains a variation in the data of about 10-15%. However, it is clear that for each set of field-on/field-off experiments, the photo-inhibition is always greater at zero magnetic field than at 200 mT.

When we define the protecting factor of magnetic field,  $Pr(B)$ , as the ratio of residual cells activity at a magnetic field B over that at zero field, we can plot  $Pr(B)$  for the different sessions. This is shown in Figure 8 where we have plotted  $Pr(200\text{mT})$  for the five sessions. It is seen that this ratio is always larger than 1, the average over the 5 independent measurements is 1.3.

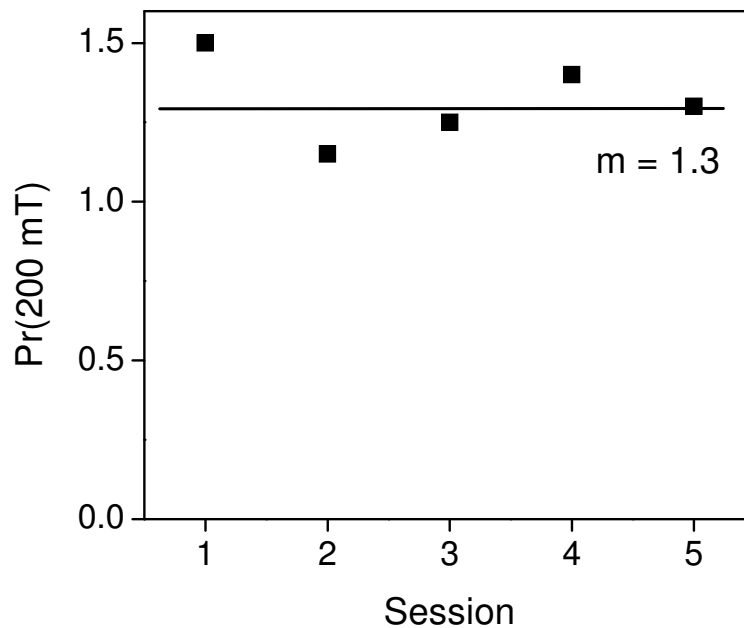


**Figure 8.**

*Ratio of residual cell activity at 200 mT magnetic field over zero-field,  $Pr(200\text{ mT})$ , plotted for 5 independent measurements.*

We have carried out similar experiments for various magnetic field strengths. At each magnetic field, the remaining cell activity after photoinhibition was measured at a certain field value, followed by the same measurement at zero-field. For each field value 3-5 independent measurements were performed. The results, shown in Figure 9, demonstrate that there is a substantial magnetic field effect on photoinhibition. At low magnetic field,  $Pr(B)$  increases from 0.98 to 1.3 at 200 mT, after which,  $Pr(B)$  decreased to about 1.1 at 800 mT. From these results it may be concluded that a magnetic field may play a protective role in the photodamage induced by high light illumination. The half magnetic field of maximum effect is observed to be  $100 \pm 35$  mT.

## Discussion

### *A magnetic field effect on photoinhibition*

In the present study, we investigated the effect of a magnetic field on

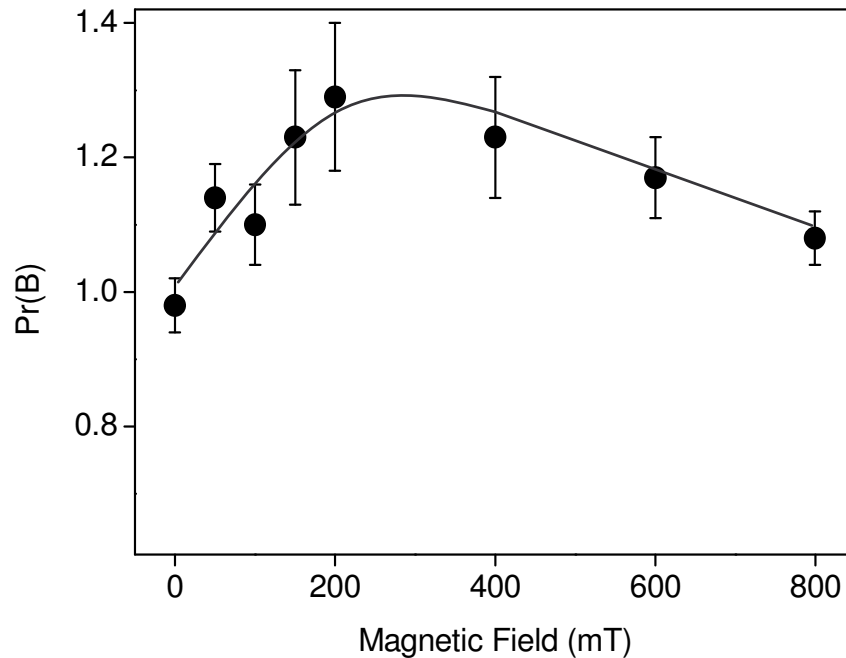


**Figure 9.**

*Pr(B)* values for various magnetic field strengths.

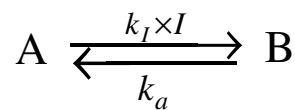
photoinhibition of PS II in *Synechocystis* cells. We found that the extent of photoinhibition is considerably less when the cells are kept in a magnetic field than at zero field: the residual activity after photoinhibition at a field of 200 mT was 30% higher than at 0 mT (Fig. 9). We explain this effect in the framework of the radical pair mechanism, RPM. This mechanism has been proposed to be the underlying mechanism for many field-dependent phenomena, including biological processes (for details, see Chapter 2).

A prerequisite for the involvement of the RPM in photoinhibition is that the damage from photoinhibition is caused by singlet oxygen and that this singlet oxygen is formed through the back reaction of a triplet state that was created via a radical pair. As mentioned in the introduction, there is considerable evidence for the involvement of singlet oxygen in photoinhibition (Hideg et al., 1994a; 1994b; Telfer et al., 1994). The formation of a triplet state through a radical pair only occurs in PS II when this triplet state is generated via recombination reaction between  $P_{680}^+$  and  $Pheo^-$  when the first quinone acceptor is reduced. The latter implies that photoinhibition occurs (partly)

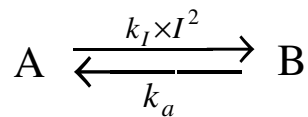
through the acceptor-side mechanism. A schematic view of such mechanism is shown in Figure 10. As the two  $\beta$ -carotenes are located too far from  $P_{680}$ , the triplet state of  $P_{680}$  cannot be quenched directly and it can form singlet oxygen in the back reaction.

### ***Extent of the magnetic field effect***

We have tried to fit the photoinhibition data from Fig 5 according to the reaction model:



in which  $A$  represents the fraction of active PS II centers,  $B$  the fraction inactive PS II centers,  $k_I$  the rate of deactivation,  $k_a$  the rate of re-activation and  $I$  the light intensity. With this model no proper fit of all 5 transients could be obtained. Better fits (drawn lines in Fig 5) were obtained when it was assumed that the inactivation depended quadratically on the light intensity:



The quadratic dependence on light intensity may reflect the involvement of a two-photon process, possibly the photo-reduction of  $Q_A$  and the light-induced triplet formation. Using this model we found  $k_I = 0.0042 \text{ min}^{-1} (\text{mE/s. m}^2)^{-2}$  and  $k_a = 0.0069 \text{ min}^{-1}$ . With the thus obtained values an estimate of the field dependence of  $k_I$  can be calculated: for the maximum value of  $Pr$  of 1.3,  $k_I$  would be  $0.003 \text{ min}^{-1} (\text{mE/s. m}^2)^{-2}$  i.e. there is a maximum reduction on the photo-induced deactivation rate of 30%.

### ***The size of $B_{1/2}$***

The essential part of the RPM is the mixing of the radical pair spin state, *i.e.* a radical pair initially formed in the singlet state, can convert to the radical pair triplet state and *vice versa*. This singlet-triplet mixing or spin-dephasing is driven by differences in g-values and by differences in electron-nuclear hyperfine interactions (hfi) of the two radicals of the pair. In bacterial photosynthesis and in PS II the radical pair is formed by  $P^+(P_{860}$  in bacteria and  $P_{680}$  in PS II) and  $(B)\text{Pheo}^-$ .



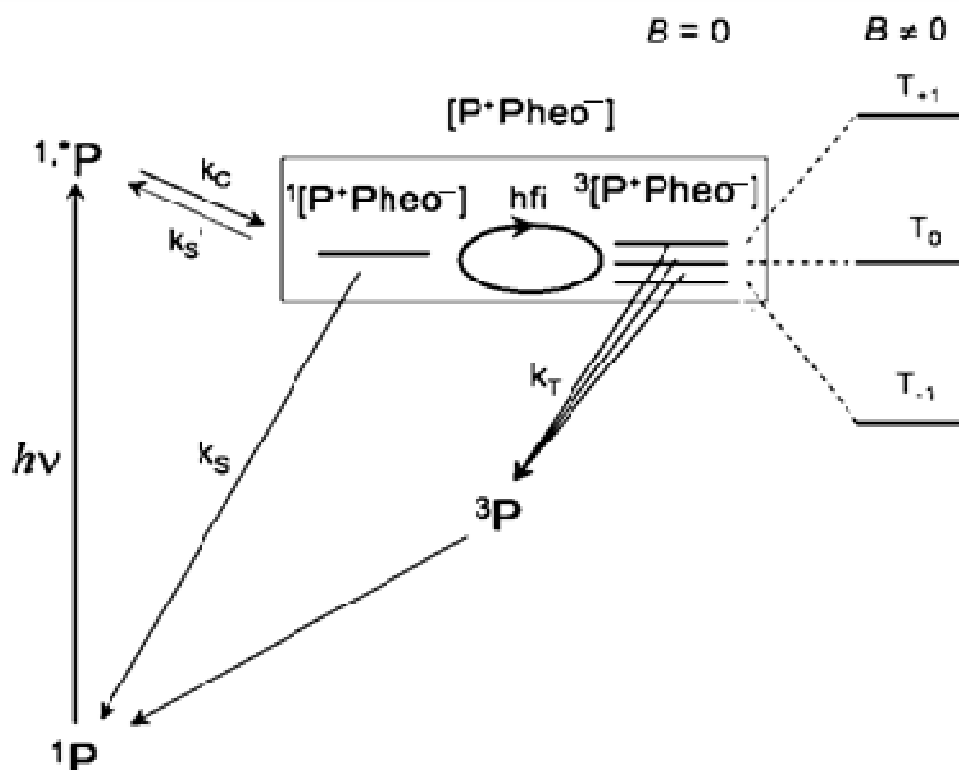


**Figure 10.**  
Schematic view of kinetic electron transfer in PS II

In the absence of a magnetic field, the energy splitting between the singlet state and the three triplet sublevels is determined by the exchange ( $J$ ) and dipolar ( $D$ ) interactions in the radical pair. Low values for  $J$  and  $D$  will result in efficient S-T mixing and subsequent formation of the donor triplet state; large values of  $J$  and  $D$ , *i.e.* strongly coupled radical pairs, will lead to low triplet yield. When a magnetic field is applied such that the Zeeman energy exceeds these interactions, two of the three triplet energy-levels will split, making the populating probability of these levels lower which results in a decreased population of the radical pair triplet state and the triplet yield will become field dependent. This field dependency is characterized by  $B_{1/2}$ , the magnetic field at which the MFE attains half its value at high field.  $B_{1/2}$  is dependent on  $k_S$  and  $k_T$ , the lifetime of the singlet and triplet radical pair state (Fig. 10), respectively, the hfi of the radical pairs and  $J$  and  $D$ , see below (Werner et al., 1978).

Magnetic field effects have been studied in photosynthesis for several decades.

The magnetic field effect was first studied on the donor triplet yield in photosynthetic purple bacteria. Hoff et al. (1977) have measured magnetic field effects in chromatophores and RCs (AUT particles) from *Rb. sphaeroides* wt and in RCs from *Rb. sphaeroides* R26 using donor triplet yield detection by time-resolved optical spectroscopy at 545 nm. In both wt and R26 mutant RCs, a  $B_{1/2}$  value was found of 5-10 mT; in chromatophores  $B_{1/2}$  was 50 mT. Blankenship et al. (1977) have determined the carotenoid triplet yield in reduced RCs from *Rb. sphaeroides* wt as a function of magnetic field by time resolved absorption spectroscopy at 545 nm. At 300 K they found a  $B_{1/2}$  value of about 40 mT. Michel-Beyerle et al. (1979) measured the triplet yield in reduced RCs from *Rb. sphaeroides* R26 using ns time-resolved absorption spectroscopy. They found a  $B_{1/2}$  of 5 mT for a delay rate of 10.5 ns and 7.5 mT for a delay rate of 16.5 ns.

Magnetic field effect measurements on PS II particles have yielded a variety of  $B_{1/2}$  values and are in general larger than in RCs from purple bacteria. Rademaker et al. (1979) measured changes in the steady state fluorescence at 685 nm in *Chlorella vulgaris* and spinach chloroplasts and found a magnetic field effect with  $B_{1/2} \approx 100$  mT. Sonneveld et al. (1980) measured on spinach chloroplasts amplitude and lifetime changes of the 150 ns luminescence component at 685 nm from PS II with reduced plastoquinone. A  $B_{1/2}$  value of 100 mT was found at 80 K; at room temperature this value was 30 mT. Klevanik et al. (1991) obtained  $B_{1/2}$  values of about 25 mT by measuring the variable chlorophyll fluorescence in digitonin particles with doubly reduced plastoquinone. Triebel et al. (1981) found in the chlorophyll fluorescence from leaves magnetic field effects with  $B_{1/2} = 20$  mT which were ascribed to PS II. Time-resolved absorption measurements of the radical pair lifetime as a function of applied magnetic field have been performed by (Volk et al. 1993b) using  $D_1D_2$ -Cytb<sub>559</sub> RCs and found  $B_{1/2}$  values varying from 34 (90 K) to 19 mT (290 K), van der Vos and Hoff (1995) have measured magnetic field effects in  $D_1D_2$ -Cytb<sub>559</sub> RCs using absorption spectroscopy at 680 nm and magnetic field modulation at low temperatures. From their data a  $B_{1/2}$  value of about 20-40 mT at 250 K can be extracted.

The  $B_{1/2}$  that we found in the study of photoinhibition has a value of  $100 \pm 35$  mT, is somewhat larger than others which were found at room temperature from 20-40 mT in PS II. In the following discussion, we will summarize and explain the factors,

which determine the size of  $B_{1/2}$ .

### **1. Relative magnitude of exchange ( $J$ ) and dipolar ( $D$ ) interactions**

It has been shown in bacteria RCs that the spin dipolar interaction  $D$  has a value of about  $6 \times 10^{-7}$  eV, which exceeds the exchange interaction  $8 \times 10^{-8} < J < 1 \times 10^{-7}$  eV by a factor of 10 (Hoff et al., 1993). In a magnetic field with a magnitude of the order of the exchange and dipolar interactions in the radical pair, the triplet products yield may increase when one of the  $T_{+1}$  or  $T_{-1}$  levels is close to the singlet energy level. This phenomenon was called  $2J$ -resonance. For relatively higher exchange interactions, a resonance will occur at higher magnetic field. In addition, the dipolar isotropy will lead to a broadened magnetic field effect that would be observed in the presence of a dipolar interaction. Either the  $2J$ -resonance occurring in a higher magnetic field or broadening will lead to an enlarged  $B_{1/2}$  value. However, these effects can only lift the  $B_{1/2}$  values only a few mT. Therefore it is not a main effect on the enlarged  $B_{1/2}$  in our measurements.

### **2. The rates of $k_S$ and $k_T$**

The quantitative determination of rates of  $k_S$ ,  $k_T$ , exchange interaction  $J$  and concentration of triplet products can be calculated (Haberkorn, 1977; Haberkorn & Michel-Beyerle, 1979; Werner et al., 1977; 1978). Qualitatively when the life time of the singlet and/or triplet states of the RP become short, it will lead to a broadening of singlet and triplet energy levels, leading to a spreading of the magnetic field effect and thus to an increased  $B_{1/2}$  value. In similar fashion the large  $B_{1/2}$  values found for PS II have been explained (Volk et al., 1993a). Although the value for the singlet recombination rate  $k_S$  in PS II is 50 times smaller than in bacterial RCs, the value for  $k_T$  ( $3 \text{ ns}^{-1}$ ) is much faster than that found in bacterial RCs ( $0.6\text{-}0.8 \text{ ns}^{-1}$ ) (Ogrodnik et al., 1988; Volk et al., 1993a). Thus it may be concluded that the differences in  $B_{1/2}$  value between what we found ( $100 \pm 35$  mT) in whole cells and those from Volk et al. (1993a) (19 mT) and van der Vos and Hoff (1995) (20-40 mT) in  $D_1D_2$ -Cytb<sub>559</sub> RCs can be explained by changes in  $k_T$  either due to the presence of antenna complexes in our cells, or by other structural differences between cells and isolated PS II RCs.

In our work, an increased photo-induced deactivation rate  $k_I$ , i.e. a decreasing  $Pr(B)$ , was observed above 300 mT (Fig. 9). Assuming that the hyperfine interaction is

about 1 mT, and  $\Delta g$  has an order of around  $10^{-3}$  in photosynthetic systems, an increased singlet oxygen generation will be expectedly observed as magnetic field increases beyond 1 T (for a more detailed explanation, see Chapter 2). Thus there is currently no clear explanation for the tendency of  $Pr(B)$  in our work.

## **Conclusions**

We have demonstrated that the activity of *Synechocystis* cells under stress conditions is dependent on magnetic field. The yield of magnetic field effect on these cells was roughly calculated and was well described by the Radical Pair Mechanism. The  $B_{1/2}$  value was roughly as expected from magnetic field effects from PS II. These results predict that a magnetic field will have a significant protective effect on plants growing under light stress conditions.

## References

- Adir N., Zer H., Shochat S., Ohad I. 2003, Photoinhibition – a historical perspective, *Photosynth. Res.* 76: 343–370.
- Allakhverdiev S.I., Murata N. 2004, Environmental stress inhibits the synthesis de novo of proteins involved in the photodamage-repair cycle of Photosystem II in *Synechocystis* sp PCC 6803, *Biochim. Biophys. Acta* 1657: 23–32.
- Anderson J.M., Park Y.I., Chow W.S. 1998, Unifying model for the photoinactivation of Photosystem II in vivo: a hypothesis. *Photosynth. Res.* 56: 1–13.
- Arnon D.I. 1949, Copper enzymes in isolated chloroplasts. Polyphenoloxidase in beta vulgaris, *Plant Physiol.* 24: 1–15.
- Aro E.M., Virgin I., Andersson B. 1993, Photoinhibition of Photosystem II. Inactivation, protein damage and turnover, *Biochim. Biophys. Acta* 1143: 113–134.
- Bartos J., Berkova E., Setlik I. 1975, A versatile chamber for gas exchange measurements in suspensions of algae and chloroplasts. *Photosynthetica* 9: 395–406.
- Blankenship R.E., Schaafsma T.J., Parson W.W. 1977, Magnetic-field effects on radical pair intermediates in bacterial photosynthesis, *Biochim. Biophys. Acta* 461: 297–305.
- Callahan F.E., Becker D.W., Cheniae G.M. 1986, Studies on the Photoactivation of the Water-Oxidizing Enzyme. II. Characterization of weak light photoinhibition of PS II and its light-induced recovery, *Plant Physiol.* 82: 261–269.
- Chen G.X., Kazimir J., Cheniae G.M. 1992, Photoinhibition of hydroxylamine extracted photosystem-II membranes –studies of the mechanism, *Biochemistry* 31: 11072–11083.
- Durrant J.R., Giorgi L.B., Barber J., Klug D.R., Porter G. 1990, Characterization of triple-states in isolated photosystem - II reaction centers- oxygen quenching as a mechanism for photodamage, *Biochim. Biophys. Acta* 1017: 167–175.
- Feikema W.O., Gast P., Klenina I.B., Proskuryakov I.I. 2005, EPR characterisation of the triplet state in photosystem II reaction centers with singly reduced primary acceptor  $Q_A$ , *Biochim. Biophys. Acta* 1709: 105–112.
- Ferreira K.N., Iverson T.M., Maghlaoui K., Barber J., Iwata S. 2004, Architecture of the photosynthetic oxygen-evolving center, *Science*, 303: 1831–1838.
- Frank H.A., Cogdell R.J. 1993, The photochemistry and function of carotenoids in photosynthesis, In *Carotenoids in photosynthesis*. Young A.J. and Britton G. (Eds.), pp. 252–326.
- Gorman A.A., Rodgers M.A. 1992, Current perspectives of singlet oxygen detection in biological environments, *J. Photochem. Photobiol.* 14: 159–176.

- Haberkorn R. 1977, Theory of magnetic field modulation of radical recombination reactions I, *Chem. Phys.* 19: 165–179.
- Haberkorn R., Michel-Beyerle M. 1979, On the mechanism of magnetic field effects in bacterial photosynthesis, *Biophys. J.* 26: 489–498.
- Hakala M., Tuominen I., Keranen M., Tyystjarvi T., Tyystjarvi E. 2005, Evidence for the role of the oxygen-evolving manganese complex in photoinhibition of Photosystem II, *Biochim. Biophys. Acta* 1706: 68–80.
- Hideg E., Kalai T., Hideg K., Vass I. 1998, Photoinhibition of photosynthesis in vivo results in singlet oxygen production: detection via nitroxide-induced fluorescence quenching in broad bean leaves, *Biochemistry* 37: 11405–11411.
- Hideg E., Ogawa K., Kalai T., Hideg K. 2001, Singlet oxygen imaging in Arabidopsis thaliana leaves under photoinhibition by excess photosynthetically active radiation, *Physiol. Plant.* 112: 10–14.
- Hideg E., Spetea C., Vass I. 1994a, Singlet oxygen production in thylakoid membranes during photoinhibition as detected by EPR spectroscopy, *Photosynth. Res.* 39: 191–199.
- Hideg E., Spetea C., Vass I. 1994b, Singlet oxygen and free-radical production during acceptor induced and donor-side induced photoinhibition – studies with spin-trapping EPR spectroscopy, *Biochim. Biophys. Acta.* 1186: 143–152.
- Hoff A.J., Gast P., van Der Vos R., Vrieze J., Franken E.M., Lous E.J. 1993, Magnetic-field effects-MARY, MIMS and MODS, *Z. Phys. Chem. - Inter. J. Res. Phys. Chem. & Chem Phys.* 180: 175–192.
- Hoff A.J., Rademaker H., van Grondelle R., Duysens L.N.M. 1977, Magnetic-field dependence of yield of triplet-state in reaction centers of photosynthetic bacteria, *Biochim. Biophys. Acta* 460: 547–554.
- Hoff A.J. 1981. Magnetic field effects on photosynthetic reactions, *Quarta. Rev. Biophys.* 14: 599–665.
- Horton P., Ruban A.V., Walters R.G. 1996, Regulation of light harvesting in green plants, *Annu. Rev. Plant Physiol. Mol. Biol.* 47: 665–684.
- Kamiya N., Shen J.R. 2003, Crystal structure of oxygen-evolving photosystem II from *Thermosynechococcus vulcanus* at 3.7 Å resolution, *Proc. Natl. Acad. Sci. USA* 100: 98–103.
- Klevanik A.V., Feyziev Y.M., Allakhverdiev S.I., Shuvalov V.A., Klimov V.V. 1991, The origin of photosystem-II variable chlorophyll fluorescence, *Biol. Membrany* 8: 1053–1065.
- Liu Y., Edge R., Henbest K., Timmel C.R., Hore P.J., Gast P. 2005, Magnetic field effect on singlet oxygen production in a biochemical system, *Chem. Commun.* 2: 174–176.

- Macpherson A.N., Telfer A., Truscott T.G., Barber J. 1993, Direct detection of singlet oxygen from isolated photosystem II reaction centers, *Biochim. Biophys. Acta* 1143: 301–309.
- Michel-Beyerle M.E., Scheer H., Seidlitz H., Tempus D., Haberkorn R. 1979, Time-resolved magnetic field effect on triplet formation in photosynthetic reaction centers of *Rhodospseudomonassphaeroides R-26*, *FEBS Lett.* 100: 9–12.
- Mishra N.P., Francke C., van Gorkom H.J., Ghanotakis D.F. 1994, Destructive role of singlet oxygen during aerobic illumination of the Photosystem II core complex, *Biochim. Biophys. Acta.* 1186: 81–90.
- Nishiyama Y., Allakhverdiev S.I., Yamamoto H., Hayashi H., Murata N. 2004, Singlet oxygen inhibits the repair of photosystem II by suppressing the translation elongation of the D1 protein in *Synechocystis* sp. PCC 6803, *Biochemistry*, 43: 11321–11330.
- Ogrodnik A., Volk M., Letterer R., Feick R., Michel-Beyerle M.E. 1988, Determination of free-energies in reaction centers of *Rb. Sphaeroids*, *Biochim. Biophys. Acta* 936: 361–371.
- Ohad I., Kyle D.J., Arntzen C.J. 1984, Membrane-protein damage and repair – removal and replacement of inactivated 32-kilodalton polypeptides in chloroplast membranes, *J. Cell Biol.* 99: 481–485.
- Ohnishi N., Allakhverdiev S.I., Takahashi S., Higashi S., Watanabe M., Nishiyama Y., Murata N. 2005, Two-step mechanism of photodamage to photosystem II: Step 1 occurs at the oxygen-evolving complex and step 2 occurs at the photochemical reaction center, *Biochemistry* 44: 8494–8499.
- Park Y.I., Chow W.S., Anderson J.M. 1995, Light inactivation of functional photosystem-II in leaves of peas grown in moderate light depends on photon exposure, *Planta*, 196: 401–411.
- Parson W.W., Clayton R.K., Cogdell R.J. 1975, Excited-states of photosynthetic reaction centers at low redox potentials, *Biochim. Biophys. Acta* 387: pp265–278.
- Prasil O., Adir N., Ohad I. 1992, Dynamics of photosystem II: mechanism of photoinhibition and recovery process. In: Barber J, ed. *Topics in photosynthesis, the photosystems: structure, function and molecular biology*, Vol. 11. Amsterdam: Elsevier: 220–250.
- Rademaker H., Hoff A.J., Duysens L.N.M. 1979. Magnetic field-induced increase of the yield of (bacterio)Chlorophyll emission of some photosynthetic bacteria and of *Chlorella vulgaris*, *Biochim. Biophys. Acta* 546: 248–255.
- Rappaport F., Guergova-Kuras M., Nixon P.J., Diner B.A., Lavergne J. 2002, Kinetics and pathways of charge recombination in photosystem II, *Biochemistry* 41: 8518–8527.

- Rutherford A.W., Paterson D.R., Mullet J.E. 1981, A light-induced spin-polarized triplet detected by electron-paramagnetic-res in photosystem-II reaction centers, *Biochim. Biophys. Acta* 635: 205–214.
- Rutherford A.W., Mullet J.E. 1981, Reaction center triplet states in photosystem I and photosystem II, *Biochim. Biophys. Acta* 635: 225–235.
- Santabarbara S., Barbato R., Zucchelli G., Garlaschi F.M., Jennings R.C. 2001, The quenching of photosystem II fluorescence does not protect the D1 protein against light induced degradation in thylakoids. *FEBS Lett.* 505: 159–162.
- Santabarbara S., Jennings R.C. 2005, The size of the population of weakly coupled chlorophyll pigments involved in thylakoid photoinhibition determined by steady-state fluorescence spectroscopy. *Biochim. Biophys. Acta* 1709: 138–149.
- Setlik I., Allakhverdiev S.I., Nedbal L., Setlikova E., Klimov V.V. 1990, 3 Types of photosystem-II photoinactivation. 1. Damaging process on the acceptor side, *Photosynth. Res.* 23: 39–48.
- Sies H., Menck C.F. 1992, Singlet oxygen induced DNA damage. *Mut. Res.* 275: 367–375.
- Sinclair J., Park Y.I., Chow W.S., Anderson J.M. 1996, Target theory and the photoinactivation of Photosystem II. *Photosynth. Res.* 50: 33–40.
- Sonneveld A., Duysens L.N.M., Moerdijk A. 1980, Magnetic field-induced increase in chlorophyll A delayed fluorescence of photosystem-II – A 100 ns to 200 ns component between 4.2 and 300 K, *Proc. Natl. Acad. Sci. USA*, 77: 5889–5893.
- Sonoike K., Terashima I. 1994, Mechanism of photosystem-I photoinhibition in leaves of *Cucumis sativus* L, *Planta*, 194: 287–293.
- Takahashi Y., Hansson O., Mathis P., Satoh K. 1987, Primary radical pair in the photosystem II reaction center. *Biochim. Biophys. Acta* 893: 49–59.
- Telfer A. 2002, What is b-carotene doing in the photosystem II reaction center? *Phil. Trans. Roy. Soc. B* 357: 1431–1440.
- Trebst A., Depka B. 1997, Role of carotene in the rapid turnover and assembly of photosystem II in *Chlamydomonas Reinhardt*. *FEBS Lett.* 400: 359–362.
- Trebst A., Depka B., Hollander-Czytko H. 2003, Function of  $\beta$ -carotene and tocopherol in photosystem II. *Z. Naturforsch., C: Biosci.* 58: 609–620.
- Triebel M.M., Frankevich E.L., Eolesnikova I.I. 1981, Magnetic field effect in primary process of photosynthesis, Abstract book of the conference on chemical induced spin polarization and magnetic field effect, pp. 119–120.
- Tyystjarvi E., Aro E.M. 1996, The rate constant of photoinhibition, measured in lincomycin-treated leaves, is directly proportional to light intensity, *Proc. Natl. Acad. Sci. USA* 93: 2213–2218.



- Tyystjarvi E., King N., Hakala M., Aro E.M. 1999, Artificial quenchers of chlorophyll fluorescence do not protect against photoinhibition, *J. Photochem. Photobiol. B.* 48: 142–147.
- van der Vos R., Hoff A.J. 1995, Optically-detected magnetic-field effects on the D1-D2- Cytb<sub>559</sub> Complex of photosystem-II – Temperature-dependence of kinetics and structure, *Biochim. Biophys. Acta* 1228: 73–85.
- van Gorkom H.J., Schelvis J.P.M. 1993, Kok's oxygen clock: what makes it tick? The structure of P680 and consequences of its oxidizing power, *Photosynth. Res.* 38: 297–301.
- van Mieghem F.J.E., Nitschke W., Mathis P., Rutherford A.W. 1989, The influence of the quinone-iron electron-acceptor complex on the reaction center photochemistry of photosystem-II, *Biochim. Biophys. Acta* 977: 207–214.
- Vass I., Styring S. 1992a, Spectroscopic Characterization of Triplet Forming States in Photosystem II, *Biochemistry* 31: 5957–5963.
- Vass I., Styring S., Hundal T., Koivuniemi A., Aro E.M., Andersson B. 1992b, Reversible and irreversible intermediates during photoinhibition of photosystem 2. Stable reduced Q<sub>A</sub> species promote chlorophyll triplet formation, *Proc. Natl. Acad. Sci. USA* 89: 1408–1412.
- Volk M., Gilbert M., Rousseau G., Richter M., Ogrodnik A., Michel-Beyerle M.E. 1993a, Similarity of primary radical pair recombination in photosystem-II and bacterial reaction centers, *FEBS Lett.* 336: 357–362.
- Volk M., Haberle T., Feick R., Ogrodnik A., Michel-Beyerle M.E. 1993b, What can be learned from the singlet-triplet splitting of the radical pair P<sup>+</sup>H<sup>-</sup> in the photosynthetic reaction-center – Conclusion from electric- field effects on the P<sup>+</sup>H<sup>-</sup> recombination dynamics, *J. Phys. Chem.* 97: 9831–9836.
- Werner H.J., Schulten Z., Schulten K. 1977, Theory of the magnetic afield modulated geminate recombination of radical ion pairs in polar solvents: application to the pyrene-N,N-dimethylaniline system, *J. Chem. Phys.* 67: 646–663.
- Werner H.J., Schulten K., Weller A. 1978, Electron transfer and spin exchange contribution to the magnetic field dependence of the primary photochemical reaction of bacterial photosynthesis, *Biochim. Biophys. Acta* 502: 255–268.

# Thesis Summary

It has been known for over three decades that magnetic fields can influence the rates and yields of certain classes of chemical reactions. How a magnetic field influences living organisms has gained great interest in scientific research. Two mechanisms have been proposed to interpret the magnetic field effect (MFE), a) the magnetite mechanism; b) the radical pair mechanism. The only mechanism that gained widespread acceptance is the one caused by the Radical Pair Mechanism (RPM). However, it has so far proved impossible to demonstrate convincingly a biological RPM effect. The studies on the biological RPM effect are therefore of importance. In photosynthetic bacteria (e.g. purple bacteria, green sulphur bacteria, cyanobacteria etc.), light is captured by pigment protein complexes constituting the antenna system, and is then transferred to a protein complex termed the reaction center (RC). The cofactors of the RC consist of a special pair of bacterio-chlorophyll molecules, acting as a primary electron donor, two bacterio-chlorophyll accessory electron acceptors, two pheophytine electron acceptors, two quinones and one carotenoid. Charge separation occurs and a radical pair is formed by the special pair and the electron acceptor after a quantum of light is absorbed. The singlet-triplet mixing of this radical pair is magnetic field dependent. This has prompted us to use these photosynthetic complexes as a model to provide a 'proof of principle' for the RPM in biological systems (**Chapter 1**).

In **Chapter 2**, the magnetic field effects on photosynthetic reaction center of *Rhodobacter (Rb.) sphaeroides* wt and of its carotenoidless mutant R26 are presented. The first part of the Chapter illustrates that the yield of light-induced singlet oxygen ( $^1\Delta_g$ ,  $^1O_2$ ) in bacterial photosynthetic reaction centers, and the ensuing oxidative damage to the protein complex and its associated cofactors are magnetic field dependent.  $^1O_2$  formed by illuminating reaction centers of the carotenoidless mutant of *Rhodobacter sphaeroides* R26 has been detected via its

luminescence at 1270 nm. The second part is devoted to study the high magnetic field effect by means of optical detection of singlet oxygen associated with photo-bleaching of N,N-dimethyl-4-nitrosoaniline (RNO). The observed singlet oxygen yield is significantly different in low and high magnetic fields. A reduced singlet oxygen yield is observed at low magnetic field (<100 mT), whereas an increased singlet oxygen yield is demonstrated when the magnetic field is above 600 mT.

In addition to the light induced photodamage, a band shift from 860 to 850 nm in the absorption spectrum of *Rhodobacter sphaeroides* R26 reaction centers takes place during illumination. Low-temperature spectroscopy and frequency-modulated absorbance detected magnetic resonance (FM-ADMR) were used to interpret the characteristic of this band shift and to investigate its influence on the functioning of the RCs of *Rhodobacter sphaeroides* R26, as shown in **Chapter 3**. The low temperature absorption spectra demonstrate clearly that the band shift from 860 to 850 nm is caused by the splitting of the donor band, which absorbs at 866 nm and 890 nm at 2K. Furthermore, the light-minus-dark difference spectra at 2 K suggest that the 850 nm band does not contribute to charge separation and consequent formation of the radical pair. The FM-ADMR study concretely proves that the RCs absorbing band of 850 nm do not produce any triplet. These findings proposed that the composition of RC proteins changed by light exposure. These damaged RCs are not photoactive and do not generate any radical pair.

The magnetic field effect studies have been extended to intact photosynthetic cells of cyanobacterium *Synechocystis* sp PCC 6803 cells (**Chapter 4**). These cells were studied under photoinhibition conditions i.e. under such high light conditions that the photodamage exceeds the photo-repair in PS II. It was demonstrated that the de-activation rate decreased with increasing magnetic field (< 200 mT) and started to increase when the magnetic field strength exceeded 300 mT. A maximum effect on the de-activation rate of 30% was found. These

observations are explained within the framework of acceptor site photoinhibition with triplet state formation through the primary radical pair. This in turn suggests that the direct or indirect singlet oxygen measurement may provide an appropriate manner for the biological magnetic field effect study.



# Samenvatting

Reeds meer dan 30 jaar is bekend dat een magneetveld de reactietijden en de opbrengsten van bepaalde chemische reacties kan beïnvloeden. Hoe echter de beïnvloeding van levende organismen door een magneetveld ontstaat, is nog onbekend en wordt thans uitgebreid onderzocht. Hiervoor zijn 2 reactiemechanismen (one word) voorgesteld die dit magneetveldeffect (MVE) zouden kunnen verklaren: 1) het magnetiet mechanisme en 2) het radicaalpaar mechanisme (RPM). In het eerste mechanisme wordt aangenomen dat kleine deeltjes van het mineraal magnetiet als een soort kompas kunnen fungeren. In het tweede mechanisme, ontstaat magneetveldafhankelijkheid door wisselwerking tussen (licht-geïnduceerde) gekoppelde paren van radicalen. Het is echter nog niet gelukt om het magneetveldeffect d.m.v. het radicaalpaar mechanisme overtuigend aan te tonen in biologisch materiaal.

In fotosynthetische bacteriën (zoals purper bacteriën, groene zwavel bacteriën en cyano bacteriën), worden pigmenten in de zogeheten antenne complexen door lichtabsorptie in de aangeslagen toestand gebracht, waarna deze toestand doorgegeven wordt aan pigmenten in het reactiecentrum eiwit complex (RC). De cofactoren in het RC bestaan uit een dimeer van (bacterio) chlorofyl moleculen, dat als electron donor fungeert, twee accessoire (bacterio) chlorofyl moleculen, twee primaire electron acceptors bestaande uit (bacterio) feofytine, twee chinonen en een caroteen molekuul. Door ladingsscheiding, die ontstaat vanuit de aangeslagen toestand van de donor, wordt een radicaalpaar gevormd bestaande uit het geoxideerde donor-dimeer en een gereduceerd bacterio feofytine molekuul.

In hoofdstuk 2 worden MVE resultaten gepresenteerd die verkregen zijn met het RC-eiwit van *Rb. sphaeroides* wilde type en zijn caroteenloze mutant R26. In het eerste gedeelte van dit hoofdstuk wordt aangetoond dat de hoeveelheid

singulet zuurstof, dat door de lichtreactie in deze RCs in geringe mate wordt aangemaakt, en de daardoor ontstane beschadiging aan het RC, afhankelijk is van het aangelegde magneetveld. De hoeveelheid singulet zuurstof werd in dit geval gemeten via de 1270 nm luminescentie van singulet zuurstof. In het tweede gedeelte wordt het MVE bestudeerd bij extra hoge magneetvelden m.b.v. de foto-bleking van RNO, die optreedt bij de reactie met singulet zuurstof. Op deze wijze werd de singulet zuurstof productie van deze RCs bepaald over een breed gebied van magneetveldsterktes: een afname van de singulet zuurstof opbrengst is waar te nemen bij lage magnetische velden (<100mT) waarna bij veldsterktes hoger dan 600 mT de singulet zuurstof opbrengst weer toenam. Het profiel van de magneetveld afhankelijkheid bleek volledig in overeenstemming met het RPM. Hiermee werd voor het eerst aangetoond dat het in principe mogelijk is dat eiwitten stoffen produceren (in dit geval singulet zuurstof) waarvan de hoeveelheid afhankelijk is van de magneetveldsterkte. Deze metingen zouden dan ook een mogelijke verklaring kunnen geven voor de magneetveld gevoeligheid van bv trekvogels.

In hoofdstuk 3 wordt de lichtgeïnduceerde en magneetveld afhankelijke oxidatieve beschadiging van het RC-eiwit nader onder de loupe genomen. De beschadigen uitten zich in de caroteenloze mutant R26 door een gedeeltelijke bleking van het absorptie-spectrum van het RC-eiwit en een schijnbare bandverschuiving van de donor band van 860 naar 850 nm. Deze effecten zijn onderzocht m.b.v. lage temperatuur absorptie spectroscopie en frequentie-gemoduleerde absorptie gedetecteerde magnetisch resonantie (ADMR). Dankzij de verhoogde spectrale resolutie bij lage temperaturen, werd aangetoond dat de bandverschuiving in feite een splitsing is van de 860 nm band in een band bij 860 en een bij 850 nm . Optische verschilspectroscopie toonde dat de 850 nm band behoorde bij RCs die geen stabieleladingsscheiding produceerden. Met FM-ADMR werd vastgesteld dat deze RCs ook geen primaire ladingsscheiding produceerden.

De resultaten in hoofdstuk 2&3 toonden aan dat de stabiliteit van het

RC-eiwit gunstig beïnvloed kan worden door deze in een magneetveld te plaatsen. Dit opmerkelijke feit heeft ons ertoe gebracht om een dergelijk onderzoek uit te voeren in een cyanobacterie. Daartoe werd de foto-inhibitie van *Synechocystis* onderzocht. Foto-inhibitie bij planten ontstaat wanneer het fotosysteem (met name fotosysteem II) door externe omstandigheden (bv lage temperatuur, zout concentratie, hoge licht intensiteit) uit balans raakt. Een gevolg hiervan is de beschadiging van het D1 eiwit. Voor het mechanisme van de D1 uitschakeling zijn er twee theorieën: de donor-kant model en de acceptor-kant model. In het acceptor-kant model gaat men ervan uit dat er singulet zuurstof gegenereerd wordt als het fotosysteem overbelast raakt waardoor D1 vernietigd wordt. De singulet zuurstof zou dan, net als in *Rb. sphaeroides* R26, ontstaan vanuit een triplet toestand, die weer zou zijn ontstaan vanuit een radicaal paar. De in hoofdstuk 4 gemeten magneetveld studies hebben nu aangetoond dat de foto-inhibitie, die ontstaat door extreme belichting, geringer is in een magneetveld dan bij nulveld. Deze metingen suggereren dat de foto-stabiliteit van planten positief beïnvloed wordt door een magneetveld.





# Curriculum Vitae

Yan Liu was born on March 29, 1978, in Jiangyan, Jiangsu, China. She followed the bachelor's program in Chemistry Department at Zhejiang University, and graduated with honor in June 1998. The same year she started the Master studies and she graduated with honor at Zhejiang University, China, with a Master's degree in Physical Chemistry in 2001. In the end of 2001, she started her PhD studies under the supervision of Dr. P. Gast at the Biophysics department in the Leiden Institute of Physics (LION).

The results of this work were presented at national and international conferences in the form of posters, notably at the 13<sup>th</sup> International Congress on Photosynthesis (Montreal, Canada), the 9<sup>th</sup> International Spin Chemistry Meeting (Oxford, UK) and the annual Dutch meeting on Molecular and Cellular Biophysics (Lunteren, The Netherlands).

Since May 2006, she joined Philips Research (Eindhoven, the Netherlands) as a research scientist.



# Nawoord

Many people have been involved in the work that I have presented in this thesis. I would like to thank Dr. Ruth Edge for inspirations during the early stage of my research. She also spent much time on helping me with the experimental setup. I would like to thank Martien van der Pijl not only for solving the problems for the electronics devices, but also for his inspiring ideas to improve the setup. I acknowledge Dr. Hans van Gorkom for careful reading of the manuscript, and great advice on photoinhibition in photosystem II. Wouter van der Meer provided me the isolated reaction centers from *Rhodobacter sphaeroides* wt. Dre de Wit helped to make the PS II preparations and was always available for discussions. John van Egmond and Willem Versluys gave me a lot of technical support. Alia shared with me valuable suggestions through many discussions. Fred Kranenburg was always willing to lend a hand when computer problems arose.

I have many pleasant memories with the colleagues: Onno, Nora, Tatiana, Jesper, Anna, Shipra, Esha, Mohammed, Marcel and Chien-Ching.

I am grateful to my friends who supported me and helped me shuffle through daily stuff: special thanks to Yinghui, Zongquan, Qianhui, Pumie, Quanjing, and Sophie. Last, but most of all, this thesis is dedicated to Hui and my family.